AMBIENT SUBMICRON PARTICLES IN NORTH AMERICA: THEIR SOURCES, FATE, AND IMPACT

A Thesis
Presented to
The Academic Faculty

by

Richard Edward Peltier, Jr

In Partial Fulfillment
Of the Requirements for the Degree
Doctor of Philosophy
In the School of Earth and Atmospheric Sciences

Georgia Institute of Technology
Dec 2007

AMBIENT SUMBICRON PARTICLES IN NORTH AMERICA: THEIR SOURCES, FATE, AND IMPACT

Approved by:

Dr. Rodney J. Weber
School of Earth and Atmospheric Sciences
Georgia Institute of Technology

Dr. Athanasios Nenes
School of Earth & Atmospheric Sciences and Chemical and Biomolecular Engineering
Georgia Institute of Technology

Dr. Michael H. Bergin
School of Civil & Environmental Engineering
Georgia Institute of Technology

Dr. L. Gregory Huey
School of Earth and Atmospheric Sciences
Georgia Institute of Technology

Dr Ellery D. Ingall
School of Earth and Atmospheric Sciences
Georgia Institute of Technology

Date Approved: Sept. 18, 2007

ACKNOWLEDGEMENTS

I am very thankful for my time with Dr. Rodney J Weber, a man who never ceases to impress me with his tenacity, intellect, and drive. I am indebted to him for taking a chance on this graduate student whose utter lack of experience was matched only by motivation to succeed. He has provided me with endless opportunities for personal and intellectual growth and offered me invaluable professional and scientific advice.

I would also like to acknowledge a number of colleagues whom have enriched my dissertation experience with humor, candor, and friendship. Former student colleagues Drs. Amy Sullivan, Steven Sjostedt, Sangil Lee and Jean-Francois Koprivnjak have each contributed greatly through advice, mutual discussion, and copious amounts of coffee. Christopher Hennigan, Arsineh Hecobian, and Saewung Kim continue to offer their time, whenever I need it, whether in the office, the lab, or the field. Lastly, I want to recognize my exam committee – a wonderful group of eminent scientists including Drs. Mike Bergin, Greg Huey, Thanos Nenes, and Ellery Ingall.

A number of people have provided invaluable assistance during some of the many field campaigns and include Drs. Adam Wollny, Ann Middlebrook, Carsten Warneke, Frank Flock, and John Holloway from NOAA Chemical Sciences Division. Dr. Elliot Atlas of the University of Miami has been a helpful ally. Dr. Jamie Schauer and David Snyder of the University of Wisconsin - Madison have graciously provided useful data and manuscript comments. I'd like to thank Drs. Jose-Luis Jimenez and Edward Dunlea of

the University of Colorado – Boulder for many years of scientific cooperation, academic discussion, and comprehensive baseball statistics discussions. Dr. Andreas Stohl of the Norwegian Institute for Air Research has been helpful in his assistance with his various model products. I especially want to acknowledge the tremendous insight of Drs. Charles Brock and Joost de Gouw from NOAA Chemical Sciences Division – their assistance has been, and will continue to be, invaluable.

Most importantly, I would like to acknowledge my incredible wife Gretchen, who has stood next to me for every minute of every day. She has put up with occasional grouchiness, obsessive-compulsive behavior, lengthy (and remote) field campaign deployments, and many bleary-eyed conversations. My life has been, and continues to be, deeply enriched by my best friend.

TABLE OF CONTENTS

LIST OF TABLES

LIST OF FIGURES

LIST OF ABBREVIATIONS

AMS: Aerosol Mass Spectrometer

AMSL: Above Mean Sea Level

AOC: Aircraft Operations Center

BL: Boundary Layer

Ca^{2+}: Calcium ion

CAA: Clean Air Act

CC: Cloud Condensation Nuclei

Cl^-: Chloride ion

CO: Carbon Monoxide

EC: Elemental Carbon

EDT: Eastern Daylight Time

EST: Eastern Standard Time

FID: Flame Ionization Detection

FRM: Federal Reference Method

FT: Free Troposphere

GCMS: Gas-Chromatograph Mass Spectrometer

HCl: Hydrochloric acid

IC: Ion Chromatograph

ICARTT: International Consortium for Atmospheric Research on Transport and Transformation

ICTC: Intercontinental Transport and Chemical Transformation

INTEX-B : Intercontinental Chemical Transport Experiment, Phase B

IMPROVE: Interagency Monitoring of Protected Visual Environments

ISE: Ion Selective Electrode

K: Kelvin (degrees)

K^+: Potassium ion

LTI: Low-Turbulence Inlet

LOD: Limit Of Detection

MACR: Methacrolein

MEK: Methyl Ethyl Ketone

Mg^{2+}: Magnesium ion

MVK: Methyl Vinyl Ketone

Na^+: Sodium ion

NAAQS: National Ambient Air Quality Standards

NCAR: National Center for Atmospheric Research

NEAQS: New England Air Quality Study

NH_3: Ammonia

NH_4^+: Ammonium ion

NMR: Nuclear Magnetic Resonance

NOAA: National Oceanic and Atmospheric Administration

NO_3^-: Nitrate ion

OC: Organic Carbon

OM: Organic Matter

OPC: Optical Particle Counter

OVOC: Oxygenated Volatile Organic Carbon

PALMS: Particle Ablation Laser Mass Spectrometer

PEEK: Polyetheretherketone

PILS: Particle-Into-Liquid Sampler

PM: Particulate Matter

PM1.0: Particulate Matter with aerodynamic diameter less than 1.0μm

PM2.5: Particulate Matter with aerodynamic diameter less than 2.5μm

PSAP: Particle Soot Absorption Photometer

PDT: Pacific Daylight Time

PTR-MS: Proton Transfer Reaction- Mass Spectrometer

RAF: Research Aviation Facility

RMS: Root Mean Square

SEC: Size-Exclusion Chomatography

SO_2: Sulfur dioxide

SO_4^{2-}: Sulfate ion

SOA: Secondary Organic Aerosol

SOAR: Study of Organic Aerosols in Riverside

TC: Total Carbon

TEOM: Tapered Element Oscillating Microbalance

TOC: Total Organic Carbon

TOR: Thermal/Optical Reflectance

TOT: Thermal/Optical Transmittance

VOC: Volatile Organic Carbon

USEPA: United States Environmental Protection Agency

UTC: Coordinated Universal Time

UV: Ultraviolet (light)

WP-3D: Lockheed P-3 Orion research aircraft operated by NOAA

WSOC: Water-Soluble Organic Carbon

SUMMARY

This thesis presents results from a number of aircraft- and ground-based observations of ambient submicron aerosol chemical composition, as well as results from work that modified a common aerosol instrument in order to measure organic carbon aerosol. We discuss aerosol sources, sinks, transport processes, and implications. The research focuses on aerosol chemical composition across North America using measurements made aboard research aircraft above the northeastern United States, northern Georgia, and the eastern Pacific Ocean and west coast of the United States.

The Particle-Into-Liquid Sampler (PILS) was successfully enhanced by replacing the impactor with a miniature cyclone. This increased droplet collection efficiency for organic carbon aerosol, and suggests that this instrument is capable of quantifying submicron organic carbon aerosol. This technique is not without limitations, as a particle size dependence was observed where insoluble particles greater than ~110 nm could not be measured.

In ambient studies, aerosol mass in the Northeastern United States was largely influenced by sulfate and water soluble organic carbon (WSOC) aerosol, with highest concentrations observed near the surface. In regions of power generation facilities, this aerosol was frequently acidic. As a result of this work, a mass balance analysis was conducted, and we estimate that organic matter (OM) can be estimated by 3.1 times the concentration of WSOC. In the Atlanta region, no significant enhancement of WSOC was observed in

highly acidic plumes, which was inconsistent with chamber studies. Lastly, transported aerosol from Asia plays a small role in submicron aerosol mass loading in the Northwestern United States. It was mainly comprised sulfate and water-soluble organic carbon, though at concentrations an order of magnitude lower than observed in the Northeastern United States. A multivariate regression analysis that related observed WSOC variability to a variety of measured volatile organic carbon (VOC) gases showed that for plumes that were mainly influenced by Asian emissions, WSOC variability was most closely related to VOCs from fossil fuel combustion, while WSOC variability in plumes mainly of North American origin was influenced by both fossil fuel combustion and biogenic VOCs.

The broader impacts of this work reflect on the importance of anthropogenic emissions on submicron aerosol mass in North America. For example, sulfate aerosol was a substantial component (by mass) of ambient aerosols in the Northeastern, Northwestern, and Southeastern United States. This is significant for aerosol control and regulation because with a few exceptions, sulfate aerosol is a secondary product emitted by anthropogenic sources. Organic carbon aerosol (in the form of WSOC) was also important throughout most regions sampled, but generally appeared in a broader, regional concentration gradient with far fewer distinct point sources. In contrast to sulfate, ambient WSOC appears to have multiple sources that may in some way be related to one another. Biomass burning clearly contributed to substantial aerosol mass loadings of WSOC, but was generally constrained to discrete, high altitude interceptions and suggests that biomass burning is a substantial source for OC aerosol through primary emission or

secondary formation (or both). This implies that while biomass burning may be a significant source of aerosol for global mass loading, its impact on lower altitudes in North America is less important. Anthropogenic sources of WSOC appear more complex, with somewhat less well-defined sources. WSOC was generally correlated with carbon monoxide (CO), a non-specific tracer of combustion, suggesting a linkage between fossil fuel combustion and WSOC. Since WSOC is not directly emitted from fossil fuel combustion, this indicating that WSOC was formed secondarily from anthropogenic emissions. However, WSOC was also generally observed throughout most low-altitude samples, including sampling periods that were not directly downwind of urban sources. This suggests that biogenic emissions, which are spatially widespread, may be linked to WSOC formation as well. Thus, WSOC may be present as a broad, regional concentration, but upwind urban sources enhance WSOC above this regional background. This implies that WSOC formation control strategies must address secondary formation that involved both underlying biogenic emissions, as well as anthropogenic emissions from fossil fuel combustion.

CHAPTER 1

AEROSOL OVERVIEW AND INTRODUCTION

1.1 Motivation and Importance of Research

Ambient aerosols are ubiquitous and play an increasingly important role in our global environment. They arise from both anthropogenic and biogenic sources, and can be formed as primary pollutants or created through complex, secondary formation processes. This complexity has led to significant uncertainty with respect to the formation and fate of aerosol, as well as with the chemical processing that aerosol undergoes as it is transported.

This work seeks to address some of the gaps in knowledge that remain in determining aerosol sources in the environment. A particular focus on organic carbon and sulfate aerosol is discussed. An improved understanding of underlying aerosol formation and transport processes will provide a better fundamental understanding relating to their control and regulation. This dissertation is divided into four sections that address essential questions by presenting salient results and analyses. Specific questions that will be addressed in this work include:

- Since organic carbon aerosol is a significant fraction of aerosol mass loading, how can existing aerosol instrumentation be modified in order to more easily quantify carbonaceous aerosol?

- How does aerosol transformation and transportation affect pollution within the northeastern United States?
- Does ambient organic aerosol form under acid-catalyzing conditions?
- To what extent does long range transport from Asia play in the role of carbonaceous aerosol in North America?

This work makes a significant contribution to the current state of understanding by identifying and analyzing specific sources and sinks for submicron aerosol in the ambient environment. Since aerosol affects many features of our environment, a comprehensive understanding of its sources and sinks is useful for identifying the most efficient way to lower emitted pollution, reduce global pollution loading, and mitigate aerosol impacts. A large portion of the observations come from the first successful deployment of a PILS-WSOC aboard an aircraft research platform. Organic carbon aerosol, which represents a substantial fraction of aerosol mass, continues to be poorly understood, and these fast, spatially distributed measurements from aircraft platforms provide novel insight in to this important aerosol component. The ability to identify variability in organic carbon across a range of atmospheric conditions will greatly contribute to our understanding of aerosol formation, fate, and potential impact on atmospheric characteristics by enhancing aerosol modeling techniques, remote sensing technology, and expand our basic science understanding of aerosols. This work is mainly focused on anthropogenic North American aerosol by first discussing how the power generation region and urban areas of the Northeastern United States have affected local aerosol climatology, then tests and refutes a specific mechanism previously thought to significantly contribute to aerosol

load, and finally by examining the sources of incoming aerosol to the west coast of North America from Asia.

1.2 Importance of aerosols

Expanding our understanding of aerosols is important because they affect many facets of our environment. They are ubiquitous throughout most of the lower atmosphere and have wide-ranging implications in the biosphere. They can be a product of our own making, yet at the same time are created without human influence. Aerosol can be formed locally, as well as at distant sources, which can then be transported and have local implications. This section will discuss the important effects of aerosol on our environment.

1.2.1 Visibility

Ambient aerosol can impair the transmission of light through our atmosphere by absorption or scattering light, thus reducing visibility. This has been linked to interference with visual navigation (e.g. aircraft and marine vessels) and can decrease our visual enjoyment of the environment. In fact, the US Congress, recognizing the importance of decreased visibility due to aerosols, included the language '…prevention of any future, and the remedying of any existing, impairment of visibility in Class I federal areas which impairment results from manmade air pollution.' as one of the goals of the 1977 Clean Air Act (CAA) amendments. The Interagency Monitoring of Protected Visual Environments (IMPROVE) actively monitors visibility throughout the United States.

1.2.2 Climate

Significant uncertainty remains with respect to the effects of aerosol on global climate. It is known that aerosols can have both indirect and direct effects on climate. These effects can have either positive or negative forcing, which can warm or cool the climate, respectively. For example, sulfate aerosol tends to have net cooling effect due to its ability to reflect incoming solar radiation [*Charlson, et al.*, 1992; *Mitchell, et al.*, 1995; *Stier, et al.*, 2006; *Verma, et al.*, 2006], a direct effect of sulfate aerosol. In contrast, black carbon can absorb radiation, which can result increased thermal absorption in the atmosphere [*Bond*, 2001; *Horvath*, 1993; *Reid, et al.*, 2005; *Stier, et al.*, 2006], as well as a decreased planetary albedo (e.g. darkening of ice surfaces) [*Law and Stohl*, 2007]}. Ambient aerosol can also have indirect effects on radiation balance. For example, sulfate can act as a cloud condensation nuclei, and therefore modify cloud properties [*Boucher and Lohmann*, 1995; *Jones, et al.*, 1994]. Alterations of freezing characteristics of cloud droplets or changes in cloud albedo [*Lohmann and Feichter*, 2005] caused by CCN may affect radiative uptake. Since aerosol in the atmosphere is comprised of a heterogeneous mixture of compounds, it is very important to understand aerosol chemical composition with respect to its influence on radiation balance.

Organic carbon aerosol has also been shown to have an indirect effect on climate. In a chemistry model by Collins, et al [2002], they show that oxidation of anthropogenic OC aerosol can act source for ozone. They also show that OC oxidation can be a significant sink for hydroxyl and peroxy radicals. These radicals can efficiently oxidize methane, thus leading to a buildup of methane in the atmosphere. Ozone and methane are well

characterized greenhouse gases, and their increase will likely have a positive forcing on global climate.

1.2.3 Human Health

Aerosols are an important component in exposure assessment studies that examine human health impacts. Unfortunately, the relationships of many of the physicochemical properties of aerosols are not fully integrated into these analyses. For example, particulate mass is often a common variable used in health outcome regression since these metrics are often publicly available and relatively easy to attain. Other studies may use small, filter-based particulate matter (PM) samplers that are deployed over long integration times for personal exposure assessment. For community-wide cohort studies, a common approach to measuring aerosol may involve a Federal Reference Method (FRM) Tapered Element Oscillating Microbalance (TEOM) instrument. The TEOM measures bulk PM mass of a known size at a single sampling location. While quantitative at the sampling site, the data may represent just a few properties (e.g. total mass) of the aerosol, and may not provide critical information specific to the exposure to the aerosol. It also may not be fully representative of spatial variability. This is reflected in somewhat conflicting research conclusions, where exposure to particulate mass is sometimes associated with excess morbidity or mortality [*Davidson, et al.*, 2005; *Delfino, et al.*, 1997; *Dockery, et al.*, 1993; *Gwynn, et al.*, 2000; *Peters, et al.*, 1997; *Pope*, 1996; 2000; *Thurston, et al.*, 2005], and sometimes this relationship is unclear [*Reiss, et al.*, 2007; *Tolbert, et al.*, 2000]. By better understanding aerosol formation processes, it may

improve the understanding on the complex linkage between exposure and health outcome.

1.2.4 Secondary effects

Aerosol also has a number of secondary effects on the atmosphere and planet. For example, aerosol has been shown to alter crop production by reflecting or absorbing radiation that is normally available for photosynthetic processes [*Greenwald, et al.*, 2006; *Yamasoe, et al.*, 2006]. Aerosol can also have detrimental secondary effects on natural features such as premature weathering of statues, buildings, and national monuments. Staining of buildings and monuments has been observed throughout Europe due to aerosol deposition and chemical processes – this was especially evident during the Industrial Revolution where emissions of aerosol from coal combustion went virtually unregulated. Thus, the Environmental Protection Agency requires compliance for not only primary air quality standards (which are mainly based on PM mass loadings considered important for protecting human health), but also require secondary standards to lessen potential secondary impacts due to particulate matter.

1.3 Aerosol Sources – A Summary

Particulate matter exists across a wide spectrum of sizes, ranging from less than 5 nm and exceeding several hundred microns. Smaller particles are typically associated with fresh combustion emissions, or from new particle formation derived from homogeneous nucleation [*Kleeman, et al.*, 2000; *Seinfeld and Pandis*, 1998]. Largest particles tend to be observed in clouds [*Brasseur, et al.*, 1999; *Seinfeld and Pandis*, 1998], typically on the

order of 25-500μm. As part of the National Ambient Air Quality Standards (NAAQS), USEPA measures and regulates particle mass, among other metrics, in two aerodynamic diameter size ranges: particles less that 10μm (e.g. coarse mode, PM_{10}), and particle mass less than 2.5μm (e.g. fine mode, $PM_{2.5}$) [*USEPA*, 2005]. Much research in aerosol science investigates submicron particles, or particles with diameters less than 1.0 microns (i.e. $PM_{1.0}$). Fine mode particles are more likely to have deleterious effects on human health as this size range is considered to be respirable. Total atmospheric mass loading tends to be driven by fine mode particles, though at times coarse mode contribution can be significant [*Seinfeld and Pandis*, 1998]. Since coarse mode particles exceed the respirable size range, they may not have significant human health effects but may play a larger role in radiation balance and ecological perturbations.

Aerosol sources are numerous and include both primary emitted particulates, and secondary aerosol. Primary aerosol has specific sources that are diverse. These include biogenic material (e.g. from biomass burning or directly emitted by plants, agriculture, etc.), combustion-based pollution, mechanical formation (e.g. from crushing of materials, tire wear that is lofted by passing vehicles and winds), and aerosol formed by breaking ocean waves. Secondary aerosol sources are considerably more diverse, and generally result from oxidation of gas precursors to more thermodynamically-stable components that can exist as particulates in the atmosphere. Specific aerosol components and sources are now discussed in further detail.

1.3.1 Inorganic components

Aerosol is comprised of many chemical constituents. A large fraction of these (by mass) are inorganic components, which are discussed below.

1.3.1.1 Ammonium Sulfate

Sulfate and ammonium aerosol – typically found in the atmosphere as ammonium sulfate and ammonium bisulfate ($(NH_4)_2SO_4$ and NH_4HSO_4, respectively) - are a significant fraction of total aerosol [*Seinfeld and Pandis*, 1998]. By mass, sulfate tends to dominate the inorganic fraction of aerosol and generally driven by fossil fuel combustion in continental regions. Anthropogenic SO_2 emissions, frequently from coal-fired power plants, are released into the atmosphere and generally comprise the largest source of sulfur for the atmosphere [*Brasseur, et al.*, 1999]. Through a complex reaction involving several intermediate steps, SO_2 is photochemically processed in the presence of water, which oxidizes the sulfur into sulfate aerosol.

There are a number of biogenic sources of sulfate aerosol, with the most abundant source of biological sulfur as dimethyl sulfide (DMS) [*Simpson, et al.*, 1999] from the ocean. Volcano emission of SO_2 also represents a significant source of sulfur (in the form of SO_2). Vegetation and biomass burning can also contribute to sulfur loading, though their fluxes are significantly smaller than anthropogenic, oceanic, and volcanic sources. These sulfur compounds are converted to sulfate aerosol through a number of complex oxidation steps. Sulfur oxidation has been well-described in the literature and can be best summarized by Singh, et al [1995]

Ammonium, on the other hand, is mainly formed by condensation of ammonia gas on a sulfuric acid particle. Ammonia is commonly emitted by biological processes [*Dentener and Crutzen*, 1994; *Langford and Fehsenfeld*, 1992], and is generally ubiquitous in the environment. On occasion where sulfur dioxide exceeds available ammonia, ammonium bisulfate can result. This leaves an acidic aerosol where the divalent negative charge of the sulfate anion is not completely neutralized by ammonium; the additional charge is balanced with a proton, thus creating an acidic particle when in an aqueous solution. Acidic aerosol has potential consequences such as additional chemical processing (e.g. acid catalyzed reactions) [*Gao, et al.*, 2004; *Iinuma, et al.*, 2004; *Jang and Kamens*, 2001; *Kalberer, et al.*, 2004; *Limbeck, et al.*, 2003; *Tolocka, et al.*, 2004] as well as an increase in adverse health effects [*Gwynn, et al.*, 2000; *Thurston, et al.*, 2005]

1.3.1.2 Nitrate

Nitrate is a semi-volatile component found in aerosol. It is often paired with ammonium or another cationic species. However, its presence in the atmosphere depends on a dynamic equilibrium with aerosol acidity – in conditions where excess acidity is present (e.g. in the presence of excess amounts of sulfuric acid), nitrate aerosol dissociates from the particle and shifts the equilibrium such that nitrate aerosol (NO_3^-) becomes nitric acid (HNO_3). Nitric acid is highly water-soluble and efficiently scavenged by clouds, fog, and ice surfaces, thus it can be difficult to quantitatively measure in aerosol [*Neuman, et al.*, 1999; *Ryerson, et al.*, 1999].

1.3.1.3 Other Ionic Components

Various other inorganic compounds can also be present in aerosol. These include ions such as calcium and magnesium, which are commonly associated with dust [*Maxwell-Meier, et al.*, 2004; *Song, et al.*, 2005]. Dust has been shown to be a significant component of aerosol that has been subjected to long-range transport from Asia and Africa [*Moulin, et al.*, 1997; *Perry, et al.*, 1997; *Prospero*, 1999]. Potassium ion has been well-documented [*Lee, et al.*, 2003; *Ma, et al.*, 2003] as a good tracer of biomass burning plumes. Sodium and chloride have multiple sources, and include sea-spray, industrial processes, and biomass burning.

1.3.2 Organic Carbon

Organic carbon (OC) represents one of the least understood fractions of atmospheric aerosols [*Decesari, et al.*, 2000; *Fuzzi, et al.*, 2001; *Novakov, et al.*, 1997; *Zappoli, et al.*, 1999]. OC is an important component since it typically comprises a large fraction of fine particle mass, thus playing roles in planetary climate [*IPCC*, 2007] by directly and indirectly affecting radiation balance. OC may also have effects on human and ecological health [*Pope*, 2000; *Thurston, et al.*, 2005]. OC is chemically complex, and spans a wide range of volatility, making quantitative OC measurements challenging.

Primary OC is typically formed by fuel combustion processes or through biogenic emissions (e.g. biomass burning or aerosol released by the ocean from wave-breaking). Biomass burning is considered to be a significant source of global OC [*Fine, et al.*, 2001; *Iinuma, et al.*, 2007; *Rogge, et al.*, 1998; *Streets, et al.*, 2003] loading. There has also

been some evidence for primary emission of OC from leaf wax, pollen, spores, bacteria, and vegetative detritus. [*Seinfeld and Pandis*, 1998]. A large fraction of primary carbonaceous aerosol stems from fossil fuel combustion that is generally found in abundance in densely populated, urban regions.

Secondary formation of OC is substantially more complex than primary emission. It involves multiple pathways of formation, many of which are unknown. The loss of organic aerosol that depends on a variety of factors, including the underlying composition of volatile organic compounds, availability of oxidizing reactants, and thermodynamic properties of the organic gases and aerosols. Since some organic aerosol is considered to be semi-volatile, these factors can influence the partitioning of the particulate between the gas and particle phases. This adds significant complexity to not only to the measurement of organic carbon aerosol, but to understanding the formation mechanisms of OC.

1.3.2.1 Water Soluble Organic Carbon

The water soluble fraction of OC comprises a substantial portion of this research and is thus described in further detail. The term 'water soluble' is operationally defined and typically comprises ~10-80% of organic carbon mass [*Decesari, et al.*, 2000; *Facchini, et al.*, 1999; *Sullivan, et al.*, 2004; *Zappoli, et al.*, 1999]. Lower WSOC/OC fractions tend to be observed in regions closer to the emission source, while higher fractions tend to be observed in more aged plumes [*Decesari, et al.*, 2002; *Kalberer, et al.*, 2004; *Lim and Turpin*, 2002; *Turpin and Huntzicker*, 1991]. Primary sources of WSOC mainly include

biomass burning. Secondary sources of WSOC are far more diverse, and may include oligermerization of oxygenated VOCs (OVOCs) [*Gao, et al.*, 2004], oxidation and subsequent condensation of VOCs and OVOCs [*Seinfeld and Pankow*, 2003], oxidization of insoluble OC to a more soluble form [*Andreae and Crutzen*, 1997; *Brock, et al.*, 2002; *Collins, et al.*, 2002; *Heald, et al.*, 2005; *Kalberer, et al.*, 2004; *Park, et al.*, 2003; *Seinfeld and Pankow*, 2003], and possible formation by hetero- or homogeneous nucleation of soluble gas-phase organics. It is believed that WSOC is mainly formed through secondary formation [*Saxena and Hildemann*, 1996] of aerosol. Considerable research has been conducted on secondary organic aerosol (SOA) formation, and has included in situ measurements at ground-based and aircraft-based sites which have spanned the globe. A significant amount of work was conducted under more controlled conditions (e.g. such as chamber studies which include oxidizers, organic gases, and seed aerosol particles), which attempt to explain fundamental questions that arise from organic aerosol formation. Fewer ambient aerosol studies examining OC aerosol have been conducted, and even less work has examined SOA formation. This topic, as well as general WSOC climatology, is discussed extensively as part of this thesis.

1.3.3 Elemental Carbon

Elemental carbon (EC) is found throughout the troposphere and typically derives from combustion of hydrocarbons. While not the only source of EC, diesel engines are significant contributors of EC. Diesel emissions, the subject of a detailed report by USEPA [*USEPA*, 2002] are thought to have considerable carcinogenic effects on human health. These emissions include both EC and organic compounds, and when combined,

form soot. Soot contains a variable amount of organic particles and vapors which include (but are not limited to) polyaromatic hydrocarbons, short- and long-chain alkanes, and various organic acids which result from incomplete oxidation of diesel fuel. Many of these compounds are considered to be hazardous air toxins and have been placed under specific regulatory scrutiny by USEPA [*USEPA*, 2005].

1.3.4 Metals

A small but measurable fraction of aerosol is comprised of trace metals. These can include arsenic, cadmium, mercury, aluminum, copper, iron, nickel, and zinc (though many known elements can, in fact, be detected in at least minute quantities). These compounds are generally emitted by industrial processes; for example, arsenic, mercury, and cadmium are often found in coal-fired power plant emissions [*Biswas and Wu*, 1998; *Lighty, et al.*, 2000], while aluminum, copper, nickel, iron, and zinc may come from mining or smelting operations [*Liu, et al.*, 2003; *McDonald, et al.*, 2003; *Prati, et al.*, 2000]. They can also be associated with dust aerosol, petroleum combustion, waste incineration, or mechanical sources such as brake dust and tire wear.

1.4 Transport and transformation

Aerosol is subjected to mesoscale and microscale meteorological influence which, at times, subjects it to transport over significant distances. For example, continental sulfate has been shown to extend for greater than 500km [*Beattie and Whelpdale*, 1989] from the northeastern United States. Likewise, Asian dust has been observed over the United States – a distance of over 6000 km [*de Gouw, et al.*, 2004; *Jaffe, et al.*, 2005]. Long

range transport events are generally episodic (i.e. dust transport from Asia; [*Husar, et al.*, 2001], though there is been recent evidence that significant long range transport from Asia occurs year round [*VanCuren and Cahill*, 2002; *VanCuren, et al.*, 2005].

Aerosol also undergoes transformation as it ages. Gas and particulate components continue to be altered by chemical and photo oxidation. Plumes of pollution can be diluted which affects concentration and gas and particle partitioning. Aerosol can be mixed with water vapor (from the surface, or in clouds), which may have an effect on reactions involving aerosol formation or loss. Specific transformation processes generally depend on background concentrations of chemical oxidants, availability of precursor gases and particles, and the initial and intermediate chemical composition of the aerosol.

Ideally, Lagrangian studies could be performed to fully analyze aerosol transformation. However, this is often not practical since transport distances often exceed thousands of kilometers, and we are often restricted to single study site locations. A common method of Lagrangian study involves the use of driftsondes (e.g. controllable weather balloons), which are released into an air mass to travel only by wind velocity and direction. Instrumentation onboard the driftsonde sends results back to an operator on the ground. There are two major types of driftsondes: one that is passive in that their buoyancy is set prior to launch and is fixed to follow a particular altitude, and a second type of driftsonde can be partially controlled by a remote operator (e.g. an investigator on the ground using satellite links to the balloon) [*Riddle, et al.*, 2006; *Voss, et al.*, 2005]. Controllable

driftsondes are advantageous in that a plume can be repeatedly sampled in cross-section (bottom of plume to top of plume) as the plume is transported. However, driftsondes are limited by their relatively small buoyancy and power capabilities and are not suitable for most aerosol sampling applications. Aircraft-based observations are useful, particularly when they are in conjunction with other aircraft that are sampling upwind air masses for comparison. Aircraft have very large research experiment payload capacities, and can travel several thousand kilometers during a single flight. At this point, remote sensing of aerosol composition and transformation still has significant uncertainty. This thesis discusses a number of aircraft-based field campaigns, and describes relatively fresh, moderately aged, and well-aged aerosol chemical composition stretching from Asia to eastern Canada.

CHAPTER 2

AEROSOL COMPOSITION MEASUREMENTS

It is useful to discuss aerosol instrumentation that was used throughout this work since there are a variety of analytical techniques that quantify and characterize aerosol. Each method has unique advantages and disadvantages that, depending on a particular research objective, make certain measurements more appropriate than others. For example, some measurements are temporally fast, but not quantitative (e.g. some mass spectrometry techniques), while other measurements are very slow yet extremely sensitive (e.g. offline gravimetric analysis of filters). Throughout this dissertation, a number of instruments are used for comparative or contrasting analysis, and therefore, it is useful here to broadly discuss the general kinds of instrumentation that are available. This discussion includes some of the strengths and limitations of each analytical technique. A more detailed specific methodology and discussion of specific instruments used for analysis is found within each subsequent chapter.

Since much of the work presented in this thesis relies on quantitative measurements of aerosol, a technique was developed to modify an existing instrument to expand its capabilities for measuring organic carbon aerosol. Instrumentation method development requires a thorough understanding of instrumentation principles, limitations constrained by uncertainty, and adequate comparison with other, similar measurements. These are discussed in detail in this chapter.

2.1 Particle-Into-Liquid Sample

The Particle-Into-Liquid Sampler (PILS) is a quantitative, online technique that condenses water vapor onto aerosol, collects the droplets, and transports them to a third-party chemical analyzer. The PILS is commonly coupled to a set of ion chromatographs (i.e. 'PILS-IC') and is capable of quantifying water-soluble inorganic ions and some organic acids. A second configuration consists of the PILS paired with a Sievers Total Organic Carbon (TOC) Analyzer (Model 800T, GE Analytical Instruments, Boulder, CO, USA), which measures the water-soluble fraction of organic carbon aerosol (i.e. 'PILS-WSOC'). Many of the results presented in this thesis rely on aerosol characterization using the PILS instrument in various configurations. A schematic diagram of the PILS system is shown in Figure 2.1. Specific operating conditions, including reagent types, flow rates, and size selection are described in further detail within each chapter.

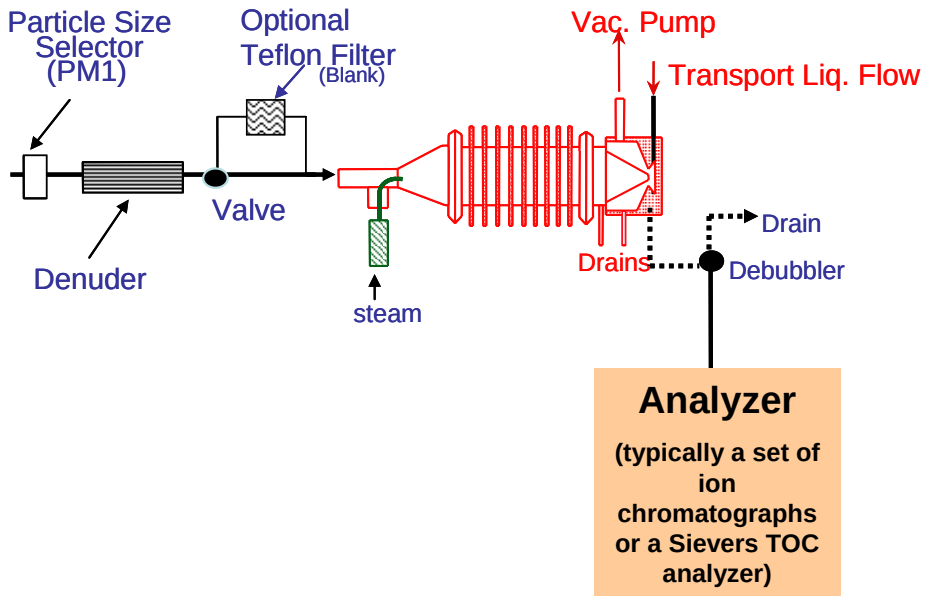

Figure 2.1. Schematic diagram of a Particle-Into-Liquid Sampler for measurement of bulk chemical composition of aerosol ($PM_{1.0}$ or $PM_{2.5}$). The PILS can be coupled to ion chromatographs (e.g. PILS-IC) or a Total Organic Carbon analyzer (e.g. PILS-WSOC)

2.2 Mass spectrometry-based analyzers

A number of mass spectrometer-based instruments are used in aerosol research. The aerosol mass spectrometer detects aerosol by ionizing a particle and observing the spectra of mass-to-charge ratios. A variety of aerosol ionization techniques are available and include chemical ionization [*Huey*, 2007; *Smith and Hearn*, 2006] and laser ionization [*Murphy and Thomson*, 1995; *Noble and Prather*, 1996]. Utility of this technique ranges from precise analysis of mass spectra of a single particle (e.g. Particle Ablation Laser Mass Spectroscopy – PALMS) [*McKeown, et al.*, 1991] to bulk composition measurements of common atmospheric components (e.g. Aerodyne Mass Spectrometer, Aerodyne Research, Billerica, MA, USA) [*Jimenez, et al.*, 2003]. These instruments are usually suitable for deployment at ground- and/or aircraft-based research platforms and provide a significant quantity of information that describes composition. Mass spectrometry-based techniques of aerosol measurement are considerably diverse and are driven by specific research objectives.

2.3 Optical methods

Optical measurements of aerosol include methods such as optical particle counters, nephalometers, and particle soot absorption photometers (PSAP). These techniques are generally fast measurements of the microphysical properties of aerosol. For example, an optical particle counter can count the number of particles in a given series of size ranges, providing a number distribution which can be converted to an estimation of particle volume. In contrast, a nephelometer measures the light scattering ability of particles and is useful in determining aerosol optical depth which can influence atmospheric albedo.

On the other hand, a PSAP collects particles on a small filter that is illuminated by a laser. As light-absorbing particles collect on the filter, the laser transmittance decreases. This change is proportional to particle absorption, which can be an indirect measurement of particulate soot (which absorbs visible light). Each instrument uses a different optical method (light attenuation, scattering, and absorption, respectively), and provides different information that describes the sampled aerosol.

2.4 Offline methods

Offline methods of aerosol quantification usually involve collecting aerosol on a filter substrate for a known period of time and air flow rate. A variety of methods can then be employed to characterize the collected aerosol. For example, gravimetric methods of aerosol measurements have been used in aerosol studies for over 20 years. By capturing aerosol on a filter substrate of previously-known weight, aerosol mass can be determined by subtracting total filter weight (filter + captured aerosol) by previous weight. This method is robust and relatively inexpensive to deploy.

Filter samples can also be coupled with more advanced laboratory techniques in which aerosol that has been captured on filters can be extracted using solvents and further processed by analytical instruments such as ion chromatography, gas chromatography-mass spectroscopy (GC-MS), nuclear magnetic resonance spectroscopy (NMR) or organic carbon oxidation [*Fine, et al.*, 2001; *Jacobson, et al.*, 2000; *Sannigrahi, et al.*, 2006; *Sullivan and Weber*, 2006a; b; *Zheng, et al.*, 2002]. This provides additional information about the composition of aerosol, depending on the analytical technique

chosen. The aerosol can be further characterized by examining the filters with a variety of microscope or laser techniques [*Chow*, 1995; *McMurry*, 2000] to provide qualitative and quantitative descriptions of the sample.

2.5 Instruments that use multiple detection methods

A number of instruments use more than one method of quantification for improved instrument response. For example, quantitative analysis of carbonaceous material captured by filters can also be determined by thermal-optical techniques following the protocols developed by Huntzicker et al [1982]. This method has become one of the most commonly used approaches for measuring the mass of ambient aerosol carbon. It quantifies the total carbon (e.g. organic and elemental fractions) mass collected on a quartz filter by heating the filter continuously or in a stepped manner to ~800 degrees in a non-oxidizing pure helium atmosphere. Organic material is volatilized and detected by Flame Ionization Detection (FID). The sample temperature is typically reduced to ~600 degrees, and the sample atmosphere is replaced with 2% oxygen (with the balance helium). The temperature is then increased to ~850 degrees C and the remaining carbonaceous material is oxidized and subsequently detected by FID. Finally, the FID signal is internally calibrated with a known quantity of methane.

A limitation to this method is that during the first heating cycle, an unknown fraction of organic carbon may char on the filter and thus not be detected. During the second heating cycle (in an oxidizing atmosphere), both the pyrolyzed (e.g. charred) organic material and elemental carbon fraction are evaporated from the filter. To delineate OC

from EC, one of two optical techniques is typically used. Thermal-optical reflectance (TOR) is used to determine the EC and OC split [*Chow, et al.*, 1993]. TOR passively illuminates the filter with a low power laser, and reflected light is constantly monitored. The filter reflectance is diminished by elemental carbon, as well as by any charred organic material that forms during the first heating cycle. As the sample analysis begins, the baseline reflectance of the filter (which is determined only from captured elemental carbon) is determined. The reflectance decreases as the organic material chars during the filter heating. During the second heating cycle (e.g. in an oxidizing atmosphere), this charred material oxidizes and results in increased filter reflectance. When filter reflectance returns to baseline, evolved carbon detected up to this point is considered the organic fraction. The remaining carbon that is detected by FID after this point is considered elemental carbon. By combining two techniques (FID detection and thermal/optical reflectance), the instrument detects the quantity of organic and elemental carbon in an aerosol sample. A sample thermogram, which depicts the EC and OC split by a related technique (thermal-optical transmittance or TOT, described in Section 2.6.2) is provided in Appendix A.

A number of other instruments are commonly used in studies of aerosol, but were not used as part of this research, thus they are not further discussed.

2.6 Modification of the PILS-WSOC to PILS-OC

We now discuss research that modifies an existing measurement technique (PILS-WSOC) to measure organic carbon aerosol.

2.6.1 The Particle-Into-Liquid Sampler (PILS)

The Particle-Into-Liquid Sampler was originally developed for measurement of water-soluble inorganic aerosol components. It operates by increasing the size of particles through condensational growth in a super saturated water vapor environment to sizes easily captured by inertial methods. The droplets formed are focused by a nozzle and inertially deposited at the center of a polycarbonate impaction plate. A film of water with dissolved aerosol components spreads from the center of the impaction plate to its edges, where a stainless steel mesh wicks the liquid from the polycarbonate impaction plate to a 0.02 inch ID polyetheretherketone (PEEK) collection tube. The mesh wick is continually washed with a stream of ultra pure deionized water injected at a known flow rate opposite to the sample collection point. Liquid sample collected from the impaction plate passes through a glass debubbler to remove entrained air bubbles, and is drawn by two glass syringes (Kloehn Ltd, Las Vegas, NV) that pump in an alternating tandem configuration to provide a smooth, continuous flow. These syringes then force the liquid sample through a 0.22μm pore polypropylene filter and deliver it to a detector. A Sievers Total Organic Carbon (TOC) analyzer (Model 800T, Boulder, CO) has been used to measure the water-soluble organic components of the ambient aerosol. This instrument will be referred to here as a PILS-WSOC.

For carbon analysis, the Sievers TOC uses a combination of 25% ammonium persulfate solution (flow rate = 0.75 μl min^{-1}) and ultraviolet light (λ = 254nm and 184nm) to oxidize the dissolved organics in the liquid sample to CO_2. The sample is acidified by adding 6M phosphoric acid (pH typically < 2). The sample is split into two equal flows.

One sample passes through a delay coil and into the CO_2 detection sensor which measures the concentration of total inorganic carbon (TIC). The second sample passes through an ultraviolet light oxidation reactor, which photochemically oxidizes the organic compounds to form CO_2. The sample is then pumped through a second CO_2 sensor which detects total carbon in the sample (TC). The CO_2 is isolated through a selective membrane into a high-purity water loop and is quantified by conductometric detection [*Carlson*, 1980]. Thus, total organic carbon (TOC) is determined by difference between the two measurements (e.g. TC-TIC = TOC). The Sievers TOC analyzer can be operated in either a 3-sec or 6-minute sample integration mode.

During PILS-WSOC operation, ambient aerosol sample is periodically diverted through a Teflon filter by an inline computer-actuated valve. This removes entrained aerosol and allows for an assessment of any background concentration of organic material. Possible sources of background interferences include semi-volatile organic carbon (SVOC) penetration through the denuder, or contamination of the ultra purified water used in the analysis. A background concentration is linearly interpolated between consecutive background measurements and is subtracted from the dataset. Further discussion of the specific operational techniques, including a discussion of possible background artifacts, can be found in Sullivan, et al [2004]. From previous studies, the PILS-WSOC uncertainty is estimated at 8% and a limit of detection of 0.1 μg Carbon m^{-3} (μgC m^{-3}). The instrument package is relatively small and is simple to operate, needing only a purified water source for daily maintenance and is reasonably inexpensive to purchase.

A consequence of using an impaction plate to collect droplets is that while not likely having an effect on soluble compounds, insoluble compounds may adhere to the surface and not be efficiently transferred to the liquid stream. In ambient urban samples, the impactor visibly darkens over time due to the adhesion of elemental carbon. It is reasonable to expect some fraction of insoluble organic carbon to also adhere to the impactor. The inline 0.22 μm liquid filter also inhibits measurements of insoluble organic particulates. Recent data from a ground site in Atlanta GA, and St. Louis, MO shows that typically the WSOC fraction of OC is 40-80% [*Sullivan and Weber*, 2006a; *Sullivan, et al.*, 2004], with the remaining fraction likely being the insoluble fraction. During short events, when local fresh emissions dominate, WSOC/OC the fraction can be considerably lower.

Attempts have already been made to measure total OC semi-continuously with a technique that in principle is similar to the PILS. Like the PILS, the steam-jet aerosol collector (SJAC) [*Khlystov, et al.*, 1995] was originally designed for inorganic aerosol measurement. After mixing aerosol with a supersaturated water vapor, particles are grown in size and collected. Rather than using an impactor to collect particles, two cyclones are used in series to achieve a sampling collection efficiency to greater than 99%. Coupled to a Total Organic Carbon analyzer, Even et al [2000] tested the SJAC performance with various soluble and insoluble organic aerosols, however, the instrument was never field tested. Their results are further discussed in this paper.

2.6.2 The Sunset Labs ECOC Analyzer

Thermal optical transmittance (TOT) is similar to TOR, except that in this case transmission of a laser beam through the filter is used to monitor concentrations of light absorbing material on the filter. The OC-EC split is defined as the point when laser transmittance returns to baseline [*Birch*, 1998]. This is used by the Sunset Labs TOT analyzer (Model 3, Sunset Labs, Forest Grove, OR), and is the basis for the National Institute of Occupational Safety and Health method 5040 [*NIOSH*, 1996].

The TOT and TOR methods previously described are generally used for offline analysis of filter samples. In general, the two methods agree, although some research has shown EC concentrations can be significantly higher using the TOR technique with lower oven temperatures [*Chow, et al.*, 2004; *Chow, et al.*, 2001]. Offline filter-based measurements of OC (which are quantified by TOR or TOT) can be limited by their lengthy sample integration time, which limits their utility when sampling from aircraft or when investigating short, transient events during ground-based studies. In contrast, online systems can provide quantitative, fast time resolution OC and EC concentrations. These systems are also typically automated and require less user handling of samples decreasing potential sample contamination and analysis cost. Sunset Labs semi-continuous ECOC instrument (Model 3F, Sunset Labs, Forest Grove, OR) is one such method, and is similar to the offline TOT analyzer, with a few exceptions. The instrument is configured with an internal filter that captures aerosol and then oxidizes and detects OC and EC using similar temperature and carrier gas profiles as the offline TOT method. Though it uses a transmittance-based pyrolysis correction, the online system uses a non-dispersed infrared

detection (NDIR) system for quantification of CO_2 (carbon dioxide). This instrument is used extensively throughout this work and is taken as the standard for comparison with the PILS-based OC measuring technique.

A Sunset Labs ECOC analyzer (Model 3F, Forest Grove, OR) was used for comparison in this study. Following NIOSH method 5040 [*Birch*, 1998; *NIOSH*, 1996], this instrument semi-continuously quantifies organic carbon that is deposited on an internal filter. The sample is denuded of volatile gases by an inline parallel plate carbon denuder [*Eatough, et al.*, 1993]. The Sunset Labs ECOC analyzer is not equipped for automated blank measurement and correction. In recent work from St Louis, MO, Bae, et al [2004] estimated the Sunset Labs blank concentration of organic carbon at ~0.94 ± 0.02 $\mu gC\ m^{-3}$ by comparing two online systems with a 24-hour integrated filter. To account for any possible positive sampling artifacts Lim et al [2003] used two Sunset Lab ECOC instruments in parallel configuration, simultaneously measuring ambient aerosol and a Teflon-filtered sample that collected SVOC only. The ambient carbonaceous particulate fraction is calculated from the difference. With this method, they report a limit of detection (LOD) of 0.3 $\mu gC\ m^{-3}$ for a one-hour integrated measurement. Takegawa et al [2005] empirically determined for an instrument with no blank correction an LOD of approximately 1.0 $\mu gC\ m^{-3}$ by comparison with an Aerosol Mass Spectrometer (Aerodyne Research, Billerica, MA). Using the commercially-available instrument in this study, we assume an instrument LOD of 0.5 $\mu gC\ m^{-3}$. The instrument was configured to collect sample for 45 minutes. Thus, higher time resolution organic carbon data from the PILS technique was averaged to this interval. Most research examining OC

measurement technique uncertainty has focused on the offline method of TOT and TOR analysis [*Bae, et al.*, 2004; *Huebert, et al.*, 2004a; *Lim, et al.*, 2003; *Schauer, et al.*, 2003; *Turpin, et al.*, 1990; *Turpin, et al.*, 1994; *Turpin, et al.*, 2000]. Offline TOT method analyzer uncertainty is typically in the range of 5-20% (depending on OC concentration, with higher uncertainty at lower concentrations). Huebert et al [2004a] estimate combined uncertainty (due to flow rates, sample handling, and analyzer) at 26%. Uncertainty in the Sunset Labs online instrument has not been clearly defined by the literature. For this work, we estimate overall uncertainty in the online version of the Sunset Labs OC analyzer to be ±20%.

This paper will discuss some of the key design changes made to the PILS-WSOC for OC measurement, compare instrument performance when measuring calibration aerosol generated under controlled conditions, as well as discuss comparison with the Sunset OCEC measurement from two urban deployments.

2.6.3 Instrument Design

Construction of a mini-cyclone

To improve transfer of insoluble OC to sample liquid, the PILS impactor was replaced with a mini cyclone constructed of polycarbonate with internal dimensions of approximately 23 mm total internal height, 8mm maximum width that tapers to ~2 mm diameter over 15 mm (see figure 2.2), following the design criteria of Gussman et al

[2002] and Kenny et al [2000]. Vacuum flow is achieved by way of a 1/8" OD stainless steel tube that is inserted through the top of the cyclone, connected to a

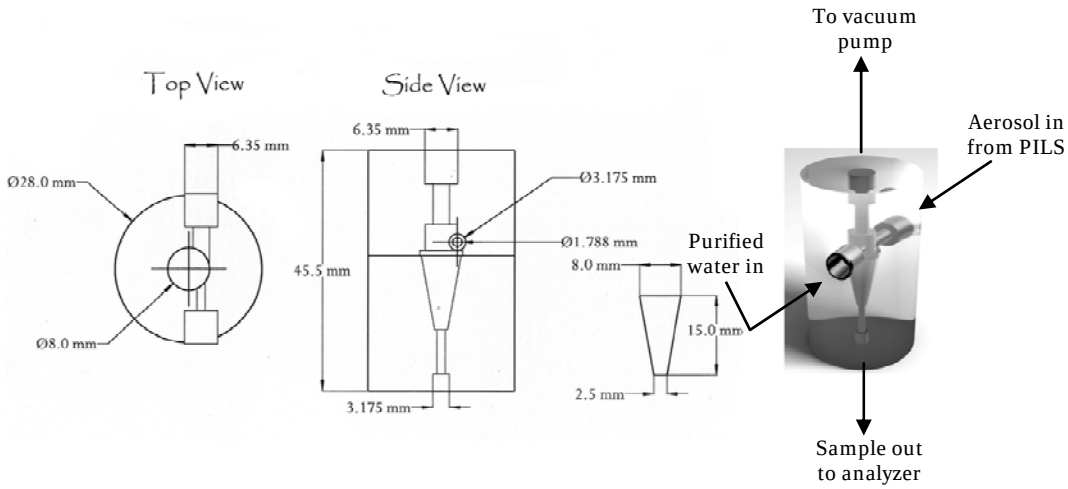

Figure 2.2. Computer Aided Diagram and rendered image of a mini cyclone attachment for the Particle Into Liquid Sampler.

critical orifice of known diameter, and then to a vacuum pump. To collect aerosol droplets, a ¼" OD (1/8" ID) stainless steel tube was press fit into the end of the standard PILS impactor nozzle, and inserted into the mini cyclone tangent to the internal wall, as shown in figure 2.2. The nozzle opening is located directly across from a small port that continually delivers 0.6 ml min^{-1} of purified liquid water into the cyclone. The liquid flow rate is the same as the transport flow of water introduced at the top of the impaction plate in the traditionally configured PILS [*Sullivan, et al.*, 2006]. This liquid creates a small, continuous ribbon of purified water and entrained aerosol as it descends the inner wall of the cyclone until reaching the bottom, where water and particles are extracted and transported to the analyzer via syringe pumps. The inline liquid filter normally present on a PILS-WSOC instrument is removed and liquid sample lines are shortened to

minimize any OC loss to the tubing wall during transport to the detector. Loss of insoluble particles is quantified in the next section. The advantage to this method is that aerosol is not impacted directly onto a plate and is less likely to adhere to the surface. This modified instrument is referred to as a PILS-OC.

2.6.4 Laboratory Calibrations

Carbonaceous aerosol was generated using an atomizer and compressed nitrogen. Approximately 0.02 grams carbon of various organic compounds (see Table 4.1) were added to 200 ml of purified water, making a ~0.1% carbon solution. Following the nebulizer, water was removed from the aerosol via silica diffusion driers and aerosol neutralized by a polonium 210 ionization source. The dried and neutralized particles were then diluted in a 4 liter glass jar with room air, which had been filtered using a High-Efficiency Particulate Air filter and denuded by an activated carbon parallel-plate denuder [*Eatough, et al.*, 1993]. The diluted aerosol was passed through a second parallel plate carbon denuder to remove any residual organic vapors. An inline, non-rotating MOUDI impactor [*Marple, et al.*, 1991] restricted particle size to less than 1.0 μm (except in the case of 1.96μm polystyrene latex aerosol, when no impactor was inline.) Finally, the sample flow was split to the PILS and Sunset Labs instrument. After the split, flow tubing material, diameter, and length were nearly identical. This resulted in aerosol concentrations delivered to each instrument of approximately 10-20 μg C m^{-3}.

2.6.5 Assessment of Mini-Cyclone Collection Efficiency

In order to assess cyclone collection efficiency, a comparative analysis between the cyclone (PILS-OC), impactor (PILS-WSOC), and Sunset Labs ECOC measurements were conducted. Laboratory-generated, polydispersed oxalate aerosol was simultaneous delivered to each instrument. Oxalate was chosen because it is highly soluble and has a relatively low vapor pressure [*CRC*, 2005]. This minimizes the risk of loss by volatilization in either system, and ensures that the PILS systems (which use liquid water to transport dissolved aerosol) is able to quantify the sample. Both results were compared with the Sunset Labs OCEC analyzer.

The ratio of OC determined by PILS-WSOC and Sunset Labs is investigated first. The experiment was repeated six times. By measuring polydispersed oxalate aerosol, the ratio of OC determined by PILS-WSOC compared to the Sunset Labs ECOC technique was 93.5% ± 1.2% (mean ± 1σ). PILS-WSOC has an instrument uncertainty of 8% [*Sullivan, et al.*, 2006], suggesting that this difference from unity is not significant.

The PILS impactor was replaced with a mini cyclone and the experiment was repeated. The ratio of oxalate aerosol concentration determined by PILS-OC (e.g. with mini cyclone) compared with the concentration determined by Sunset Labs ECOC was 69.3% ± 1.7% (1σ) which is significantly lower than the PILS-WSOC/Sunset Labs ratio. The comparison was repeated 8 times. Since the instrument configuration for each experiment was identical (with the exception of using a mini cyclone instead of the impactor on the PILS), this difference is most likely due to a lower collection efficiency

for the mini cyclone. Because the cyclone system has a collection efficiency of 69.3% ± 1.7% (1σ) compared to the Sunset Labs method, this factor has been applied to the data throughout the remainder of the results. Since the PILS-OC method is similar to the PILS-WSOC method (with the exception of using a mini cyclone for droplet collection), combined uncertainty (e.g. uncertainty associated with the PILS-WSOC plus the standard deviation of the collection efficiency) of the PILS-OC instrument is estimated to be similar to PILS-WSOC at ±10%.

2.6.6 Tests with Calibration Aerosol

A variety of organic carbon aerosol was generated from single standard solutions and sampled using the PILS with mini cyclone and TOC detection. It is not possible to test the full range of ambient organic aerosols due to the myriad of organic compounds that have been observed. Therefore, several selected organic compounds that varied in molecular weight, vapor pressure, and solubility in water were tested. These compounds were chosen based partly on those described by Saxena and Hildemann [1996] and are listed in Table 2.1.

Table 2.1: Summary of compounds tested for technique comparison. The table also includes molecular formula, vapor pressure of compound, and solubility in water.

	Molecular Formula	Vapor pressure (mmHg at 20° C)[†]	Solubility (g/L at 20° C)
Organics:			
Oxalate	$C_2H_2O_4$	$1x10^{-3}$	12
4-nitrophenol	$C_6H_5NO_3$	$2.4x10^{-5}$	1.7
Phthalic Acid	$C_8H_6O_4$	$6x10^{-3}$	0.43
Humic Acid	n/a[‡]	n/a[‡]	Miscible
Benzoic Acid	$C_7H_6O_2$	$7.5x10^{-4}$	3.4
Other:			
Monodispersed PSL	$[CH_2CH(C_6H_5)]_n$	very low	Insoluble
Elemental carbon[a]	C	Very low	Insoluble
DI water blank	H_2O	24	n/a

[†] Vapor pressure at 25° C; [‡] Humic acid is a bulk carbonaceous material that is involved in many processes involving soil and natural water. It is considered to be water-soluble and have a low vapor pressure. A specific molecular formula is not available. For additional information, consult the International Humic Substances Society at http://www.ihss.gatech.edu.; [a] Elemental carbon as Carbon Black, Alfa Aesar, Stock #39724

The fraction of aerosol measured by PILS-OC compared with Sunset Labs is shown in Figure 2.3 for the detected compounds. Oxalate, phthalic acid, and humic acid aerosol compared well, with agreement between the two instruments exceeding 95%. Benzoic acid and 4-nitrophenol aerosol was somewhat lower; PILS-OC typically measured ~78% of the mass when compared to Sunset Labs, though the error bars (Fig 2.3) span 100%. Elemental carbon (EC) was also not detected by the Sievers analyzer. Elemental carbon calibration aerosol was, however, detected by the Sunset Labs analyzer in the form of EC implying that EC aerosol was successfully delivered to the instruments. Error bars are plotted for each compound and are calculated as the sum of squares of repeated

measurement standard deviation, and estimated instrument uncertainty in the PILS-OC and Sunset Labs analyzer.

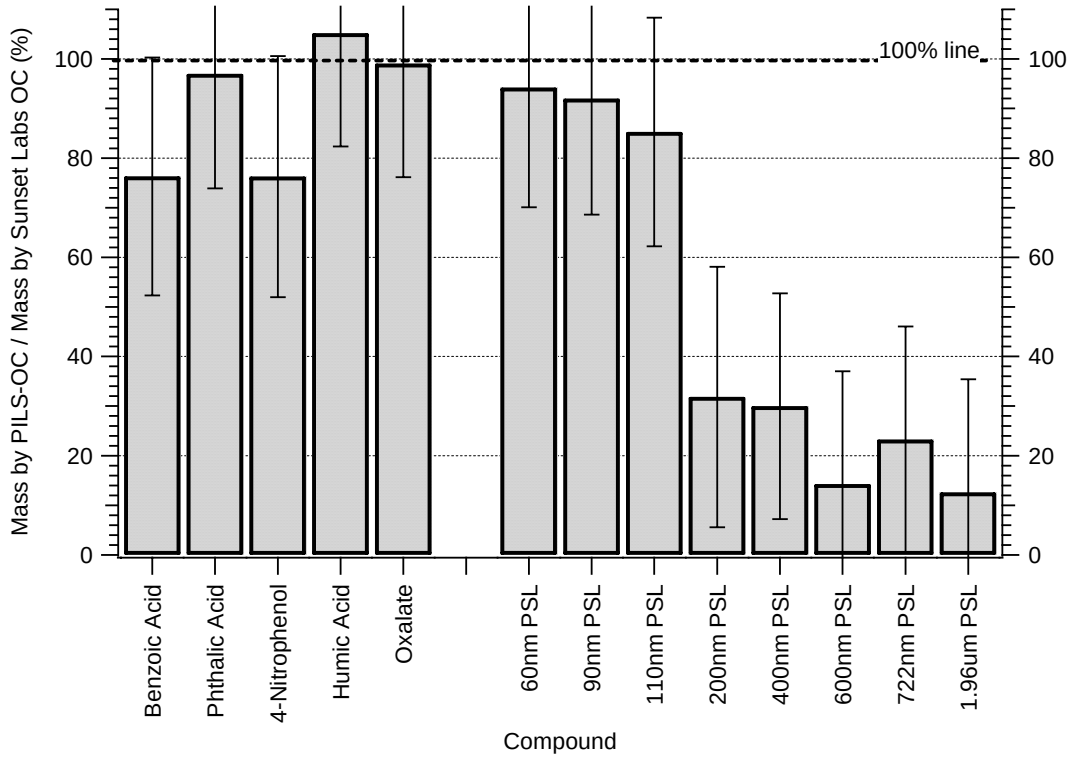

Figure 2.3 Recovery fractions of various aerosols by PILS-OC when compared to Sunset Labs OC method. Water-soluble compounds are on the left side of figure, while insoluble compounds are on the right side of the figure. Error bars are quadratic sum of squares of propagated error including standard deviations of at least 8 repeated measurements and instrument uncertainty.

Similar findings were reported by Even et al [2000], who tested a variety of organic compound standards in solution (i.e. not generated as aerosol) by measuring with a Shimadzu TOC analyzer and Sievers TOC analyzer. The Shimadzu analyzer is a combustion-based catalytic oxidation method that efficiently quantifies all carbonaceous material in a liquid sample regardless of its solubility. Even, et al. tested benzoic acid

and humic acid standards which were equally measured by both the Sievers TOC analyzer and the Shimadzu analyzer (recovery = ~100%). Black carbon was also tested, and was not efficiently recovered (~0%) by the Sievers analyzer, but was detected by the Shimadzu.

2.6.7 Insoluble Calibration Aerosol

To test completely insoluble particles, monodispersed polystyrene latex (PSL) spheres (for all sizes: 10% w/w, Duke Scientific, Palo Alto, CA) were generated in the lab using the technique previously described and used to compare measurements of purely insoluble aerosol. For the tested PSL sizes, an apparent size dependence was observed – as particle size increases, the comparison between PILS-OC and Sunset Labs decreases, as shown in figure 2.3. When compared to Sunset Labs, PILS-OC effectively measures insoluble particles that are less than ~110 nm in diameter. For 200nm monodispersed PSL, PILS-OC measures approximately 31% of the mass that Sunset Labs OCEC detects. This is likely a result of the TOC analyzer's inability to adequately oxidize and detect large, insoluble organic particles. 90nm and 200nm PSL spheres in solution were also tested by Even et al. [2000]. As compared to the Shimadzu analyzer, the 90 nm spheres were well recovered (~100%), and the 200 nm spheres where poorly recovered (~25%) by the Sievers analyzer, similar to our results. Note that while trace concentrations of water-soluble organic surfactants were present in all PSL solutions, they are likely insignificant when compared to the carbon mass derived from PSL spheres. For example, no carbonaceous material (from PSL or from surfactants) was detected by PILS-OC when testing 1.96μm PSL (Fig. 2.3).

The inability of the TOC analyzer to quantify solid insoluble particles larger than ~0.11 μm may be of little consequence when measuring ambient aerosols under most conditions. Purely insoluble organic aerosol typically originates from fresh combustion processes, and has been shown to be generally less than 150nm in size [*Kleeman, et al.*, 2000] (e.g. most insoluble material is likely to be oxidized and detected). Particle growth processes, such as heterogeneous nucleation or coalescing, can produce bulk particles with sizes larger than those that can be detected by this instrument if they were completely insoluble. However, the PILS-OC collection method reduces the size of aerosol by dissolving most of the soluble components within an internally-mixed aerosol leaving the remaining insoluble core. Before sampling, additional photochemical and oxidative chemistry can oxidize the insoluble core, which further increases the solubility of the particulate [*Saxena and Hildemann*, 1996; *Turpin and Lim*, 2001]. Insoluble vegetative detritus, however, can be significant larger than ~0.11 μm and so is likely not measured by this technique.

Increasing the Sievers TOC oxidizer flow rate had little effect on the instrument's measurement efficiency for insoluble particles larger than 200nm. Doubling the oxidizer flow rate to 1.5 μl min^{-1} had less than 5% improvement when measuring 200nm PSL aerosol. Compared to Sunset Labs, this corresponds to PILS-OC measuring just ~35% of the mass of 200nm PSL. Oxidizer flow rates can not be further increased because gas bubbles form within the analyzer's liquid flow system causing erroneous carbon mass concentrations.

To quantify large insoluble OC, a combustion-based analytical technique, such as the Shimadzu TOC-Vcs (Shimadzu Scientific Instruments, Columbia, MD) could be coupled with the PILS instead of the liquid-based oxidation system of the Sievers TOC. Although the Shimadzu is significantly larger and more expensive, it is capable of on line analysis with 3-4 minute sample integration times.

2.6.8 Loss to Sample Tubing and TOC Oxidizer Flow Rate

Replacing the impactor with a cyclone to capture the large droplets formed in the PILS appeared to improve collection of insoluble particles. The penetration of insoluble particles suspended in liquid while transported from the cyclone to detector was also tested. In order to assess particle loss within the liquid sample transport tubing, various lengths of polyetheretherketone (PEEK) tubing were used to connect the mini cyclone with the syringes used to pump the sample. 110nm PSL aerosol was generated and sampled by PILS-OC using various tubing lengths of internal diameter 0.02 inches. The longest length tested, 75 cm, resulted in an apparent loss of ~6% of PSL aerosol (compared to Sunset Labs measurement). No detectable loss of large, insoluble particles was observed when tubing length was less than 30 cm. Under normal operating conditions, tubing length is generally less than 15 cm. During this study, the length of tubing from the syringes to the TOC analyzer sample inlet was approximately 13 centimeters.

2.6.9 Ambient Studies

Ambient comparison studies were conducted during field studies in Atlanta GA and Riverside CA to investigate the capabilities of the PILS-OC for measuring urban emissions.

2.6.9.1 Atlanta, Georgia

A PILS-WSOC (e.g. water soluble organic carbon system) and a Sunset Labs ECOC analyzer were co-located at a sampling site in Atlanta, Georgia from 17 Apr-13 Sep 2004. The sampling site is located within 400 m of a major highway and may be subjected to relatively fresh - and therefore less soluble – highway (mainly non-diesel) emissions. Heavy duty truck traffic (e.g. diesel powered) is not permitted on the highway so emissions are mainly from gasoline vehicles. Atlanta has been shown to have significant sources of both biogenic and anthropogenic aerosol, with a significant fraction of secondary organic aerosol [*Lim and Turpin*, 2002; *Sullivan and Weber*, 2006a; *Weber, et al.*, 2007]. Since secondary organic aerosols tend to be water soluble [*Kondo, et al.*, 2007], this fraction of organic aerosol can be detected by PILS-WSOC in Atlanta. Median carbon monoxide (CO) concentration in Atlanta during the comparison period was 0.5 ppmv. Figure 2.4 compares PILS-WSOC measurement of WSOC with Sunset Labs measurement of OC during this period. From the regression slope, WSOC measured by PILS-WSOC (e.g. use of impaction plate) measured approximately 72% ± 1% (1σ) of the organic carbon mass determined by the Sunset Labs instrument. Combined measurement uncertainty for both instruments (10% PILS and 20% Sunset Labs), shown as error bars in Figure 3, does not account for this difference from unity,

thus, the remaining ~28% is likely the insoluble fraction of OC that is not quantified by the PILS-WSOC.

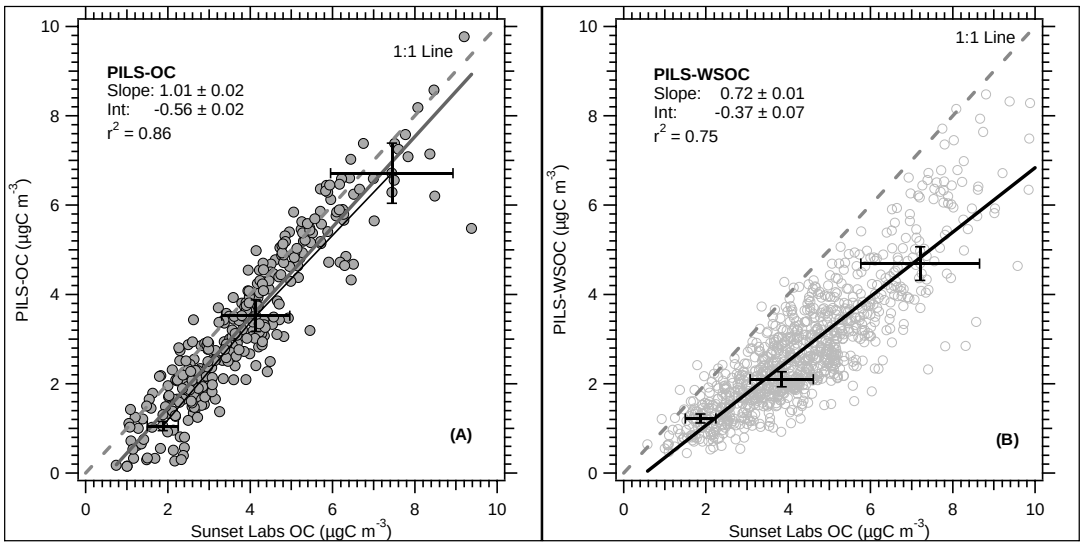

Figure 2.4 PILS-OC (A) and PILS-WSOC (B) measurement of ambient organic carbon compared with Sunset Labs measured in Atlanta, Georgia. PILS-OC measurements are from 09 May-06 Jun, 2005. PILS-WSOC measurements are from 17 Apr - 13 Sep, 2004. PILS measurements are averaged to 45 minute integral of Sunset Labs OC measurement. Slope, intercept, and r^2 are calculated from univariate linear regression. Error bars are uncertainty associated with instrument.

In contrast, a PILS-OC (e.g. with mini cyclone in place of the impactor) was deployed in the same location from 09 May-06 Jun, 2005 using the same inlet and sampling configuration. By univariate linear regression, the PILS-OC measured ~101% (± 2%, 1σ) of the organic carbon compared to Sunset Labs measurement of organic carbon (Figure 2.4), a significant enhancement over PILS-WSOC. Considering the measurement uncertainty (included in Fig 3), the regression slope for PILS-OC is statistically indistinguishable from unity. PILS-OC also has a higher correlation coefficient (r^2 = 0.87) with the Sunset Labs measurement, suggesting that the variability in organic carbon concentration is well captured by the PILS-OC instrument. For both PILS-WSOC and

PILS-OC comparisons, a small but significant intercept was observed (Fig 2.4). This intercept is discussed in detail in Section 2.6.10.

In order to possibly examine different aerosol sources, the comparison of PILS-OC and Sunset Labs organic carbon in Atlanta was categorized as rush-hour or non-rush-hour samples (Figure 2.5). Rush hour samples are comprised of a higher fraction of mobile sources, and due to the proximity of the nearby highway, are more likely to be freshly emitted than non-rush hour samples. For example, during this experiment, the median elemental carbon concentrations for both rush hour and non-rush hour periods were similar at 1.0 $\mu gC\ m^{-3}$, however, rush hour periods were observed to have higher variability in concentration ($1\sigma = 0.9\ \mu gC\ m^{-3}$ for rush hour samples, and $1\sigma = 0.5\ \mu gC\ m^{-3}$ for non-rush hour samples). Short spikes of EC were usually observed during rush hour periods, with concentrations exceeding 2-3 $\mu gC\ m^{-3}$. If the insoluble organic aerosol associated with mobile source emissions went unmeasured, this would result in a change of regression slope. However, no significant difference is observed in regression slopes or intercepts between the data sets. The intercept in both rush hour and non-rush hour samples are statistically identical (Fig 2.5), where the Sunset Labs measures $\sim 0.5 \pm 0.1\ \mu gC\ m^{-3}$ when the PILS-OC measures zero.

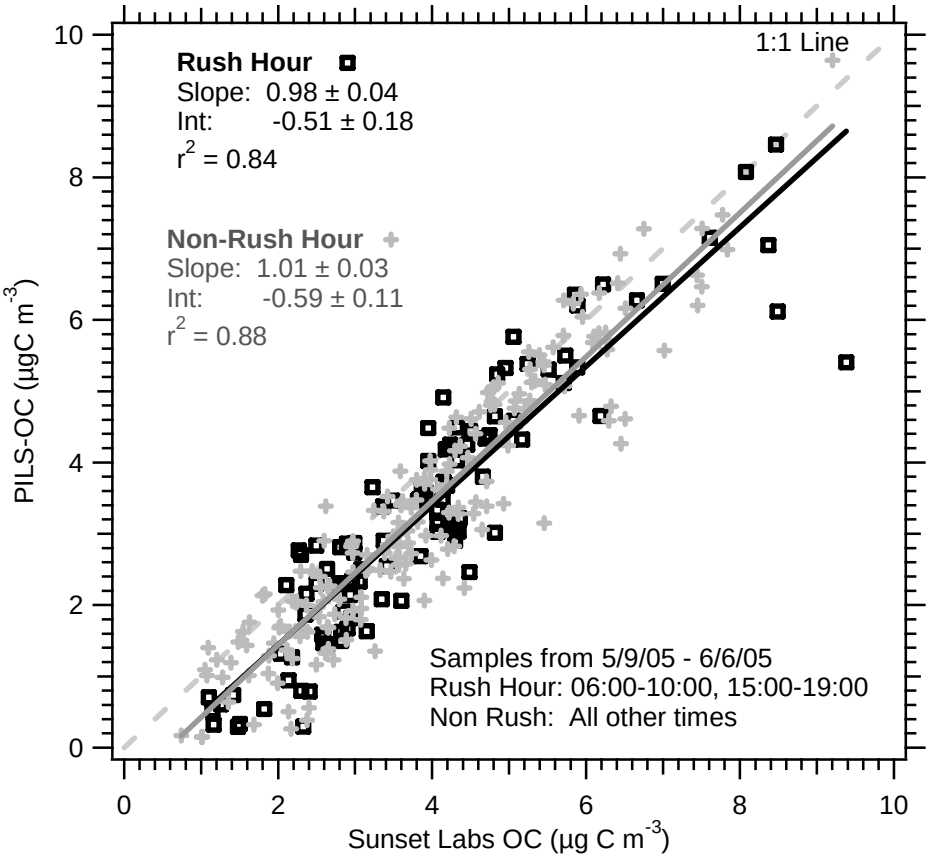

Figure 2.5 Linear correlated between PILS-OC and Sunset Labs OC in Atlanta (09 May -06 Jun, 2006), separated by rush hour and non-rush hour data.

2.6.9.2 Riverside, California

An additional field deployment was conducted in Riverside, California as part of the Study of Organic Aerosols at Riverside (SOAR) field campaign. Conducted on the campus of the University of California/Riverside from 18 July to 15 August, 2005, the sampling location was located approximately 600 meters from a major highway leading into Los Angeles, California. Organic aerosol in this region is thought to be largely primary emissions from condensed organic vapors from mobile sources [*Hughes, et al.*, 2000; *Pang, et al.*, 2002; *Sardar, et al.*, 2005a; *Sardar, et al.*, 2005b], including mobile

sources from the nearby highway, as well as those transported from the Los Angeles basin along with secondary OC formed during transport. Elemental carbon, a tracer for mobile source emissions, had distinct peaks during rush hours and often exceeded 3-4 $\mu gC\ m^{-3}$ providing evidence that a significant fraction of sampling was from mobile source emissions. Median ($\pm 1\sigma$) morning rush hour elemental carbon concentrations were $1.5 \pm 0.95\ \mu gC\ m^{-3}$. A PILS-WSOC system and a Sunset Labs ECOC analyzer were co-located at the sampling site.

Figure 2.6 shows a comparison between PILS and Sunset Labs organic carbon measurements in Riverside. By univariate linear regression fit, PILS-WSOC (e.g. impactor) measured approximately $52\% \pm 2\%$ (1σ) of carbonaceous material as compared to Sunset Labs method. This is lower than the percentage observed in Atlanta by PILS-WSOC and is consistent with a higher fraction of organic aerosol being from insoluble primary emissions. During the Riverside field campaign, median CO concentration was 0.65 ppmv which is ~30% higher than Atlanta during PILS-OC test period in 2004. A larger fraction of insoluble organics were likely present in Riverside due to its proximity to the large highway and significant mobile source emissions from the Los Angeles, CA basin (i.e. higher fraction of primary emissions).

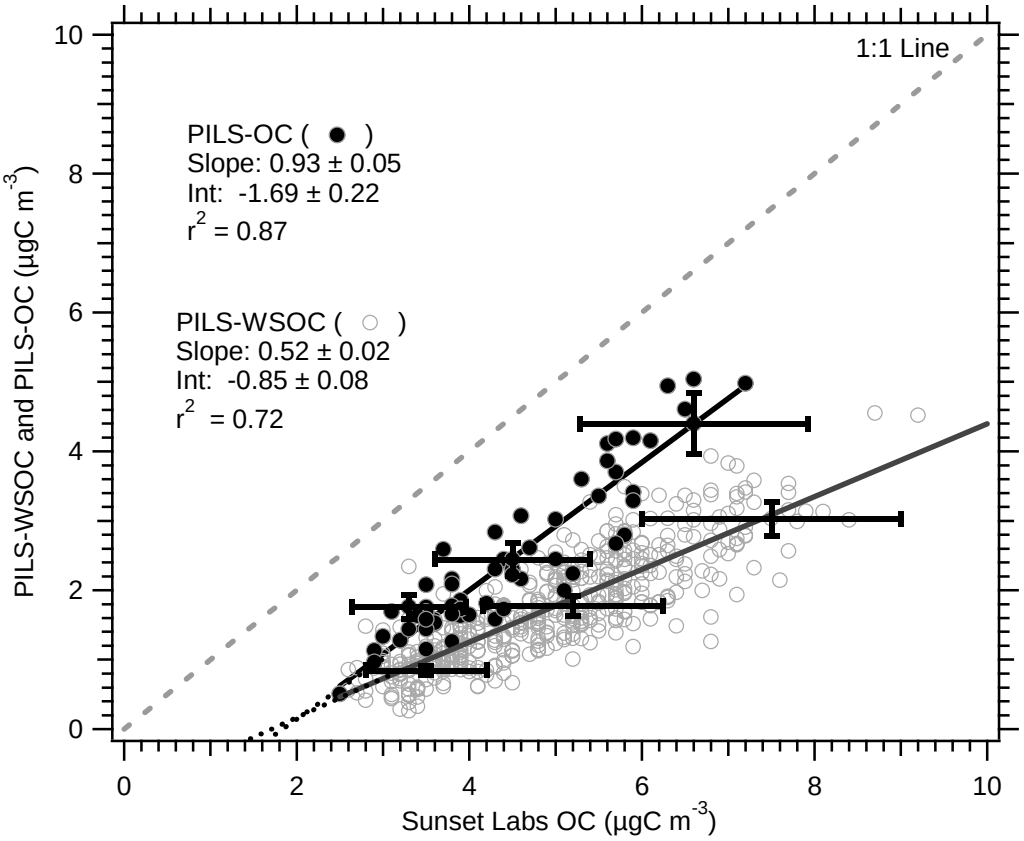

Figure 2.6 Comparisons between PILS-OC and Sunset Labs and PILS-WSOC and Sunset Labs in Riverside, California. PILS-OC measurements from 27 Jul – 30 Jul, 2005, and PILS-WSOC measurements are from 22 Jul – 27 Jul and 31 Jul – 09 Aug, 2005. Lines through data are univariate regression least-squares fit, and have been extended to the intercept (dashed lines). Error bars are uncertainty associated with instrument.

The PILS-WSOC impactor was replaced with a mini cyclone for approximately three days (27 Jul to 30 Jul) near the middle of the measurement campaign, and a comparison with Sunset Labs is also provided in Figure 2.6. By univariate linear regression slope, PILS-OC technique measured ~93% ± 5% of the Sunset Labs OC mass, representing an enhancement over the PILS-WSOC method (though slightly less than the slope observed in Atlanta). The correlation coefficient was high with $r^2 = 0.87$.

As observed in Atlanta, there was significant intercept (Figure 2.6) when PILS-OC is compared to Sunset Labs OC. By extrapolation, Sunset Labs tended to report approximately ~1.7 μgC m^{-3} when PILS-OC detected ~0 μgC m^{-3}. Uncertainty associated with each measurement (error bars, Fig. 5) does not explain this intercept. This is discussed further in Section 2.6.10.

2.6.10 OC Regression Intercept

The significant intercept detected when comparing the PILS-OC technique with a measurement of OC by Sunset Labs could be caused by a combination of potential biases. Interestingly, the intercept is higher in the urban region with higher primary emissions (CO or EC) and higher fractions of insoluble (hence primary) particles. Sampling a significant fraction of large (e.g. > 110nm) insoluble carbon particles, which are not detected by the PILS-OC method, would result in lower reported OC concentrations by PILS-OC, consistent with the observed intercept. It is also possible there was a positive artifact caused by penetration of SVOCs through the denuder in the Sunset Labs system that were absorbed by the filter and then detected by the analyzer as OC. For the OCEC data presented here, instruments blanks were not performed. It is noteworthy that the intercept in the Atlanta study (0.56 μgC/m^3) is similar to the typical blank values reported in St Louis (0.90 ± 0.02 μg m^{-3}, Bae, et al [2004]. (Note that Atlanta and St. Louis emissions are more similar than Los Angeles versus St Louis). To further investigate possible causes for the intercepts, the Sunset Labs measurements of OC were compared with an online measurement of aerosol mass.

In Atlanta, $PM_{2.5}$ mass was measured by the State of Georgia Environmental Protection Division (GAEPD) with a Tapered Element Oscillating Microbalance (TEOM, model 1400ab, Thermo-Electron) located approximately 15km to the southeast of our PILS-OC and Sunset Labs ECOC instruments. The GAEPD TEOM operates with a case temperature of 30 degrees C, and utilizes a Nafion drier system to remove water vapor from the sample (resulting RH = ~15%). It is noted that this configuration may result in some loss of semi-volatile compounds.

For data collected throughout the summer of 2004, a regression intercept of 2.0 ± 0.04 $\mu gC\ m^{-3}$ (r^2 =0.58) was observed when comparing a Sunset Labs OC measurement with the GAEPD TEOM (not plotted, i.e., ~2 $\mu gC\ m^{-3}$ of OC at zero mass). In May 2005 (the period of PILS-OC and Sunset OC comparison), the Sunset Labs instrument had an intercept of 1.4 ± 0.12 $\mu gC\ m^{-3}$ (r^2 = 0.66) compared to the TEOM. In contrast, the PILS-OC, when compared to the TEOM during this same period in May, had an intercept of 0.17 ± 0.11 $\mu gC\ m^{-3}$. Furthermore, the PILS-WSOC (e.g. water-soluble fraction of OC) had an intercept of 0.66 ± 0.06 $\mu gC\ m^{-3}$ when compared to the TEOM during summer 2004, which is a factor of three times lower than Sunset Labs during the same time period (when the OC intercept was 2.0 $\mu gC\ m^{-3}$). Since the instruments were not collocated (and thus at times possibly not sampling identical sources), there is some scatter throughout the data. These results suggest that the Sunset Labs - TEOM intercept might be caused by two possibilities: there may be substantial volatilization of aerosol within the TEOM that results in decreased observed aerosol mass. However, this also requires a significant and nearly equal amount of undetected OC by the PILS-OC since

this system was more consistent with TEOM with the intercept closer to 0 μgC m^{-3}. Or, there was a positive artifact associated with the Sunset Labs OC measurement caused by SVOC penetration through the denuder, and unlike the PILS-OC had no instrument blank correction. Although a combination of these various factors is possible, however, both PILS-OC and TEOM comparisons to Sunset Labs OC are consistent with a significant Sunset OC blank.

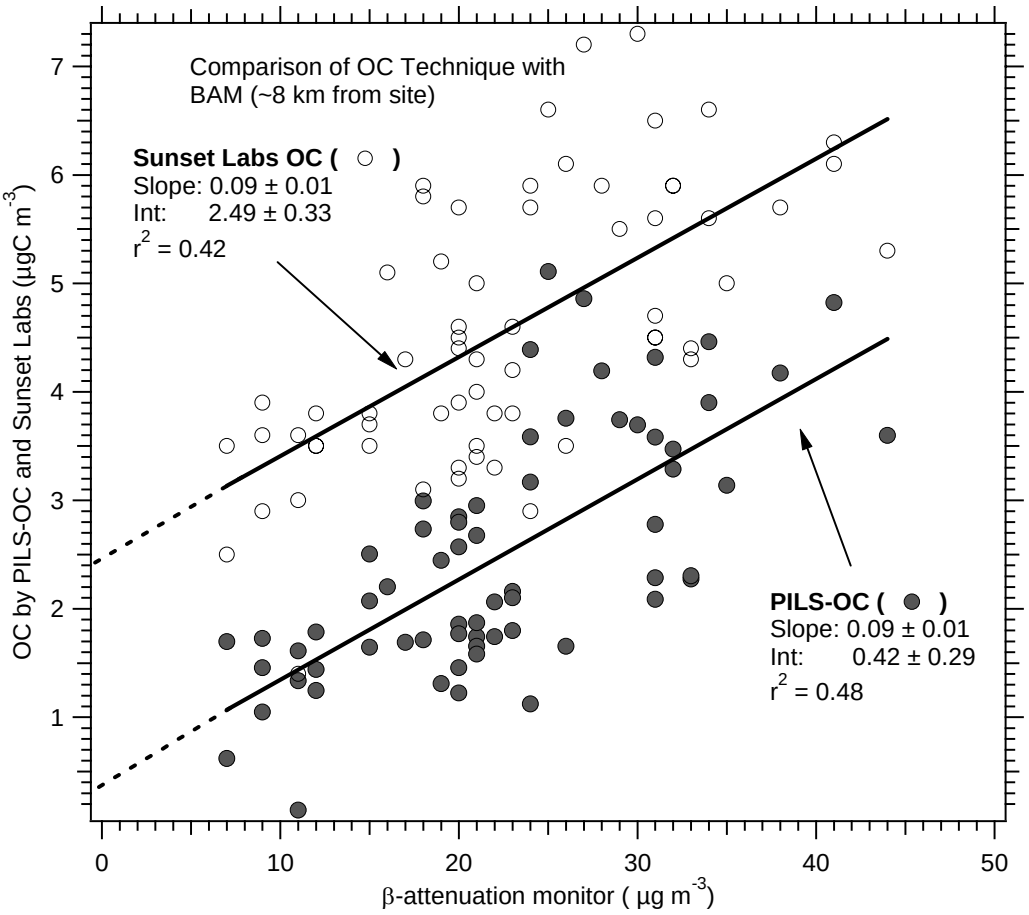

Figure 2.7 PILS-OC and Sunset Labs measurements of organic carbon compared to a beta attenuation monitor in Riverside, California. Sample period was 27 Jul – 30 Jul, 2005.

Similar to the analysis in Atlanta, the Riverside Sunset Labs and PILS-OC measurements were compared with a PM2.5 mass measurement, in this case a beta attenuation monitor (BAM-1020, Met-One, Grants Pass, OR) operated by the California Air Resources Board during the co-sampling period (28Jul-30Jul, 2005). The BAM site was located at Rubidoux-Riverside, CA, ~8 km from the Riverside OC sampling site. When the BAM sample relative humidity exceeded 55%, the sample was heated to ~3 degrees above ambient temperature to avoid condensed water on the filter tape. With slight heating, it is possible for semi-volatile particle loss. By linear regression, the Riverside Sunset Labs OC measurement had an intercept of 2.49 ± 0.33 μgC m^{-3} compared to the BAM measurement, as shown in Figure 2.7. In contrast, the intercept is ~0.4 ± 0.3 μgC m^{-3} in the PILS-OC measurement. Like the Atlanta study, the instruments were not collocated and in this case there is significant scatter throughout the data (r^2 = 0.42). However, the results are consistent with the Atlanta comparison; Sunset Labs intercept is significantly larger than that of the PILS-OC, despite similar regression slopes and r statistics. Similar trends have also been observed in other studies. Although not plotted, a linear regression between a Sunset Labs analyzer (with activated carbon denuder) and a co-located TEOM (inlet heated to 35 degrees C and utilizing a Nafion drier) at a site ~20 km to the north-northeast of Mexico City had an intercept of 3.62 ± 0.16 μgC m^{-3} (r^2 =0.40).

It is not possible with this data to conclusively specify what caused the intercept between Sunset Labs and bulk aerosol mass; positive Sunset OC artifact or negative artifact from in the PM measurement. Some studies suggest online mass measurements with the TEOM are subject to substantial loss of semi-volatile mass [*Wilson, et al.*, 2006], and

other studies show positive artifacts associated with the online Sunset Labs OC measurement [*Bae, et al.*, 2004]. However, our results are more consistent with a positive OC artifact, since in comparison to mass measurements, the PILS measurements (both PILS-OC and PILS-WSOC) had significantly smaller regression intercepts in Atlanta and Riverside. The intercept was higher in Riverside, CA (and highest in Mexico City), which are locations strongly influenced by mobile source emissions and thus high concentrations of semi-volatile VOCs and particulate OC. While a significant PILS-OC – Sunset Labs intercept would suggest poor measurement performance by PILS-OC at lower concentrations, it appears unlikely that this intercept was due mainly to organic carbon particles and cannot be solely explained by the inability of the PILS-OC to detect large (> 0.11 μm diameter), insoluble organic carbon particles.

2.6.11 Conclusions

Replacement of the PILS impactor with a mini cyclone appears to increase collection efficiency of small, insoluble particles. When coupled with a Sievers TOC analyzer for carbonaceous aerosol detection, this method leads to good agreement between the PILS-OC method of analysis and a Sunset Labs ECOC analyzer. However, there are limitations. A size dependence on insoluble particles was observed. Calibration with purely insoluble PSL spheres showed that particles greater than approximately 110nm are not efficiently quantified by the Sievers TOC analyzer. Alternate methods of carbon detection, such as combustion techniques, could be used to solve this limitation, but such methods are generally not as fast as the Sievers analyzer and are significantly more expensive.

The PILS-OC technique was deployed in Atlanta, Georgia and Riverside, California to measure ambient aerosol carbon and was compared to OC determined by a Sunset Labs instrument. By linear regression slope (± 1σ), the PILS-OC measured ~101% ± 2% of OC in Atlanta, and ~93% ± 5% of OC in Riverside, not statistically different from one considering the combined uncertainties associated with each measurement (10% PILS-OC, 20% Sunset Labs OCEC). The measurements were also highly correlated in each location ($r^2 = 0.86$, $r^2 = 0.87$, respectively). However, in both cases, a significant positive intercept was observed, where the Sunset OC measurement was significantly higher than PILS-OC. Both measurements were also compared to bulk aerosol mass measurements. At zero mass, the PILS-OC intercept was small whereas the Sunset Labs OC intercept was significantly larger than zero, with a larger intercept in regions of higher mobile source emissions. The observed intercepts could be associated with a number of causes, including the PILS-OC method's inability to adequately detect large insoluble OC and negative artifacts associated with the online mass measurements. However, for all comparisons a consistent but uncertain explanation for a significant portion of the intercept is a positive bias due to absorption and analysis of SVOCs by the Sunset Labs instrument.

Overall, this analysis suggests that the PILS-OC shows some promise as a fast (3s to 6 min), sensitive (0.1 μgC m^{-3}), and relatively inexpensive method for measuring carbonaceous aerosol in urban environments.

CHAPTER 3

NEW ENGLAND AIR QUALITY STUDY

The Northeastern United States is of particular interest in aerosol science because it is frequently influenced by upwind sources of aerosol pollution. For instance, the Ohio River Valley has a high number of SO_2 sources, mainly consisting of coal-fired power generation facilities, and is frequently has a substantial upwind influence on air masses that advect across the northeastern US. This can result in substantially acidic aerosol conditions, which may have significant health and ecological consequences [*Brauer, et al.*, 1995; *Brook, et al.*, 1997; *Gwynn, et al.*, 2000; *Keeler, et al.*, 1991; *Likens, et al.*, 1996; *Pandis, et al.*, 1995; *Schindler*, 1988; *Talbot, et al.*, 1992] The Clean Air Act Amendments of 1990 specifically sought to reduce SO_2 emissions from this region because of high concentration of points source in the Ohio River Valley and because of the densely populated region (the Washington-New York-Boston megalopolis) that may be affected by these emissions [*Lynch, et al.*, 2000].

While the mission objectives focused on a comprehensive examination of Northeastern US outflow, a number of biomass burning interceptions are also discussed. This work is a result of an unusually active forest fire season in the boreal regions of Yukon Territory, CA, and Alaska, US. These results are discussed in detail, and compared with typical urban and rural outflow more often associated with conditions in the northeastern US.

The International Consortium for Atmospheric Research on Transport and Transformation (ICARTT), a multinational and multiplatform research initiative, recently studied the transport of pollutants and atmospheric chemistry of the Northeastern United States and Canada [*Fehsenfeld, et al.*, 2006]. The National Oceanic and Atmospheric Administration's (NOAA) WP-3D research aircraft participated in these experiments. Based in Portsmouth, NH (43.08N, -70.82W), research flights were conducted over regions that included the Canadian Maritime provinces, northern Quebec, New England, the Ohio River Valley, and western edge of the North Atlantic. Measurements were made during the period of 05 July to 15 August, 2004.

This paper identifies the main chemical components, their sources and the resulting spatial distribution of the bulk $PM_{1.0}$ aerosol (aerodynamic diameters less than 1.0μm) that were sampled throughout the summer field campaign. Other papers focus on specific plumes to investigate the evolution of fine particles from anthropogenic emissions along the urban corridor from Washington D.C. to Boston MA [*Sullivan, et al.*, 2006], [Brock et al, manuscript in preparation, 2007].

3.1 Experimental Methods

Fine particle bulk chemical composition was measured online from the NOAA WP-3D aircraft with two automated systems, each involving a Particle-Into-Liquid Sampler (PILS). One PILS was coupled to two Metrohm® ion chromatographs (Model 761, Houston, TX), while the second was coupled to a Sievers total organic carbon analyzer (GE Water Systems, Model 800T, Boulder, CO). The first instrument package is referred

to as PILS-IC (ion chromatography), and the second as PILS-WSOC (water soluble organic carbon). PILS-IC has been described in previous research [*Ma, et al.*, 2004; *Orsini, et al.*, 2003; *Weber, et al.*, 2001]. The PILS-WSOC instrument is described in detail by Sullivan et al (2006). Both instruments sampled ambient aerosol from a shared low-turbulence inlet (LTI) [*Wilson, et al.*, 2004], each sampling at 15.0 l/min. Upstream of the instruments, a non-rotating micro-orifice impactor [*Marple, et al.*, 1991] with 1.0 μm cut size (at 1 atmosphere) removed particles with aerodynamic diameters greater than 1.0 μm aerodynamic diameter at relative humidity that may have been significantly lower than ambient due to sample heating within the aircraft.

3.1.1 PILS-IC

The PILS-IC was operated using a chromatographic separation of 2.45 minutes for both the cations (ammonium, sodium, calcium, potassium, magnesium) and anions (chloride, sulfate, and nitrate). A "Cation 1-2" column and "Anion A Supp 5 (100 mm)" column (Metrohm-Peak, Houston, TX) was operated at an eluent flow rate of 1.5 ml min^{-1}, and 1.05 ml min^{-1}, respectively. Eluents used during this campaign were 11 mM Na_2CO_3 (sodium carbonate) , 6mM $NaHCO_3$ (sodium bicarbonate) for anion exchange, and 8.5 mM L-tartaric acid, 4.1 mM dipicolinic acid for cation exchange. With the liquid flow rates used in this campaign, limit of detection ranged from 0.2 μg m^{-3} for cation species (except potassium ion, which was 0.5 μg m^{-3}) to 0.02-0.04 μg m^{-3} for anions. The PILS impactor was continuously washed with a transport flow of 0.19 ml min^{-1} of ultrapure deionized water spiked with lithium fluoride as an internal standard. Liquid sample from the PILS was split between the anion and cation ICs. Each flow was continuously drawn

via syringe pumps into a 150 μl sample loop at a rate of 100 μl min^{-1}, resulting in a 90 second sample integration time. The resulting measurement interval was 2.45 minutes, with each sample representing a 90-second collection time.

To eliminate interferences from gases, sample air passed through a carbon monolith denuder and a set of etched glass honeycomb denuders prior to entering the PILS-IC. One etched glass denuder was coated with citric acid (for removal of gases such as NH_3 (ammonia)), and the second was coated with sodium carbonate (for removal of gases such as HNO_3 (nitric acid), SO_2 (sulfur dioxide), and HCl (hydrochloric acid)). Before each flight, a valve diverted the sampled aerosol through a HEPA filter for an assessment of denuder function, as well as a quantification of backgrounds. Sulfate was the only ionic compound measured with detectable background interference, which was generally constant at 0.015 μg l^{-1} (equivalent to ambient aerosol concentration of 10 ng m^{-3}). The sulfate background was subtracted from the dataset.

The ion chromatographs were calibrated using known dilutions of NIST-traceable liquid anion and cation stock standards. Linear calibration curves forced through zero were determined from five different concentrations of anions and cations that spanned the range of ionic concentrations typical for aerosol liquid samples collected from the PILS. The cation IC was calibrated before the mission began, and was re-calibrated near the middle and at the end of the mission. Sensitivity changed by less than 5% over the 6-week project. The anion column was calibrated before the mission; however, the column

was replaced and calibrated on 29 July 2004 and the system was re-calibrated at the end of the mission (again, with no significant change in calibration constants).

3.1.2 PILS-WSOC

A Particle-Into-Liquid Sampler coupled to a total organic carbon (TOC) analyzer (GE Water Systems, 800T, Boulder, CO) was used to measure the water-soluble organic carbon (WSOC) component of fine particles. WSOC was measured with a PILS-WSOC that functions similar to a PILS-IC, however, in this case the PILS liquid sample is quantified for carbon mass. The PILS was operated so that the collected particles were mixed with a transport flow of ultrapure deionized water to produce a total liquid flow rate of 1.3 ml min^{-1}. This sample liquid was pumped through a 0.5 μm PEEK filter via two 2.5 ml glass syringe pumps (Versa 3, Kloehn Inc.) operating in an alternating tandem mode to provide a smooth continuous flow. The TOC analyzed most of this flow by running at a sample flow rate of 1.2ml min^{-1}. The instrument quantifies the carbon mass by converting carbon in the liquid sample to CO_2 (carbon dioxide) through a combination of chemical and UV oxidation. The CO_2 is then detected by conductivity. This instrument operated at a 3-sec measurement rate with a detection limit of approximately 0.1 μgC m^{-3} and estimated measurement uncertainty of ± 8% + 0.3 μgC m^{-3} [*Sullivan, et al.*, 2006]. Liquid concentrations (in parts per billion carbon, or ppbC) of WSOC ranged from 10 ppbC to approximately 300 ppbC for the flow rates employed and regions investigated during the airborne experiment.

Upstream to the PILS-WSOC, sample air is passed through an activated carbon parallel-plate denuder [*Eatough, et al.*, 1993] to remove organic vapors. Throughout all flights, a computer-activated valve was triggered every 3 hours to direct the sample through a Teflon filter for quantifying the backgrounds by assessing any positive artifacts due to gas penetration through the denuders and absorption in PILS, and organic artifacts in the sample water. This background was assumed constant between consecutive background measurements and subtracted from the dataset. Although the TOC analyzer is factory calibrated, a series of oxalic acid standards were used to verify calibration stability. Calibrations were typically within 5% of the factory calibration.

Data were recorded continuously at 3-second integrals. In the following analysis, the data have been averaged to 1 minute, where the average would only be computed if at least 75% of possible data points were valid within the one-minute window. For a more detailed discussion on the PILS-WSOC, see Sullivan et al [2006].

3.1.3 Other Instrumentation

Additional supporting measurements were used throughout the analysis and include 1s observations of sulfur dioxide (SO_2) and carbon monoxide (CO) [*Holloway, et al.*, 2000] and gaseous organic compounds measured by a proton transfer reaction-mass spectroscopy (PTR-MS) with an approximate sampling frequency of 18s [*de Gouw, et al.*, 2003b]. $PM_{1.0}$ volume, which is used extensively in the following analysis, was measured at 1s resolution using a combination of three instruments: a battery of 5 condensation particle counters (CPC), a modified Lasair 1001 optical particle counter

(OPC), and a white light optical particle counter (WLOPC) [*Brock, et al.*, 2004; *Brock, et al.*, 2003]. Located in a pod under an aircraft wing, the CPC measured total concentrations in five cumulative particle size ranges (0.004μm to 0.055 μm). The OPC measured concentrations in 64 size bins spanning the size range from 0.15μm to 0.95μm diameter. Sampled air was heated to 35 degrees C for the CPC, and was not heated in the case of the OPC. However, relative humidity was measured in the inlet of the OPC, and the data were corrected to RH of 40% using a fitted curve of hygroscopic diameter growth for mixed sulfate/organic particles as described by Santarpia et al [2004]. Lastly, the WLOPC was located inside the aircraft and measured size bins from 0.7μm to 8.0 μm. The data are processed by an inversion technique which determines a smooth and continuous size distribution that is consistent with the data and experimental response of the instruments, as well as with the instrument uncertainty. A more detailed description of volume measurement methodology, calibration, and uncertainty can be seen in Brock et al [2000; 2007; 2002], and Wollny, et al (manuscript in prep, 2007). Ambient pressure and temperature were recorded while in flight and used to adjust all aerosol particle concentration data reported here to standard conditions (20°C and 1 atmosphere).

3.2. Results

Airborne measurements provide the opportunity to sample with a single set of instruments large geographic regions and a range of altitudes. A map, including aircraft flight paths during the deployment based out of Portsmouth, New Hampshire is shown in Figure 3.1. During this experiment, a majority (~69%) of observations took place at altitudes less than 2000 meters above sea level.

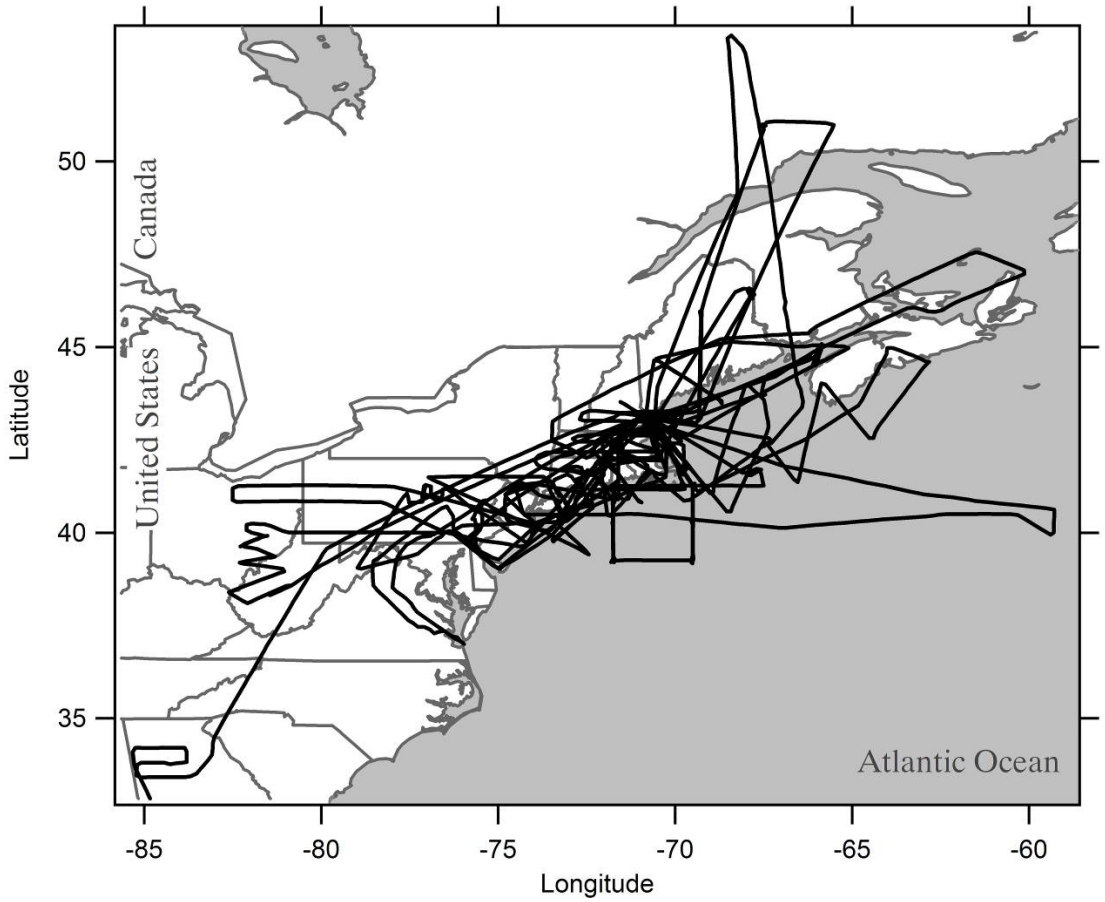

Figure 3.1 Overview of all WP-3D flight tracks flown during the NEAQS experiment. The aircraft was based at Pease Airfield in Portsmouth, NH. 17 research flights were conducted and were typically 8-9 hours in duration.

3.2.1 Aerosol Composition - Main Chemical Components of $PM_{1.0}$

Table 3.1 summarizes the bulk aerosol composition measurements that were made from the NOAA WP-3D during the NEAQS field campaign. For the species measured, both below and above 2 km altitude, the two main components by mass were sulfate and WSOC. Sulfate was observed throughout the field campaign with a mean concentration of 3.86 μg m^{-3}, although the range of observation spanned from the limit of detection (LOD, see Table 3.1) to 30.96 μg m^{-3}. Ammonium ion was also commonly observed, with a mean concentration of 1.1 μg m^{-3} (range: LOD to 6.5 μg m^{-3}) and was well

correlated with sulfate ($r^2 = 0.74$). Water-soluble organic carbon (WSOC) averaged 2.2 μg C m^{-3}, and ranged from the LOD to 25.6 μg C m^{-3}, with highest concentrations measured within biomass burning plumes.

The other measured ions were nearly always below the limit of detection, with the exception of periodic encounters with unique plumes. For example, at the detection limit of 0.04 μg m^{-3}, nitrate ion was almost exclusively observed in biomass burning plumes and was often correlated with the ammonium ion. This finding was expected since nitrate is a known component of biomass burning smoke [*Chow, et al.*, 1994] and is unlikely to be observed at significant concentrations in fine particles during the summertime in the northeastern U.S. [*Tolocka, et al.*, 2001].

Compounds associated mainly with mineral dust, calcium (Ca^{2+}) and magnesium (Mg^{2+}), and sea-salt particle components, sodium (Na^+) and chloride (Cl^-), were usually near or below the detection limits for the $PM_{1.0}$ particles sampled in this mission. Potassium (K^+) ion was typically below the LOD, even during biomass burning plume sampling. This is significant because these plumes contained the highest concentrations of aerosol mass measured during the experiment and other studies have shown that K^+ is prevalent in fine particle biomass burning smoke, [*Lee, et al.*, 2003; *Ma, et al.*, 2003]. Assuming ΔK^+ concentration equals 0.25 μg m^{-3}, (one-half the instrument LOD for K^+, and background K^+ concentrations were 0), $\Delta K^+/\Delta CO$ ranged from 1.2 to 3.9 pptv $ppbv^{-1}$ (mean = 2.07 pptv $ppbv^{-1}$). These ratios are generally consistent, although somewhat lower than those reported in other studies [*Andreae and Crutzen*, 1997; *Ma, et al.*, 2003; *Reiner, et al.*,

2001], where ratios were in the range of 1.3 to 4.9 pptv $ppbv^{-1}$. Minor differences in K^+ relative to CO compared to other studies could be due to differences in emissions (material and method of burning), and the fact that in some cases the plumes had undergone long-range transport with evidence for precipitation scavenging (Wollny et al, manuscript in prep, 2007[2]), a process that may have depleted the particulate K^+ relative to CO (Brock et al, manuscript in prep, 2007[1]) [*de Gouw, et al.*, 2006; *Warneke, et al.*, 2006]. Thus, we conclude the lack of K^+ in the observed biomass burning plumes was due to expected concentrations near or below the LOD, rather than a complete absence of K^+.

3.2.2 Air Mass Classification

Sulfate, ammonium, WSOC, and aerosol volume varied significantly from their means and medians reflecting high spatial variability over the region sampled (Table 3.1). To investigate the physico-chemical properties of $PM_{1.0}$ from different sources, in the following analysis the data are divided into air masses with and without a clear indication of a biomass burning influence. Biomass burning emissions were identified using acetonitrile as a unique tracer [*de Gouw, et al.*, 2003b], with acetonitrile concentrations below 250 pptv indicating minimal biomass burning influence. In a few cases, biomass-burning emissions from long range transport appeared to have mixed with more regionally polluted air masses. These air masses were encountered near the surface and contained fine particles with high inorganic ion concentrations (e.g. ammonium and sulfate), and both high acetonitrile and WSOC concentrations.

3.2.3 Segregation of Data Into Three Air Masses Types

In the following analysis, the data are binned into three groups: 1) relatively pure biomass burning air masses - acetonitrile concentrations greater than 250 pptv and sulfate less than 4 μg m^{-3}; 2) sulfate-enhanced biomass burning air masses - acetonitrile greater than 250 pptv, and sulfate concentrations greater than 4 μg m^{-3}; and 3) non-biomass burning influenced air masses - acetonitrile concentrations less than 250 pptv. (Note that 250 pptv level of acetonitrile was chosen to select for plumes which were strongly influenced by biomass burning; while plumes with lower concentrations (e.g. 0-250pptv) may have been influenced by biomass burning, this analysis focuses on biomass burning air masses that were relatively pure and contain high concentrations of acetonitrile. Also, 4 $\mu g/m^3$ of sulfate is chosen as the cutoff since it is the approximate average sulfate concentration observed throughout all altitudes in this study. The identification of the pure and sulfate-enhanced biomass burning air masses is not sensitive to this number). These three generalized air masses were observed multiple times in different locations throughout the experiment.

Table 3.1: Statistical overview of observed species throughout all flights during NEAQS separated into three bins: All altitudes (top), samples below 2000m (middle), and samples above 2000m (bottom). For statistical purposes, ½ the LOD value is substituted when observation was below LOD. Inorganic ions are sampled over a 90-second averaging time. Fine Volume is averaged to PILS-IC integration time (90s) with estimated water content (see text) subtracted, and WSOC is averaged over 60 seconds. (For Min column, most data is ½ LOD). For fine particle mass, calculated density, calculated OM, OM/PM mass, and Sulfate/PM mass, all data was averaged to PILS-IC integration time (90s). WSOC was converted to OM using $C_{wsoc} = 3.1$; see mass closure section for additional methodology. All statistics include biomass burning data except numbers in parentheses (biomass data is excluded for these calculations/estimations).

All Altitudes

	LOD[a,b]	% above LOD	Mean	Median	Std Dev	Min	Max
Chloride[a]	0.02	1.7%	0.02	0.01	0.12	0.01	3.77
Sulfate[a]	0.03	97.0%	3.98	2.07	4.69	0.04	30.96
Nitrate[a]	0.04	15.0%	0.06	0.02	0.24	0.02	4.66
Sodium[a]	0.2	1.3%	0.1	0.1	0.1	0.1	2.7
Ammonium[a]	0.2	79.2%	1.1	0.6	1.1	0.1	6.5
Calcium[a]	0.2	0.5%	0.1	0.1	0.0	0.1	0.7
Potassium[a]	0.5	0.1%	0.3	0.3	0.0	0.3	0.6
Magnesium[a]	0.2	0.1%	0.1	0.1	0.0	0.1	0.4
WSOC[b]	0.1	100%	2.2	1.6	2.2	0.1	25.6
Fine Volume[c]	n/a	n/a	9.30	6.80	8.65	0.18	90.89
Fine Particle Mass[a]	n/a		16.23 (15.48)	11.27 (11.09)	14.23 (11.82)	0.06 (0.06)	123.1 (85.7)
Calculated Density[d]	n/a		1.47 (1.48)	1.48 (1.48)	0.10 (0.10)	1.22 (1.23)	1.71 (1.71)
Calculated OM[a]	n/a		6.2 (5.8)	4.7 (4.5)	6.2 (3.9)	0.6 (0.6)	71.9 (31.6)
OM/PM Mass	n/a		0.43 (0.43)	0.40 (0.40)	0.20 (0.20)	0.05 (0.05)	0.99 (0.99)
Sulfate/PM Mass	n/a		0.29 (0.30)	0.26 (0.26)	0.17 (0.17)	0.00 (0.01)	0.99 (0.99)

Table 3.1 (continued)

Altitudes less than 2000m

LOD[a,b]		% above LOD	Mean	Median	Std Dev	Min	Max
Chloride[a]	0.02	1.2%	0.01	0.01	0.05	0.01	1.60
Sulfate[a]	0.03	98.5%	4.97	3.18	4.92	0.04	30.96
Nitrate[a]	0.04	14.8%	0.05	0.02	0.13	0.02	2.41
Sodium[a]	0.2	0.1%	0.1	0.1	0.0	0.1	0.6
Ammonium[a]	0.2	97.9%	1.5	1.0	1.2	0.2	6.5
Calcium[a]	0.2	0.3%	0.1	0.1	0.0	0.1	0.7
Potassium[a]	0.5	0%	0.3	0.3	0.0	0.3	0.3
Magnesium[a]	0.2	0%	0.1	0.1	0.0	0.1	0.1
WSOC[b]	0.1	100%	2.0	0.8	4.0	0.1	25.6
Fine Volume[c]	n/a	n/a	9.62	7.63	6.53	0.64	37.31
Fine Particle Mass[a]	n/a		16.35 (16.29)	12.13 (11.87)	11.87 (11.87)	0.06 (0.06)	85.70 (85.70)
Calculated Density[d]	n/a		1.48 (1.48)	1.48 (1.48)	0.10 (0.10)	1.24 (1.24)	1.71 (1.71)
Calculated OM[a]	n/a		6.1 (6.0)	5.0 (5.0)	4.0 (4.0)	0.6 (0.6)	31.6 (31.6)
OM/PM Mass	n/a		0.43 (0.43)	0.40 (0.40)	0.20 (0.20)	0.05 (0.05)	0.98 (0.98)
Sulfate/PM Mass	n/a		0.29 (0.29)	0.26 (0.26)	0.17 (0.17)	0.01 (0.01)	0.97 (0.97)

Table 3.1 (continued)

Altitudes less than 2000m							
LOD[a,b]		% above LOD	Mean	Median	Std Dev	Min	Max
Chloride[a]	0.02	1.2%	0.01	0.01	0.05	0.01	1.60
Sulfate[a]	0.03	98.5%	4.97	3.18	4.92	0.04	30.96
Nitrate[a]	0.04	14.8%	0.05	0.02	0.13	0.02	2.41
Sodium[a]	0.2	0.1%	0.1	0.1	0.0	0.1	0.6
Ammonium[a]	0.2	97.9%	1.5	1.0	1.2	0.2	6.5
Calcium[a]	0.2	0.3%	0.1	0.1	0.0	0.1	0.7
Potassium[a]	0.5	0%	0.3	0.3	0.0	0.3	0.3
Magnesium[a]	0.2	0%	0.1	0.1	0.0	0.1	0.1
WSOC[b]	0.1	100%	2.0	0.8	4.0	0.1	25.6
Fine Volume[c]	n/a	n/a	9.62	7.63	6.53	0.64	37.31
Fine Particle Mass[a]	n/a		16.35 (16.29)	12.13 (11.87)	11.87 (11.87)	0.06 (0.06)	85.70 (85.70)
Calculated Density[d]	n/a		1.48 (1.48)	1.48 (1.48)	0.10 (0.10)	1.24 (1.24)	1.71 (1.71)
Calculated OM[a]	n/a		6.1 (6.0)	5.0 (5.0)	4.0 (4.0)	0.6 (0.6)	31.6 (31.6)
OM/PM Mass	n/a		0.43 (0.43)	0.40 (0.40)	0.20 (0.20)	0.05 (0.05)	0.98 (0.98)
Sulfate/PM Mass	n/a		0.29 (0.29)	0.26 (0.26)	0.17 (0.17)	0.01 (0.01)	0.97 (0.97)

[a] In $\mu g\ m^{-3}$ for ions; [b] in μg Carbon m^{-3}; [c] in $\mu m^3\ cm^{-3}$; [d] $g\ cm^{-3}$.

3.2.4 Sources of WSOC

The sources of anthropogenic WSOC are investigated in greater detail by Sullivan et al [2006], Peltier, et al, [2007b], and Brock et al. [2007] and are discussed only briefly here. FLEXPART [*Stohl, et al.*, 1998] transport model shows that the larger biomass burning plumes encountered originated from fires in the Alaska/Yukon region [*de Gouw, et al.*, 2006; *Pfister, et al.*, 2005; *Warneke, et al.*, 2006]. The highest $PM_{1.0}$ volumes in this study were observed in these distinct biomass burning plume layers. WSOC and acetonitrile were well correlated in these plumes ($r^2 = 0.73$), but were not correlated ($r^2 =$

0.06) when acetonitrile was below 250 pptv in air masses with minimal biomass burning influence. Correlations between WSOC and carbon monoxide (CO) were observed throughout this study and suggest a WSOC source linked in some manner to combustion emissions. Other studies [*de Gouw, et al.*, 2005; *Sullivan, et al.*, 2006; *Weber, et al.*, 2007] identify a significant source of WSOC from secondary organic aerosol production. Incomplete combustion is a significant source for CO and can occur in burning of biomass materials [*Chow, et al.*, 1994] or fossil fuels combustion [*Mayol-Bracero, et al.*, 2002]. The CO - WSOC correlation was observed in all the types of air masses investigated with $r^2 = 0.64$ in relatively pure biomass burning plumes, $r^2 = 0.67$ in biomass burning emissions mixed with sulfate, and $r^2 = 0.54$ in air masses with no biomass burning influence (Figure 3.2).

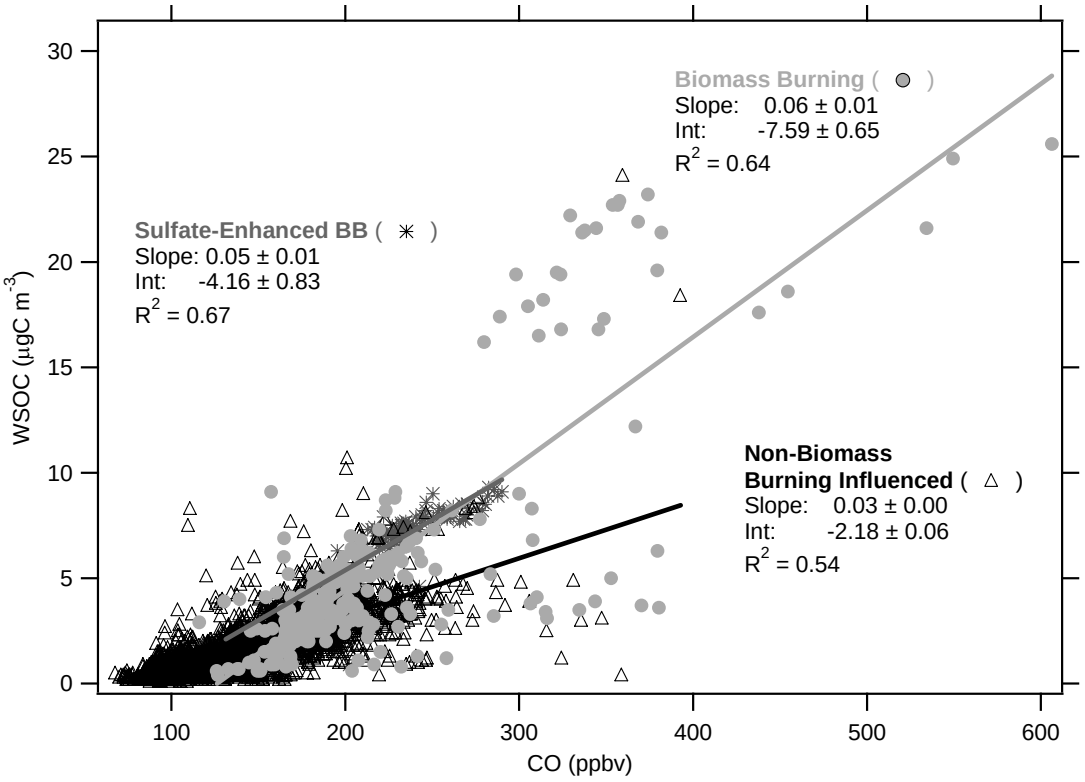

Figure 3.2 WSOC plotted as a function of CO, classified by airmass regime. Lines are univariate least-squares linear regression fits. Slope and r^2 for all plotted data were 0.038 and 0.61, respectively. Individual regime slope, intercept, and r^2 values are described in legend. CO data were averaged to 60 seconds to match WSOC integration time.

3.2.5 Sulfate Sources

As expected, high sulfate concentrations detected in this study were linked to power plant plume emissions. The urban plumes also often contained sulfate, mainly from sources of SO_2 near the urban centers [*Brock, et al.*, 2007]. Very distinct power plant plumes of high sulfate and SO_2 were also encountered away from urban sources. For example, high sulfate mass was observed in the Ohio River Valley region of the U.S. at altitudes less than ~2000m. This region has many power generation facilities that emit SO_2 and were

the apparent sources for the observed sulfate. Sulfate and WSOC measured in the regions of western Pennsylvania are discussed in more detail (Section 4) where results from a specific flight are presented.

3.2.6 WSOC-Sulfate Correlations

WSOC and sulfate were not highly correlated in the regions sampled. The highest correlation of sulfate-WSOC was observed in the sulfate-enhanced biomass burning air mass (r^2 =0.37) where biomass plumes from long range transport had mixed with regionally polluted air masses (Figure 3.3). WSOC - sulfate r^2 within the biomass burning plumes was low (r^2 = 0.06), while WSOC - sulfate r^2 = 0.29 in non-biomass burning regimes. This suggests that WSOC and sulfate did not have co-located sources, or they have highly different removal efficiencies.

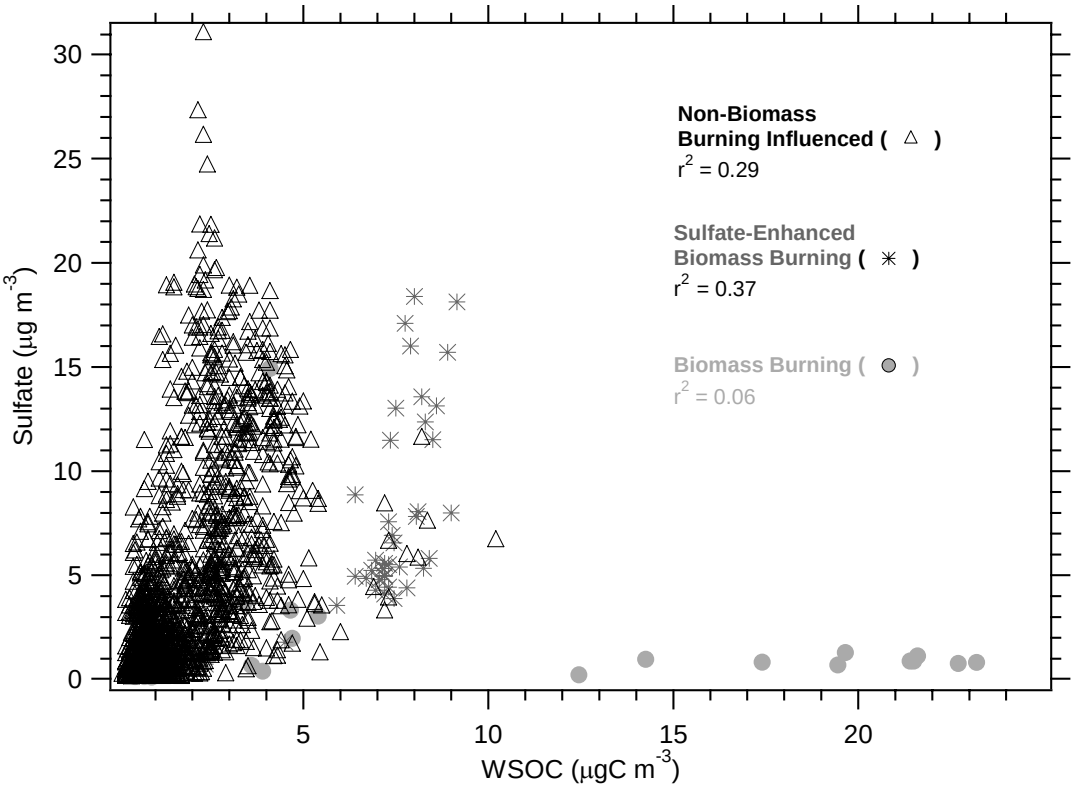

Figure 3.3 Sulfate plotted as a function of WSOC for all flights, classified by air mass regime. WSOC data were averaged to 90 seconds to match sampling time of sulfate.

3.2.7 Sulfate, WSOC, Versus Fine Particle Volume

Although species-specific aerosol chemical mass fractions are of most interest, we first compare speciated mass to particle volume since this only involves directly measured quantities. In the next section, the particle mass is estimated from the particle volume, and sulfate and carbonaceous mass fractions are then estimated.

The mean ratio of sulfate to fine particle volume, was 0.54 μg m^{-3}/μm^3 cm^{-3} and these two parameters were highly correlated (r^2 = 0.75) in samples without a biomass burning influence. For the sulfate-influenced biomass burning plume, the ratio of sulfate to fine

particle volume was 0.47 μg m^{-3}/μm^3 cm^{-3}, and was also highly correlated (r^2 = 0.87). The biomass burning plumes that had not mixed to the surface had a different aerosol profile; sulfate was not a significant fraction of fine particle volume and thus was not correlated (r^2 = 0.01, Figure 3.4) with fine particle volume.

In contrast, WSOC was highly correlated (r^2 =0.89) with fine particle volume within biomass burning plumes, with a WSOC to fine volume ratio of 0.20 μgC m^{-3} / μm^3 cm^{-3}.

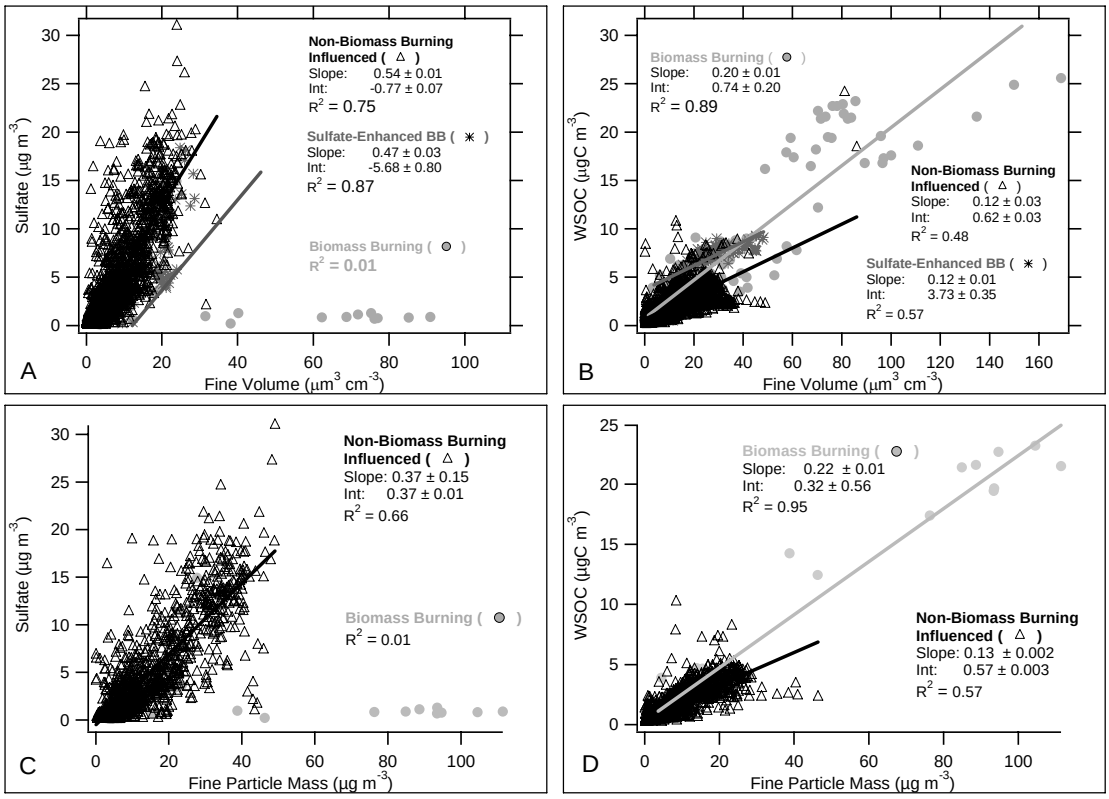

Figure 3.4 Sulfate (A) and WSOC (B) plotted as a function of submicron particle volume. Sulfate (C) and WSOC (D) plotted as function of estimated fine particle mass (see text). Symbols indicated data assigned to non-biomass burning, sulfate-enhanced biomass burning, and biomass burning classifications. Lines and legends give univariate linear least-squares regression fits and statistics for each regime. Fine particle volume averaged to 90 second in A, and 60 seconds in B to match integration time of respective measurements. Fine particle volume averaged to 90 seconds in C and D to match integration time of ion measurement. In C and D, cation data were unavailable for sulfate-enhanced biomass burning case; these data are not plotted.

This may not represent typical emission ratios since it may have been altered during transport due to precipitation scavenging [*de Gouw, et al.*, 2006]. The ratio of WSOC to fine particle volume was lower (0.12 μgC $m^{-3}/\mu m^3$ cm^{-3}) in non-biomass burning plumes and in sulfate enhanced biomass burning plumes (Figure 3.4).

The majority of measurements made during this campaign were non-biomass burning influenced and were likely representative of typical conditions observed in the northeastern United States during the summer of 2004. For all data, and based on regression analysis, sulfate was highly correlated with $PM_{1.0}$ volume in the regions sampled ($r^2 = 0.75$), while WSOC was less well correlated ($r^2 = 0.57$). An example of the relative importance of sulfate and WSOC in controlling total submicron particle mass is discussed in a case study in Section 4.

3.3 Calculation of Fine Particle Mass and Organic Mass from Volume and WSOC Measurements

In this section, the WSOC to OM (organic matter) ratio, C_{WSOC}, is estimated and then used in subsequent analysis to convert WSOC to OM. For this purpose, fine particle volume and PILS-WSOC data were averaged to 90 seconds, the time integral of PILS-IC measurements. All data (including biomass burning interceptions) from this field campaign are included in this calculation. Assuming a constant density for organic aerosol mass and a constant WSOC to OM ratio (C_{WSOC}), sulfate and OM fractions of $PM_{1.0}$ mass are calculated and summarized (Table 3.1).

To calculate mass from submicron particle volume, no correction is made for the effect of composition on the optical measurements (e.g. influence on particle refractive index). We assume a particle density of 1.78 g cm^{-3} for inorganic ionic aerosol mass (e.g., ammonium sulfate and ammonium bisulfate), and a density of 1.2 g cm^{-3} for the organic aerosol component [*Turpin and Lim*, 2001]. The overall density was determined by a volume-weighted average based on concentrations of the measured inorganic ions and OM. Fine particle volume was reported at ~40% relative humidity, and thus included condensed water vapor in the particle volume measurement. This was quantified by assuming all condensed water was associated with the measured NH_4^+ and SO_4^{2-} and using the model ISORROPIA [*Nenes, et al.*, 1998]. The predicted water volume associated with the particle at the measurement relative humidity of 40% was subtracted from the particle volume measurement.

Conversion of WSOC to organic matter (OM) can be accomplished by calculating a ratio of OM to WSOC (units: μg μgC^{-1}). This conversion factor has two components: one accounts for the insoluble portion of carbon mass associated with the organic carbon (OC) that was unmeasured (OC/WSOC, units: μgC μgC^{-1}); the second factor converts organic carbon (OC) to organic matter (OM) (OM/OC, units: μg μgC^{-1}), which accounts for the elemental groups (e.g., oxygen, nitrogen, hydrogen, etc.) that are associated with the carbon. The ratio of summertime WSOC/OC from a variety of studies has been reported by Jaffrezo et al [2005, references therein] to range from 31%-77%, with lower ratios generally found in fresh plumes and higher ratios in more aged plumes. In

addition, as reported by Turpin and Lim [2001], OM/OC ratios range from 1.6 (urban) to 2.1 (non-urban, more aged). The relationship between particle age and OM/WSOC ratio is complicated in that as a particle ages, the WSOC/OC component increases (i.e. OC/WSOC decreases) while the OM/OC component increases. This creates conditions where the calculation of the OM/WSOC ratio, defined as OM/WSOC = (OM/OC) x (OC/WSOC), is somewhat self-compensating resulting in a smaller variability of OM/WSOC than otherwise might be expected.

The mass calculated from fine particle volume (PM_{vol}) can be compared to that observed by PILS (PM_{PILS}) by Eq. 3.1:

$$\underbrace{V_{fine} \times \left(\frac{\left(C_{WSOC} \times WSOC\right) + \sum ion}{\left(\frac{C_{WSOC} \times WSOC}{\rho_{om}} \right) + \frac{\sum ion}{\rho_{ion}}} \right)}_{PM_{vol}} = \underbrace{\left(\sum ion + \left(C_{WSOC} \times WSOC\right) + M_{unmeasured} \right)}_{PM_{PILS}} \qquad \text{Equation 3.1}$$

This equation includes terms that describe fine particle volume (V_{fine}), weighted density of organic matter and ions (ρ_{om} and ρ_{ion}), sum of measured ions (Σ_{ion}), organic matter, which is defined as WSOC multiplied by C_{WSOC}, and an estimate of the unmeasured fraction that may include species such as elemental carbon, metals, and crustal material ($M_{unmeasured}$). Rearranging the mass balance equation and using an iterative equation solver, the balance equation can be solved for C_{WSOC}. Occasionally (< 4% of

calculations), C_{WSOC} was less than 1 (OM less than WSOC); these data, which are likely associated with instrumental uncertainties, are excluded from this analysis. The median C_{WSOC} ratio ($\pm 1\sigma$ for all data was 3.1 ($\pm$ 1.6) μgC μg^{-1}. The sum of squares of the uncertainty associated with each measurement (particle volume, anion, cation, WSOC) results in an overall uncertainty of ~50% in this value. Using C_{WSOC}= 3.1, PM_{vol} and PM_{PILS} are highly correlated ($r^2 = 0.77$, Figure 3.5) for all data recorded during this mission. There were no discernable patterns for the WSOC-to-OM ratio across sampled longitude, latitude, or altitudes.

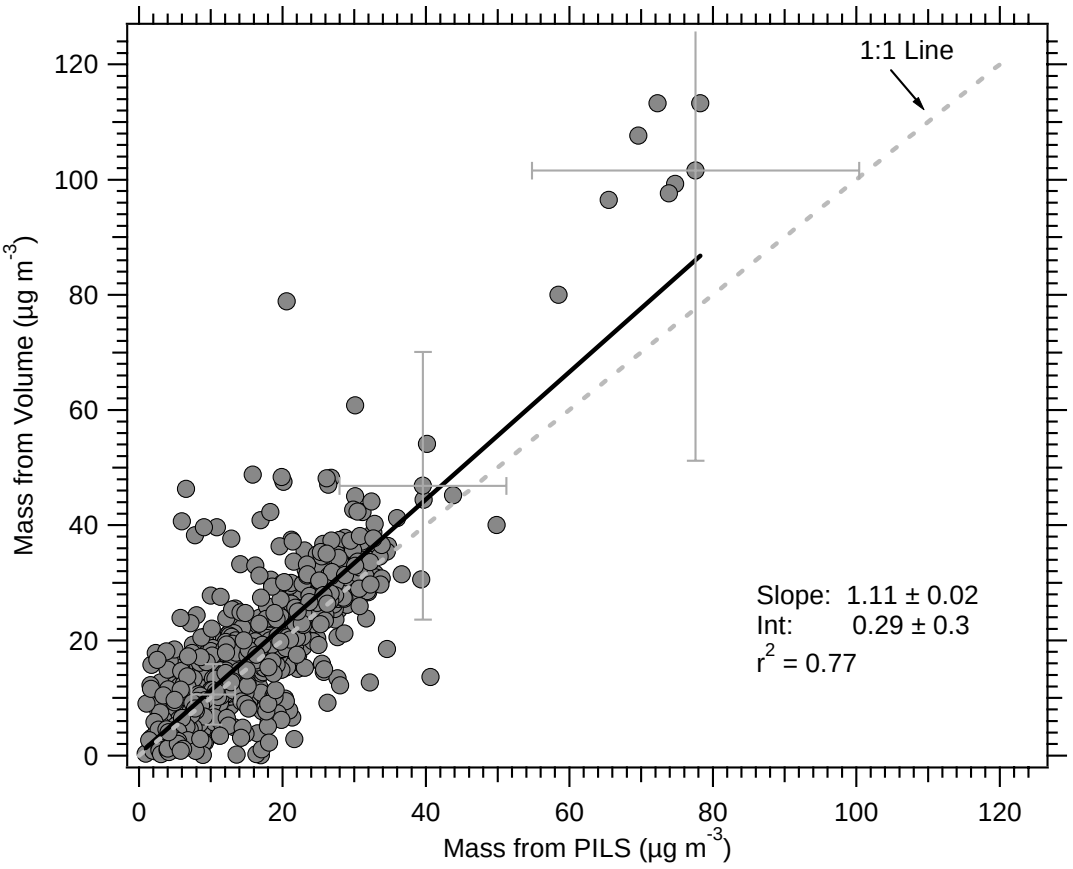

Figure 3.5 Particle mass estimated from submicron volume measurements plotted as a function of mass from directly measured composition (see text). Error bars are instrument uncertainties propagated in quadrature.

The derived value C_{WSOC} = 3.1 is similar to what is expected based on reasonable values of WSOC/OC and OM/OC previously discussed. For example, a value of C_{WSOC} = 3.1 can be derived if OM/OC is presumed to be 1.9 and WSOC is 61% of OC. This is consistent with what has been found in other studies. For example, in St. Louis, MO, a summer time WSOC/OC ratio of ~61 to 64% is reported by Sullivan et al [*Sullivan, et al.*, 2004] and OM/OC of 1.95±0.17 [*Bae, et al.*, 2006].

Recall that the calculated ratio from mass balance assumes an unmeasured aerosol volume as 8%. Using data from EPAs Interagency Monitoring of Protected Visual Environments (IMPROVE) sites located within the sampling region, elemental carbon was, on average, observed to be less than ~5% of $PM_{2.5}$ mass at the IMPROVE ground sites; metals and crustal materials at the IMPROVE sites account for an additional 2-3% of $PM_{2.5}$ mass. None of these compounds were measured aboard the WP-3D aircraft. The IMPROVE data are only used as an estimate of the unmeasured aerosol in order to complete the mass closure and may not be fully representative of the conditions sampled by the WP-3D; IMPROVE sites tend to measure background concentrations of aerosol whereas the WP-3D focused mainly on specific power plant and urban plumes. If the fraction of unmeasured aerosol was larger than 8%, C_{WSOC} would be slightly lower.

The influence of particle chemical composition on this mass comparison was investigated by segregating the data into periods when the constructed chemical mass was dominated by either sulfate mass or WSOC (and thus OM). For data in which sulfate was less than 25% of the mass inferred from the chemically speciated measurements (for these cases

WSOC was, on average, approximately three times the mass of sulfate) C_{WSOC} is 3.3 ± 1.9. In contrast, for data where sulfate was greater than 80% of the mass, C_{WSOC} is 2.8 ± 1.4.

Surprisingly, the derived value of C_{WSOC} was similar for biomass burning plumes and non-biomass burning. In biomass burning plumes (acetonitrile concentration above 250 pptv), the C_{WSOC} was 3.3 ± 1.3 and 3.0 ± 1.7 for outside of biomass burning plumes (acetonitrile concentration below 250 pptv). Higher values of C_{WSOC} within biomass burning plumes are consistent with additional insoluble organics not included in the WSOC measurement.

Using the results of this analysis, Table 3.1 describes aerosol statistics after converting WSOC to OM and calculating mass from fine particle volume. Estimated condensed water was subtracted from the fine particle volume measurement. Across all altitudes, the calculated median concentration of submicron particle mass was 11.27 μg m^{-3}. Median fine particle mass concentration was higher at lower altitudes (12.13 μg m^{-3}) and lower at higher altitudes (4.88 μg m^{-3}, though with a significant standard deviation due to biomass burning plumes). Average particle density, which was weighted by particle composition determined by PILS, was 1.47 g cm^{-3}. Median density was slightly lower at higher altitudes, consistent with increasing ratios of organic material to fine particle volume (discussed in next section and in Figure 3.7) and an assumed organic aerosol density of 1.2 g cm^{-3}. On average, organic matter was 6.2 μg m^{-3}, although OM ranged from 0.6 μg m^{-3} to 71.9 μg m^{-3}. The median ratio of calculated OM to fine particle mass

was 0.40 μg m^{-3} / μg m^{-3} for the entire dataset and 0.46 μg m^{-3} / μg m^{-3} above 2000m altitude.

Mass fractions of sulfate and WSOC can also be computed. Sulfate (Fig 3.4c) represents ~37% of fine particle mass in non-biomass burning influenced samples (determined by regression slope), providing further evidence that sulfate is a significant fraction of fine particle mass within the sampling domain. WSOC accounts for 22% (μgC m^{-3} / μg m^{-3}) of fine particle mass in biomass burning sampling, and 13% in non-biomass burning air masses within the sampling domain (Fig 3.4d). Thus, using the WSOC-to-OM conversion technique previously discussed, we estimate the organic matter mass fraction of fine particle mass to be ~68% (μg m^{-3} / μg m^{-3}) in biomass burning plumes and 42% in non biomass burning air masses.

3.4 Variation in Concentration with Altitude

The NOAA WP-3D aircraft operated in an altitude range of approximately 250m to 6100m (above sea level). Altitude profiles of sulfate, ammonium, nitrate, and WSOC for all data collected during ICARTT in the northeastern United States are shown in Figure 3.6. The sampling region was focused heavily on urban outflow from New York City, NY and Boston, MA, but also included several transects of the Ohio River Valley, US region (approximately 37° to 41° N latitude, -82° to -87° longitude). Additional sampling was conducted in northern Quebec to sample biomass burning plumes, as well as over the Gulf of Maine and western regions of Canadian Maritimes to sample aged urban air masses. Aircraft interceptions of distinct biomass burning plumes between 3 and 4 km

altitude can be observed in the WSOC (OM), nitrate, and ammonium plots (Figure 3.6). Additional discussion of altitude profiles can be found in Sullivan et al [2006] and Warneke et al. [2006]

In air not significantly influenced by biomass burning, measurement throughout the sampled column showed that sulfate and ammonium concentrations were generally highest at altitudes below 2000m (i.e. within the boundary layer). WSOC and estimated OM had a similar profile with highest concentrations near the surface. Aerosol nitrate concentrations did not vary systematically with altitude. Since concentrations of these species, with the exception of nitrate, were highest at lower altitudes, it appears that the major sources of sulfate, ammonium, and WSOC are from the surface and that that these compounds are not efficiently dispersed above ~2000m, a finding supported by a modeling analysis of these data [*Heald, et al.*, 2006a].

The altitude profile of SO_2 (not shown) was similar to that of sulfate, with higher concentrations occurring at lower altitudes. The highest concentrations of SO_2 were observed near 1000m (~40 ppbv). The profile of CO (not shown) was similar to WSOC (recall that CO and WSOC are correlated, Figure 3.2), and decrease with increasing altitude, CO approached a background free troposphere concentration of approximately 75 ppbv. WSOC was also measured throughout the sampled altitude range. Excluding measurements below 2000m and biomass burning interceptions above 2000m, WSOC measurements were higher than the instrument LOD 35% of the time (535 samples). Substituting one-half LOD value (0.05 μgC m^{-3}) in cases where the measurement was

less than LOD (note, in Table 3.1, the calculated OM does not substitute one-half LOD value, and averages are therefore higher), mean WSOC concentration (± 1σ) above the planetary boundary layer was 0.3 μgC m^{-3} (± 0.5 μgC m^{-3}). Since large sources of WSOC (e.g. biomass burning plumes) are excluded from this calculation, this finding suggests a free troposphere background concentration of WSOC of approximately 0.3 μgC m^{-3}. Converting this to organic matter, we estimated the free troposphere concentration of organic matter is approximately 1.0 μg m^{-3}. This estimate is consistent with the findings of Heald et al [2005], Maria et al [2003], Park et al [2003] and Jaffe et al [2005] where background concentrations of organic matter ranged from 0.43 to ~3 μg m^{-3}.

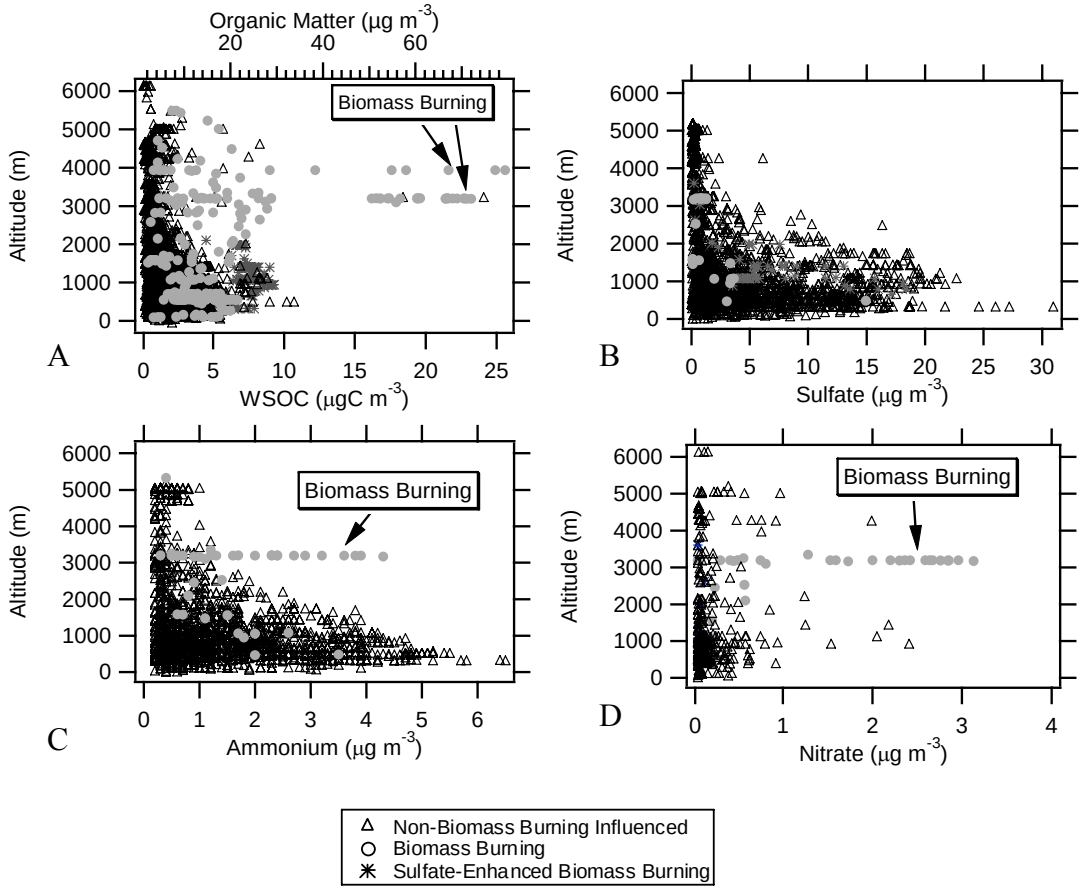

Figure 3.6 Altitude profiles for WSOC (and estimated OM), sulfate, ammonium, and nitrate ion. Specific biomass plumes are indicated.

Although absolute concentrations of WSOC (and hence, OM) and sulfate dropped sharply with increasing altitude, the ratio of sulfate to OM, ratio of sulfate to fine particle mass, and ratio of OM to fine particle mass did not follow this profile. To improve signal, the OM, sulfate, and particle mass data were binned into 250m intervals for altitudes less than 2km and 500m intervals for altitudes greater than 2km. The median of the ratio was calculated for each bin. The median values for the highest and lowest altitude bins are more uncertain since these bins include fewer data points. In air masses not significantly affected by biomass burning (acetonitrile < 250 pptv), the median ratio of SO_2 to total sulfur (SO_2 / (SO_2 + sulfate)) and of SO_4^{2-} to fine particle mass (μg m^{-3} /

μg m^{-3}) in each altitude bin was calculated (Figure 3.7a). Between the altitudes of ~1000-3000 m, SO_2/(SO_2 + sulfate) was lowest and sulfate/fine particle mass was highest, suggesting that in this altitude range, oxidation of SO_2 to particulate sulfate had occurred at a rate faster than that of particle removal processes. Below this altitude, sufficient time may not have occurred since emission to allow for substantial oxidation and sulfate formation. Between 3000 and 4000 m, particle removal processes (such as precipitation scavenging) may have efficiently removed sulfate particles at a rate faster than production of sulfate by SO_2 oxidation. Finally, at altitudes > 4000 m, slower removal processes may have resulted in a higher ratio of sulfate to total sulfur.

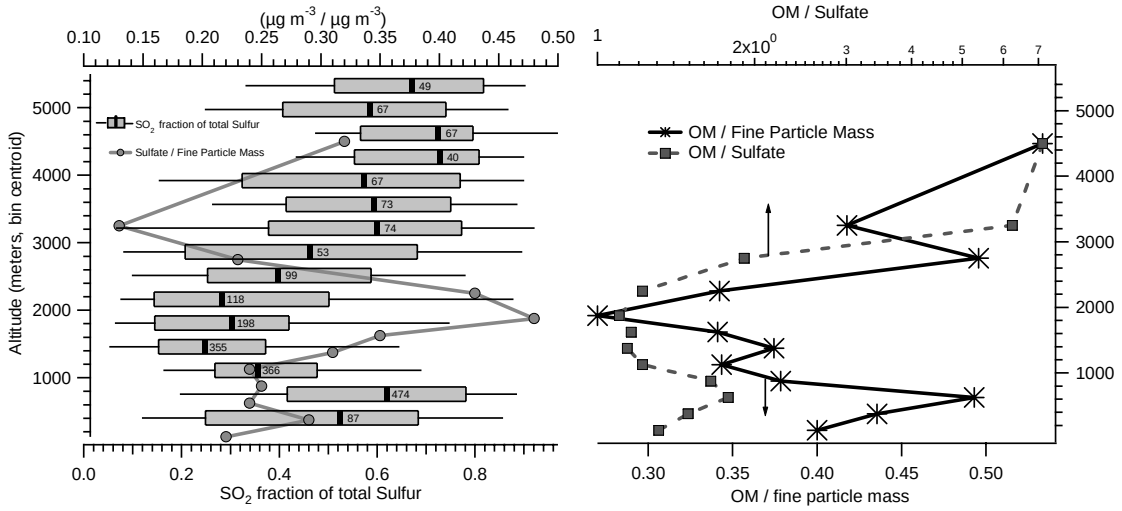

Figure 3.7 A) Altitude profile of ratio of sulfate to fine particle mass (grey line, top axis), and SO_2 fraction of total observed sulfur (box and whisker plot, bottom axis). Markers represent median data point of 250 meter binned data at altitudes less than 2000m, and 500m binned data at altitudes greater than 2000m. Box and whisker plot gives, 10^{th} and 90^{th} percentiles (ends of whiskers), 25^{th} and 75^{th} percentile (ends of boxes), median value (dark line), and number of observations within each bin (to immediate right of median line). B) Altitude profiles of ratio of organic matter (OM) to fine particle mass. Organic matter/sulfate is also plotted (dashed line). Biomass burning samples have been excluded from this analysis.

While absolute concentrations of sulfate and OM were much higher below 3 km altitude than above this altitude (Figure 3.6), the ratio of OM to fine particle mass ($\mu gC\ m^{-3}$ / $\mu g\ m^{-3}$) substantially increased with altitude in the non-biomass burning influenced air masses, with the highest ratios occurring above 3000 m in the free troposphere (Figure 3.7b). The variation in the ratio of OM to sulfate ion with altitude is also plotted and has a similar profile as the ratio of OM to $PM_{1.0}$ mass. This result is consistent with Novakov, et al [1997] , who reported an increase of total organic carbon mass fraction as altitude increased from 0 – 3.5 km from aircraft measurements near Virginia, US in 1996. Similarly, Murphy, et al [1998] reported that in upper tropospheric (5-19km) measurements near Texas, internally-mixed aerosol with higher fractions of organics relative to sulfate were observed.

The vertical profile of ratios in composition (Figure 3.7a) suggests that relative to sulfate, OM is either more efficiently lofted, is removed less efficiently, and/or produced in situ at faster rates at altitudes between 3 and 5 km. Compared to sulfate particles, those containing significant mass fractions of OM may be less efficiently activated to form cloud condensation nuclei and thus may not be as likely to undergo wet deposition when lofted. However, Heald, et al. [2005] performed a covariance analysis of this data set and suggest that an unknown, possibly heterogeneous, pathway for secondary organic aerosol formation is a likely contributor to free troposphere aerosol mass. Biomass burning, which likely contributes to the observed background concentrations of acetonitrile (~200-250 pptv), may also be responsible for some of the additional free troposphere OM concentrations that are not fully explained in modeling studies.

3.5 Charge Balance Between Measured Ions

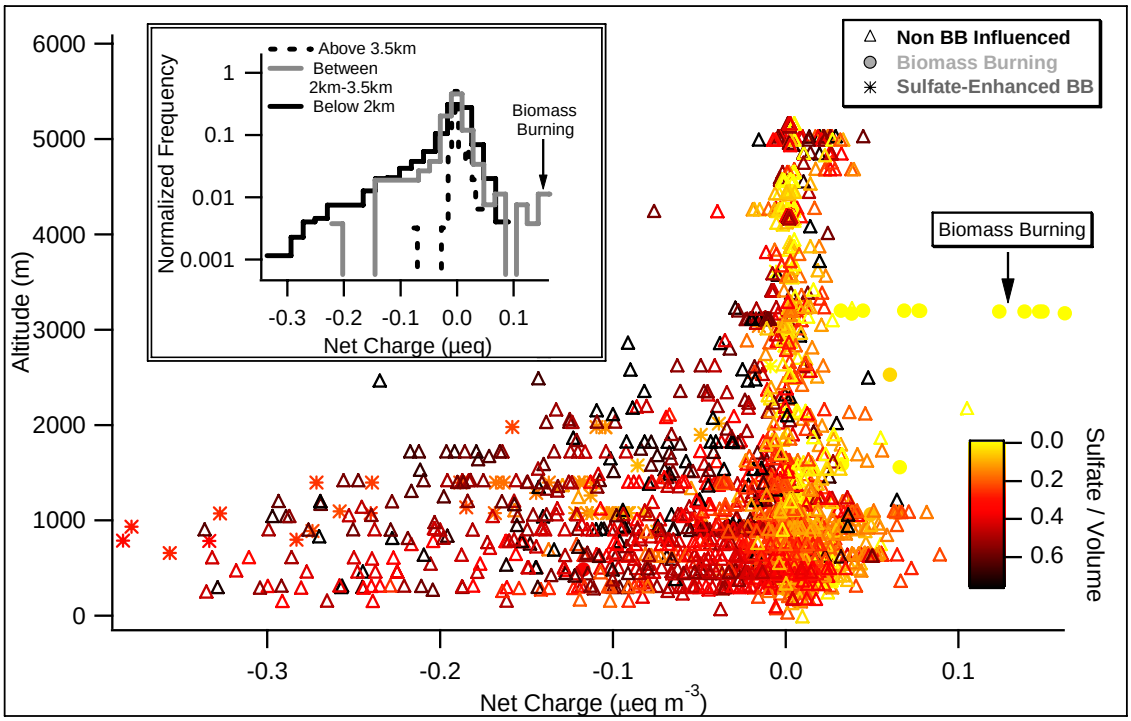

Figure 3.8 Altitude profile of charge balance for sulfate, ammonium, and nitrate ions, colored by the ratio of sulfate to fine particle volume. Values < LOD assigned value of 0. Embedded plot on upper left is normalized frequency histogram of observed charge balances in 3 altitude ranges (less than 2 km, 2-3.5 km, and above 3.5 km).

The spatially heterogeneous and strong emissions of some of the aerosol sources encountered in this study led to wide variability in other aerosol properties, such as balance between measured anions and cations. Comparing concentrations of measured anions to cations can provide insight into the presence of unmeasured ions. In the following analysis, an ion balance is calculated from the sum of measured cations minus the sum of measured anions, in equivalence concentrations. Large positive or negative deviations from zero suggest unmeasured ionic constituents in the sampled aerosol

particles. In the following analysis, if a specific ion was at the LOD, the ion was not considered in the ion balance calculation. This is to reduce a bias that would have been caused by differences in cation and anion LODs. Often, a balance between measured anions and cations was observed; however, in many cases the net charge was negative, suggesting an unmeasured cation, most likely H^+, suggesting a more acidic aerosol. Figure 3.8 illustrates the calculated net charge of observed ions over the altitude range of the measurements. On average, the net charge was zero, indicating that most anion-cation pairs were measured (Figure 3.8). The charge balance was within the range of -0.05 to +0.05 μeq m^{-3} 67% of the time.

The measured aerosol ion balance is always near zero at altitudes from 3000-5000 m, when biomass burning plumes are excluded. However, many low-altitude charge balance calculations were observed to be highly negative. During periods of highest negative charge balance, sulfate tends to be a larger fraction of $PM_{1.0}$ volume (Figure 3.8). Net charge on the particles also tended to become more negative when absolute concentrations of sulfate increased (not plotted). This implies that strong SO_2 sources leading to sulfate formation overwhelm sources for ammonia, the precursor for sulfate's commonly-paired cation species. This was most clearly seen in power generation regions (see Section 4).

A composite, normalized histogram that bins all observations of charge balance into three altitudes – low (<2 km), middle (2-3.5 km) and high (>3.5 km), - shows that a net charge of approximately 0 μeq was observed most frequently throughout each altitude bin (inset

in Figure 3.8). In the lowest altitude bin, there is a significant tail toward negative values suggesting a more acidic aerosol composition. Some occurrences of positive ion balances were observed in the middle altitude range during biomass burning plume interceptions. Biomass burning particles were found to have relatively high ammonium and low sulfate concentrations; thus a net positive charge balance may result from an unmeasured organic acid associated with NH_4^+. The WSOC concentration, which includes organic acids, is correlated (not plotted) with the positive charge balance in biomass burning plumes ($r^2 = 0.58$).

The general chemical and physical characteristics of the sampled fine aerosol have been discussed. Measurements from a specific flight are now investigated in detail.

3.6 Case Study: Nighttime Sulfate and WSOC in Industrial and Urban Areas

A nighttime flight on August 9, 2004 presented an opportunity to contrast on a single flight air masses measured over the power generation regions of eastern Ohio and western Pennsylvania to air masses influenced by urban regions on the eastern seaboard. The flight was conducted at night between ~19:00 and ~02:00 EDT. This flight is also discussed in detail by Brown et al [2006] where the affect of nocturnal nitrogen oxide processing on air quality was investigated.

Figure 3.9 shows the flight path colored by SO_2 and CO, the aircraft altitude, and the observed spatial distribution of fine particle volume, sulfate, WSOC, and ammonium to sulfate (NH_4^+/SO_4^{2-}) molar ratios. The Pennsylvania and eastern Ohio portion of the

flight was sampled from approximately 00:00-04:00 UTC (20:00-00:00 EDT). The wind direction was generally from the southwest at ~8 m s^{-1}, although direction was more south-southwesterly during the westernmost portions of the flight. Based on the combined transport and emission inventory model FLEXPART [*Stohl, et al.*, 1998] SO_2 was largely derived from power plants located along the Ohio River and in western Pennsylvania, whereas CO was generally from the Columbus and Cincinnati Ohio, Detroit, Michigan, and Pittsburgh, Pennsylvania areas. The FLEXPART simulation indicates that both SO_2 and CO were aged approximately 1-4 days since the time of emission.

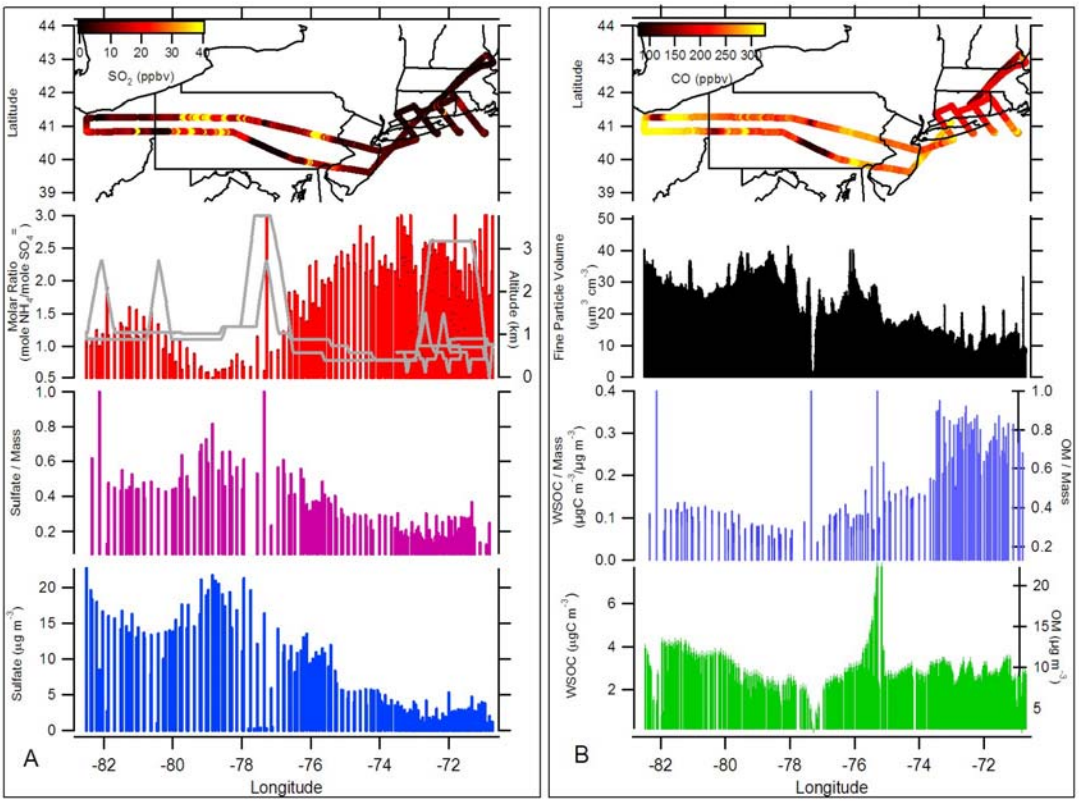

Figure 3.9: A) Track of WP-3D aircraft on 2004/08/09 colored by SO_2, and molar ratio, altitude, sulfate fraction of fine particle mass, and sulfate mass as a function of longitude. B) As in (A), but colored by CO, and fine particle volume, WSOC fraction of fine particle mass, and WSOC as a function of longitude

The eastern seaboard leg included a flight pattern designed to characterize the outflow of New York City from approximately 04:05-07:00 UTC (00:05-03:00 EDT) as the WP-3D returned to Portsmouth, New Hampshire. A FLEXPART analysis for this region shows that the majority of CO and SO_2 that was observed originated from the New York City metropolitan region. These pollutants were aged generally less than one day. Wind direction was westerly, with average wind speeds around 6 m s^{-1}. These nighttime measurements had somewhat low CO concentrations, typically ranging from 150-200 ppbv in the NYC outflow, versus daytime flights where CO concentrations typically ranged from 230 to 240 ppbv. The Ohio River Valley region had similar CO concentrations, apart from the 200-225 ppbv of CO observed in the westernmost region of the flight in the vicinity of Columbus and Cleveland, Ohio.

As expected, based on the spatial distribution of coal-fired power plants, sulfate concentrations were factors of four to five times higher over the power generation regions on the western leg of the flight compared to the eastern regions. Fine particle mass was estimated from measured volume as discussed in a previous section. Sulfate was ~60% and WSOC ~10% (OM ~33%, assuming OM/WSOC is constant at 3.1, see Section 3.4) of total submicron mass in the power generation regions of western Pennsylvania. For all of this flight, the spatial variability in $PM_{1.0}$ was driven by sulfate. WSOC concentrations were more spatially uniform, although slightly higher WSOC, and hence OM, in the extreme western portion of the flight was correlated with higher CO from Columbus and Cincinnati, Ohio.

High sulfate concentrations in the power production regions of western Pennsylvania (-80 to –78° longitude) produced an apparently acidic aerosol. In these regions NH_4^+/SO_4^{2-} molar ratios were one or less compared to the eastern portion of the flight were the ratio was 2 or higher (Figure 3.9). No general enhancements in WSOC concentrations are seen in the region of lower NH_4^+/SO_4^{2-} molar ratios, consistent with [*Zhang, et al.*, 2004], who found no evidence for acid-catalyzed enhancements in organic aerosol during another study conducted in this region.

On the eastern leg of the flight an influence from urban emissions can be detected. For example, the slight oscillating pattern in WSOC concentration from about –74 to about –77 degrees longitude (Figure 3.9) is due to entering and leaving the NYC plume. WSOC mass was about 20% to 30% higher in the area of NYC outflow compared to the surrounding regions. However, substantially larger increases in WSOC (200 to 500%) relative to background were observed during the daytime downwind from NYC on other flights [*Sullivan, et al.*, 2006] compared to these nighttime data. Over the wide longitudinal range of this flight, the WSOC (and thus likely OM) concentration was fairly uniform (standard deviation = 0.8 $\mu gC\ m^{-3}$). Due to a decrease in sulfate concentration as sampling moved eastward, the WSOC fraction of fine particle mass increased from about 10% to ~30% (Figure 3.9) (OM mass fraction increased from ~40% to ~80%). Overall, the distinct longitudinal distribution of higher sulfate and $PM_{1.0}$ volume (mass) to the west, in contrast to more uniform WSOC and OM concentrations, clearly demonstrates the dominating influence of large SO_2 sources on air quality over wide spatial regions (e.g. the western longitudes of this flight). WSOC and OM, on the other hand, appears to

have fewer well-defined point sources during this flight, suggesting a more regional background from distant sources.

3.7 Conclusions

Airborne measurements in July and August 2004 of fine particle ($PM_{1.0}$) bulk chemical composition were made from the surface to ~6 km altitude over northeastern United States and Canada, but with a focus on regions along the eastern seaboard. This paper summarizes the overall particle chemical climatology. The online measurements included ionic species chloride, nitrate, sulfate, sodium, ammonium, potassium, calcium and magnesium, and the water-soluble organic carbon (WSOC) fraction of the organic aerosol. In addition, measurements were made of particle volume and a suite of trace gases.

The bulk aerosol chemistry data were combined with fine particle volume data through a mass closure analysis to infer particle density and the ratio of organic matter (OM) to WSOC. The measured $PM_{1.0}$ particle volume concentrations and inferred density were then used to estimate $PM_{1.0}$ particle mass concentrations. Although the particle density varied with composition, the analysis predicted a fairly constant ratio of OM to WSOC of 3.1 ± 1.6 μg μgC^{-1}.

In this study, sulfate aerosol was ubiquitous with highest masses downwind of power generating regions (e.g., Ohio River Valley). Sulfate was also frequently observed in urban plumes. Sulfate concentrations were typically on the order of 2 to 4 μg m^{-3}.

Ammonium was often present and apparently associated with sulfate, with an ammonium to sulfate molar ratio near 2. However, in regions of high sulfate concentration, the calculated molar ratio was significantly less than 2, typically near 1. Nitrate was rarely present above the limit of detection (0.04 $\mu g\ m^{-3}$), and was found to be mainly associated with biomass burning plumes originating from the Yukon/Alaska region of North America. Significant concentrations of ammonium were also observed in these biomass burning plumes. All other measured aerosol ionic species were generally below detection limits (typically < 0.2 $\mu g\ m^{-3}$ for cation species; 0.04 $\mu g\ m^{-3}$ for anion species). Sulfate and ammonium concentrations tended to be highest at lower altitudes, while the vertical distribution of nitrate had no discernable pattern.

WSOC, and hence inferred OM, was detected throughout the measurement domain, and was observed in highest concentrations (WSOC >25 $\mu gC\ m^{-3}$, inferred OM > 75 $\mu g\ m^{-3}$) within the Yukon/Alaskan biomass burning plumes. Apart from biomass burning plumes, WSOC was more spatially uniform than sulfate and highest concentrations appeared to be mainly associated with urban emissions and WSOC concentrations generally ranged in between 2 and 4 $\mu gC\ m^{-3}$. Although, like sulfate, WSOC concentrations decreased rapidly with increasing altitude, the ratio of WSOC to sulfate increased sharply at about 2.5 km altitude, in the region of transition from the boundary layer to the free troposphere. Overall, in this study, sulfate comprised roughly 35 % of the $PM_{1.0}$ mass and OM roughly 55%, however, the fractions varied depending on altitude, and the proximity to various sources, such as power generating facilities and urban regions.

CHAPTER 4

ACID-CATALYZED REACTIONS

Compounds containing organic carbon (OC) are a large fraction of ambient fine particles in the southeastern United States (U.S.), and during the summer when air quality generally worsens, secondary organic aerosol (SOA) is a large component of this particulate OC. Many laboratory studies with both biogenic and anthropogenic volatile organic compounds (VOCs) have suggested that heterogeneous reactions involving acid aerosols can catalyze the formation of secondary organic aerosol through polymerization reactions[*Gao, et al.*, 2004; *Iinuma, et al.*, 2004; *Jang and Kamens*, 2001; *Kalberer, et al.*, 2004; *Limbeck, et al.*, 2003; *Tolocka, et al.*, 2004]. However, little ambient data exists to test these experiments, and from the few observations, the results tend to be mixed. Ambient measurements in Houston, TX by Brock et al. [2003] show that measured particle volumes increased at much higher rates than what could be explained by SO_2 oxidation and condensation in plumes that contained both high levels of VOCs and SO_2, whereas plumes mainly of VOCs did not exhibit this increase. Chamber studies by Jang and Kamens [*Jang and Kamens*, 2001] show that SOA yield from a variety of aldehydes was enhanced in the presence of acidic seed particles, compared with neutralized seed aerosol. In contrast, Gao et al. [2006] found no evidence for oligomer formation and no correlation between particle-inferred acidity and a large number of organic acids measured in the southeastern United States. Zhang et al. [2004] found no significant enhancement of organic carbon concentration during the Pittsburgh Supersite experiment during acidic aerosol events, suggesting that acid-catalyzed formation of

secondary organic aerosol is not a significant contributor during these conditions. The findings of this paper adds to these ambient results by presenting recent airborne measurements conducted over metropolitan Atlanta to investigate evidence for acid-catalyzed reactions that may lead to organic aerosol formation. In this work, measurements and discussion of WSOC concentrations in acidic aerosol conditions caused by power plant plumes are compared with WSOC concentrations under apparently more neutralized aerosol conditions occurring immediately surrounding each plume. This is a more direct measurement compared to other studies that rely on correlations between apparent aerosol acidity and organic aerosol concentration from ground-based data. Elucidating the sources of fine PM is important since, for example, the Atlanta metropolitan region often fails to meet National Ambient Air Quality Standards for particulate matter. If acid-catalyzed aerosol formation is an important process as some smog chamber studies suggest, it is likely to occur in the Atlanta metropolitan region since it is rich in both biogenic and anthropogenic VOCs and is surrounded by large coal-fired power plants that generate acidic sulfur-containing aerosols.

In support of the New England Air Quality Study in the summer of 2004, US National Oceanic and Atmospheric Administration's WP-3D research aircraft was deployed for airborne sampling of atmospheric components. The payload included measurements of CO, SO_2, ozone, VOCs, particle size and number distribution, and fine particle bulk composition. For the majority of the mission, the aircraft was stationed at Portsmouth, NH (43.08N, -70.82W). Most of the research flights concentrated on the northeastern

US, eastern Canada, and Ohio River Valley with particular emphasis on urban and power generation facility outflow. Near the end of the study, while the aircraft was transiting to its home base in Florida, US, a large region of northern Georgia was sampled for approximately 105 minutes.

SOA is thought to be formed through oxidation of VOCs, which increases polarity and decreases its vapor pressure [*Seinfeld and Pankow*, 2003]. Thus, a large fraction of the compounds comprising SOA are likely oxygenated and soluble or partially soluble in water. Recent studies in Tokyo confirm this; WSOC was highly correlated with oxygenated organic aerosol (OOA), determined by multivariate analysis of organic spectrum by Aerosol Mass Spectrometry (Aerodyne Research, Inc, Billerica, MA), and comprised roughly 75% of the oxygenated aerosol mass [*Kondo, et al.*, 2007]. Comparisons between Tokyo WSOC and SOA mass estimated via the EC tracer method found similar results [*Miyazaki, et al.*, 2006]. Furthermore, these studies and others [*Weber, et al.*, 2007] have also found little or no evidence for significant concentrations of primarily emitted WSOC, in the absence of biomass burning emissions. Because biomass burning trace gases were at background concentrations in the region sampled (e.g. mean acetonitrile = 130pptv ± 11pptv), in this analysis we use WSOC as a reasonable (though not necessarily complete) measure of secondary organic aerosol mass fraction.

4.1 Methods

This study was conducted as part of the broader research described in Chapter 3. Therefore, the methods are only briefly summarized here.

Fine particle ($PM_{1.0}$) bulk chemical composition was measured onboard the WP-3D by two, automated Particle-Into-Liquid Samplers (PILS). One PILS was coupled to ion chromatographs (instrument package is referred to as PILS-IC), and another PILS was coupled to a Total Organic Carbon analyzer (referred to as PILS-TOC). PILS-IC has been described in previous research [*Ma, et al.*, 2003; *Orsini, et al.*, 2003; *Weber, et al.*, 2001]. The PILS-TOC instrument is described in detail by Sullivan et al [2006]. PILS-IC measures aerosol inorganic ion concentrations (sulfate, nitrate, chloride, sodium, ammonium, calcium, potassium, and magnesium ions) at a rate of a 90-second integrated sample every 2.45 minutes. The ion chromatographs were calibrated using dilutions of NIST-traceable stock solutions in concentrations that bracketed expected sampled PILS effluent flow. PILS-TOC measures the water-soluble fraction of organic carbon (WSOC) every three seconds. The TOC instrument is factory-calibrated, though this was verified by calibration standards both before and after the completion of the field campaign. Both instruments, including specific operating parameters, are described in greater detail in Peltier, et al [*Peltier, et al.*, 2007a], and Sullivan, et al [2006]. The PILS-IC instrument has a reported uncertainty of 10%, while the PILS-TOC instrument has an uncertainty of approximately 8%.

Aerosol was sampled from a single Low-Turbulence Inlet [*Wilson, et al.*, 2004] at a volumetric flow rate of 15 liters per minute for each instrument (total flow = 30 liters per minute). Upstream of the instruments, particle size was restricted to PM1.0 by a non-rotating micro-orifice impactor [*Marple, et al.*, 1991]. Both instruments utilized

denuders to minimize potential interferences from gases; in the case of PILS-IC, sampled aerosol passed through a monolithic carbon denuder and a set of etched-glass honeycomb denuders. One denuder was coated with a solution of citric acid and another with sodium carbonate. PILS-TOC sample was denuded by a parallel plate denuder consisting of activated carbon paper [*Eatough, et al.*, 1993]. In order to minimize volatile losses from particles due to re-equilibrium, denuders were located as close as possible to the PILS entrance (residence time ~ 0.15s). Aerosol flow from each instrument was periodically diverted through a filter to remove sampled particles. This allowed for an assessment of gas phase interferences that penetrated the denuders, as well as an assessment of background interferences present within the reagents (e.g. eluents, purified water) used in each technique.

Additional supporting measurements were used throughout the analysis and include 1s sulfur dioxide (SO_2) and carbon monoxide (CO) [*Holloway, et al.*, 2000]. PM1.0 volume was measured at 1 s resolution using a combination of three instruments: a condensation particle counter (CPC), a modified Lasair 1001 optical particle counter (OPC), and a white light optical particle counter (WLOPC) [*Brock, et al.*, 2000]. Particle volume reported here includes size ranges from 150nm to 1.0 μm at a relative humidity of ~40%. Volatile organic compounds, such as toluene, isoprene, methacrolein, and methyl vinyl ketone, were measured by 10s integration whole air sampling canister, and then analyzed offline by Gas Chromatography – Mass Spectroscopy (GC-MS).

4.2 Results

A low altitude (~1000m) flight segment lasting for 105 minutes was performed over the Atlanta metropolitan region. Wind speed and direction measured on the WP-3D were typically less than 5 m s^{-1} and variable throughout the sampled region suggesting stagnant ambient conditions. The flight path is depicted in Figure 4.1. Measurements of high $PM_{1.0}$ particle volume concentrations show a polluted air mass within the planetary boundary layer (PBL) amplified in several locations by local power plant plumes that can be readily identified by SO_2 spikes (see Figure 4.2). These plumes are identified by letters A through E in Figures 4.1 and 4.2.

The time series for PM1.0 volume, sulfate, and WSOC, and gases SO_2, various VOCs, and CO in Figure 4.2 show that all these components rapidly increased in concentration

as the aircraft descended into the PBL, which was delineated by a weak temperature

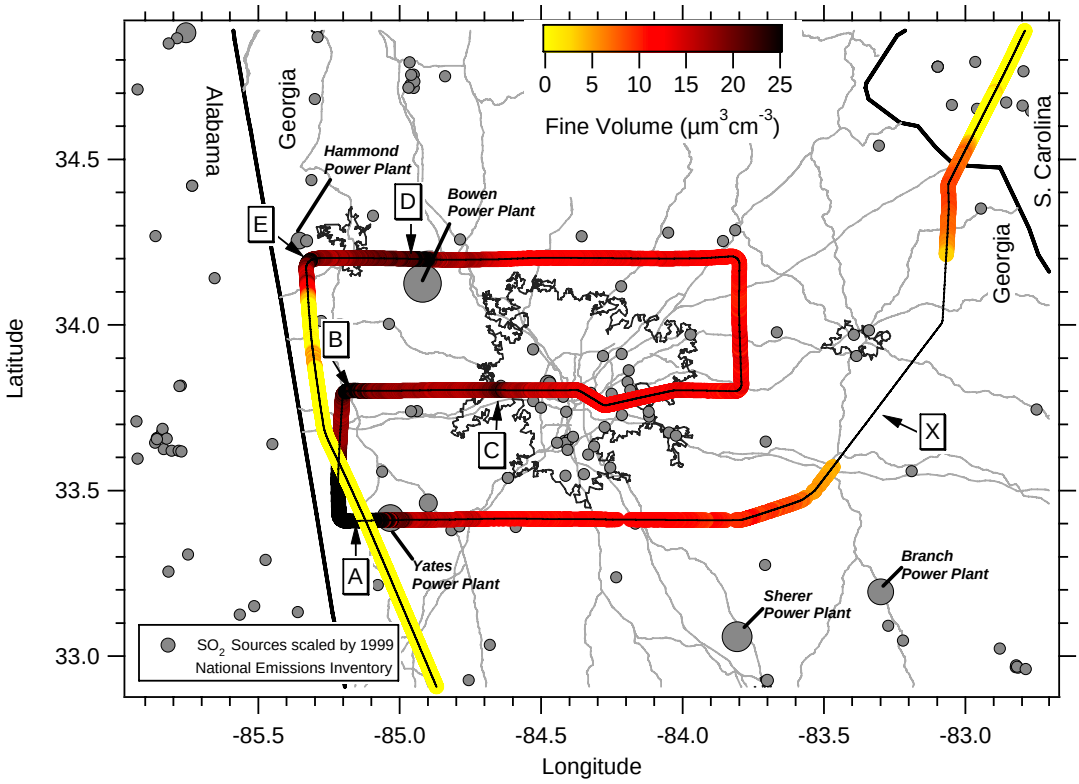

Figure 4.1: Flight path colored by fine particle volume ($\mu m^3\ cm^{-3}$) on research flight around Atlanta, USA. Letters A-E indicate specific SO_2 plumes, and X indicated region where aircraft passed through clouds and data is not analyzed. Local SO_2 sources are also indicated and marker size is scaled by the 1999 National Emissions Inventory.

inversion ($\Delta T = 1°C$) at ~2500m. Concentrations remained elevated throughout the entire region sampled for altitudes below ~2500 m. Ambient relative humidity (not plotted) ranged from 60-78% throughout the sampling period.

Measurements of liquid water indicate the aircraft penetrated a cloud in the region identified by X in Figures 4.1 and 4.2, and were not included in the analysis since the aerosol inlets were not equipped to handle in-cloud sampling. While some cumulus clouds were present at altitudes above the aircraft, all data that are discussed were from

cloud-free samples. In-cloud heterogeneous reactions have been shown to enhance oxalate aerosol formation [*Sorooshian, et al.*, 2006b] which would lead to increased WSOC concentration. This route for gas-to-particle conversion is not investigated.

There appears to be a regional sulfate concentration of 5-8 $\mu g\ m^{-3}$ that is present throughout most of the flight within the PBL. Superimposed on this regional sulfate, there are several spikes in sulfate concentration that are correlated with clear SO_2 spikes from local power plants. These plumes were typically 12-40 km in width, based on the higher time resolution SO_2 measurements. Despite the nearby power plants, identifying specific sources for each intercepted plume is not straightforward as the winds tended to be light and variable during the measurement period. Sulfate aerosol and fine particle volume are sharply elevated within these plumes. Thus, overall sulfate from local power plants accounts for much of the spatial variability in the fine particle volumes recorded within Atlanta and the surrounding region PBL. These increases in sulfate are significant. For example, in the SO_2 spike labeled A, the sulfate increased from about 5 to 19.5 $\mu g\ m^{-3}$ and the fine particle volume increased from about 20 to over 45 $\mu m^3\ cm^{-3}$. In this experiment the PILS-IC samples were integrated over 90 seconds and cannot accurately identify very narrow plumes (under typical flight speeds, plumes less than 16 km wide). These power plant plumes thus likely have sulfate concentrations on smaller spatial scales that are significantly larger than the more averaged values recorded by the PILS-IC.

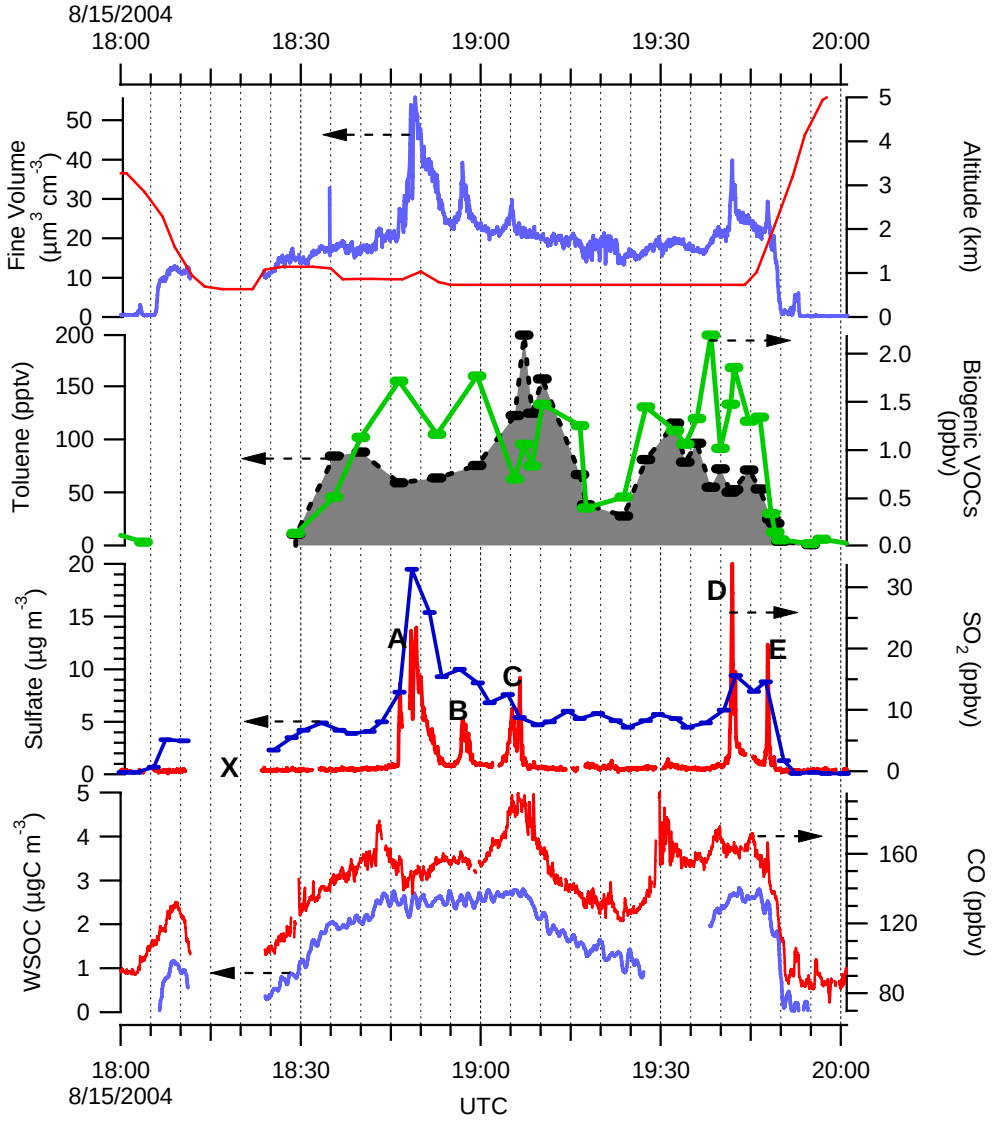

Figure 4.2: Time series of a flight on 2004/08/15, including data below 2400m surrounding the Atlanta, GA region. Horizontal arrows indicate appropriate axis for specific trace. A, B, C, D, and E refer to specific SO_2 plumes as discussed in the paper. X refers to a time period where the aircraft passed through a cloud, and aerosol data was ignored since the inlet it not equipped to sample aerosol within clouds. Gap in WSOC data between ~19:29 and ~19:39 is due to periodic background assessment in the instrument. Biogenic VOCs are defined as (isoprene + methyl vinyl ketone + methacrolein). Biogenic VOC and toluene were measured by a whole air sampler and represent 10-second integrated measurements (lines added for emphasis).

Air masses were characterized as either in-plume or out-of-plume as determined by 1 second SO_2 measurements for all PBL data. Summarized in Table 2.1, on average across all five plumes, sulfate concentration was a factor of 2 higher inside the plume, and SO_2 mixing ratio was larger by nearly a factor of 8 (though with a large standard deviation), when compared to outside of plume conditions. Median molar ratio of ammonium to sulfate ion was 2.0 outside of the plumes compared to 1.1 inside of the plumes. It should be noted that NH_4^+/SO_4^{2-} molar ratios may be slightly higher due to loss of NH_4^+ in the PILS [*Sorooshian, et al.*, 2006a]. Because NH_4^+ and SO_4^{2-} were the dominant fine particle cations and anions observed, the much larger imbalance is most likely due to unmeasured H^+, suggesting that, as expected, aerosol H^+ concentration (e.g. aerosol acidity) was higher in power plant plumes. The apparent molar ratios observed above Atlanta in this study were consistent with estimated molar ratios in the chamber studies conducted by Jang and Kamens [2001] (assuming similar atomization efficiencies for sulfuric acid and ammonium sulfate solutions, estimated molar ratio in the reaction chamber was 0.9). By assuming a particle density of 1.8 g cm^{-3} for the Jang and Kamens work, somewhat lower mass loadings were observed in Atlanta, compared with the seed aerosol used chamber studies (typical reported particle volumes in chamber studies: ~2-66 μm^{-3} cm^{-3}). This difference may be one reason why acid catalyzed reactions were not significant in the ambient atmosphere. Furthermore, their model results are from experimental reaction times between 10 minutes and 6 hours. This is approximately consistent with the plume ages observed in the ambient measurements above Atlanta, though we can not be certain due to the light and variable winds encountered during sample (making precise air mass aging techniques difficult).

	CO, (ppbv)	SO_2, (ppbv)	NH_4^+/SO_4^{2-}	Biogenic VOCs, (ppbv)	Toluene, (pptv)	SO_4^{2-}, ($\mu g/m^3$)	NH_4^+, ($\mu g/m^3$)	WSOC, ($\mu gC/m^3$)
Within plume	140.4 ± 26.3	3.3 ± 5.4	1.1 ± 0.5	1.10 ± 0.49	71.2 ± 52.8	8.8 ± 4.54	2.0 ± 0.3	2.5 ± 0.2
Out of plume	157.6 ± 15.1	0.4 ± 0.5	2.0 ± 1.1	0.94 ± 0.63	62.9 ± 40.7	5.0 ± 2.34	1.8 ± 0.8	2.4 ± 0.2

Table 4.1: Median plume concentrations/ratio of various compounds within the plume and out of the plume. Standard deviation is also included. Biogenic VOCs are defined as isoprene + methyl vinyl ketone + methacrolein

The water-soluble fraction of organic aerosol was somewhat spatially uniform; small-scale plumes characterized by sharp increases in WSOC were generally not observed within the PBL suggesting that much of the WSOC in Atlanta was regional in nature. The overall large-scale trend of CO was matched well by WSOC. WSOC and CO were highly spatially correlated in Atlanta and surrounding region (inside the PBL) with r^2 = 0.80 and a slope of 32 μgC m^{-3}/ppmv for all data plotted in Figure 4.2. There are a few notable exceptions to this correlation. For example, in Figure 4.2 during the period of 19:01 to 19:08 UTC (local eastern daylight time is UTC - 4 hours), and corresponding to the SO_2 spike labeled C, the aircraft was sampling almost directly over Atlanta, and CO concentrations were significantly higher than the surrounding area. The toluene mixing ratio, a measure of anthropogenic VOC emissions, also spiked, and ozone (not plotted) showed a similar trend to CO in this region. In contrast, WSOC remained essentially unchanged in these regions of more fresh emissions suggesting that WSOC is largely not composed of primary vehicle emissions, but possibly indirectly linked to them via SOA formation given the overall high correlation between WSOC and CO on larger regional spatial scales [*Weber, et al.*, 2007].

Table 4.2: For all plumes sampled, percent change in concentration/ratio of various compounds between in-plume and out-of-plume. CO, SO_2, and WSOC compare in-plume concentrations with the mean concentration of 90 seconds of data immediately before and after the plume interception (as determined by 1s SO_2 concentration). Sulfate and ammonium ion compares in-plume conditions with the mean ratio/concentration of one data point just before and after plume interception. In the case of biogenic VOCs and toluene, percent change compares in-plume measurements with average out-of-plume concentrations for entire low-level flyby of Atlanta (Table 4.1) due to insufficient number of data points just outside of individual plumes. With the exception of plumes A and C, plume interception time was less than the time integral of the ion measurement which adds some uncertainty to this measurement.

	Plume A	**Plume B**	**Plume C**	**Plume D**	**Plume E**
Approx. time	18:46:11-18:53:08	18:56:02 - 18:58:44	19:03:39 - 19:07:16	19:41:24 - 19:42:41	19:47:18 - 19:48:30
% ΔCO	-5.1%	1.5%	7.1%	-2.5%	3.4%
% ΔSO_2	651.6%	277.3%	351.1%	345.2%	360.8%
MR, (NH_4^+/SO_4^{-2})	0.9	1.1	1.3	1.3	0.9
% ΔBiogenic VOC	81.9%	n/a	-6.4%	77.7%	-63.8%
% Δ Toluene	-6.2%	n/a	154.8%	-18.2%	-60.6%
% ΔSO_4^{2-}	99.1%	11.1%	24.6%	34.3%	91.3%
% ΔNH_4^+	23.8%	2.6%	5.6%	9.5%	42.9%
% ΔWSOC	-3.4%	1.6%	4.2%	7.2%	5.9%

In-plume versus out-of-plume percent changes in WSOC concentrations ranged from -3.4% to +7.2%. On average across all five plumes, the net change in WSOC concentration was just +0.1μgC m^{-3}, corresponding to a 4.2% increase, which is less than the uncertainty of the WSOC measurement. Focusing on individual plumes as shown in table 4.2, the net WSOC change in plume A was lower in the plume by 3.4%, or 0.1 μgC m^{-3}, despite a low NH_4^+/SO_4^{2-} molar ratio (~0.9). Plumes B and C had slight increases of 1.6% and 4.2%, respectively, (below instrument LOD, and 0.1 μg C m^{-3}, respectively). Plumes D and E had net WSOC increases of 7.2% and 5.9% (or 0.2 and 0.1 μgC m^{-3}, respectively). Plume C is noteworthy in that it was located directly over urban Atlanta where CO and toluene (mobile source emissions) are significantly higher than

surrounding regions, yet little enhancement in WSOC within the plume is observed. Plumes A and E had the lowest NH_4^+/SO_4^{2-} molar ratios observed and hence likely highest aerosol H^+ concentrations, yet increases in WSOC were not significant. In contrast, plume D had the largest increase in WSOC (+0.2 μgC m^{-3}), yet this increase is not greater than the 8% uncertainty of the instrument (see supplementary material). Therefore, these plumes do not provide evidence for measurable SOA under conditions of a more acidic aerosol.

As summarized in Table 4.1, biogenic and anthopogenic VOCs were spatially variable (i.e., large standard deviation for each VOC). Median concentration of toluene, a representative of anthropogenic VOCs that has the potential for SOA formation, was 71 pptv within plumes and 62 pptv outside of plumes. Median biogenic VOCs (isoprene + methacrolein + methyl vinyl ketone) were ~1.1 ppbv within the plumes and 0.94 ppbv outside of the plumes. VOCs, both in and outside the plume, are of sufficient concentration that there should be secondary semi-volatile organic carbon (SVOC) available for SOA formation. However, lack of WSOC enhancement inside the plumes relative to outside the plumes indicates that acid catalyzed formation of secondary organic aerosol is insignificant.

In summary, these limited measurements show that more acidic conditions in freshly emitted power plant plumes with PM1.0 NH_4^+/SO_4^{2-} molar ratios in the range of ~0.9 – 1.4 do not lead to substantial increases in the water-soluble organic component (i.e., SOA) of ambient particles in metropolitan Atlanta, Georgia and the surrounding region.

Despite adequate concentrations of biogenic and anthropogenic VOCs that can lead to SOA formation, preferential heterogeneous acid catalyzed reactions in many of the coal-fired power plant plumes are likely not a major contributor to the secondary organic aerosol formed in the Atlanta metropolitan area and surrounding region. In regions where less NH_3 is available to neutralize sulfate formed from strong point sources (e.g., leading to NH_4^+/SO_4^{2-} molar ratios less than ~1.0), acid-catalyzed reactions may be important. It is also possible that acid-catalyzed SOA formation may occur on timescales that are longer than those observed within the relatively fresh power-plant plumes sampled here, but before the particles are neutralized by ammonia. The results of this study also do not preclude that other regions with a substantially different mix of VOCs may significantly involve acid-catalyzed SOA production. However, the regions sampled in this study contain both anthropogenic and biogenic VOCs suggesting that these results may be applicable to many regions.

CHAPTER 5

INTEX-B

5.5 Introduction

Expanding arid regions and biomass burning in Asia, along with the rapid industrialization of China, has lead to emissions from the Asian continent that are a significant global source of tropospheric aerosols [*Streets*, 2007; *Streets, et al.*, 2003; *Streets and Waldhoff*, 2000]. Numerous studies have investigated the long range transport of Asian mineral dust and pollution [*Bertschi and Jaffe*, 2005; *Huebert, et al.*, 2003, and references therein, Jaffe, 1999 #306; *Jaffe, et al.*, 2003; *Jaffe, et al.*, 2005], including extensive airborne measurements made near the Asian coast during the ACE-Asia [*Huebert, et al.*, 2003] and TRACE-P [*Jacob, et al.*, 2003] research campaigns in the spring of 2001. Other studies have examined transported Asian aerosol as it approached the North American continent [*de Gouw, et al.*, 2004; *Heald, et al.*, 2005; *Jaffe, et al.*, 2005; *Park, et al.*, 2003].

Airborne measurements during TRACE-P and ASIA-ASIA of fine particle chemical composition identified relatively pure and mixed plumes of mineral dust, biomass burning, and anthropogenic emissions. Biomass burning plumes consisted of fine particle ammonium, nitrate, water-soluble potassium, as well as organic carbon and elemental carbon [*Ma, et al.*, 2003]. Anthropogenic plumes were comprised mainly of sulfate and nitrate, with associated ammonium [*Lee, et al.*, 2003], and carbonaceous material that was mainly organic carbon (OC) (Huebert, 2004 #218; Maria et al 2003}. From

soundings conducted off the coast of Asia, sulfate concentrations on average dropped from ~4 μg m^{-3} near the surface to less than 1 μg m^{-3} in the free troposphere. Elemental carbon (EC) had a similar shaped profile (see Heald et al, 2005 and references therein). In contrast, OC concentrations ranged from on average ~ 4 to 5 μg m^{-3} and were fairly uniform from the surface up to the upper measurement range of 6 to 7 km above sea level (asl). This resulted in OC/sulfate mass ratios near one below ~2 km asl, but increased to 3 to 4 in the 3 to ~ 6 km asl altitude range. A similar profile demonstrating the importance of OC in the free troposphere was recently recorded in the anthropogenic-influenced Northeastern United States measured during ICARTT [*Peltier, et al.*, 2007a]

Numerical simulations aimed at understanding the sources and atmospheric processing of sulfate and organic carbon in these study domains demonstrated limitations with current understandings of OC sources and processing [*Heald, et al.*, 2005; *Heald, et al.*, 2006b]. For the ACE-ASIA study, sulfate and EC were well predicted by GEOS-Chem, but OC was significantly under predicted, indicating unknown and unaccounted for OC sources [*Heald, et al.*, 2005]. For the eastern United States data, the OC mass (actually the mass of water-soluble OC) was predicted fairly well by GEOS-Chem, a 3-D model of atmospheric composition, but not the spatial distribution, suggesting a poor understanding of atmospheric processing.

A number of other recent studies have also demonstrated a lack of understanding of OC sources and processing in regions impacted by urban anthropogenic emissions [*de Gouw, et al.*, 2007; *de Gouw, et al.*, 2005; *Johnson, et al.*, 2006; *Volkamer, et al.*, 2006]. These

studies indicated there is a significant yet unknown anthropogenic source for secondary organic aerosol. OC is a substantial fraction of fine particle aerosol mass and a poor understanding of its sources and processing impedes development of control strategies. Understanding OC has been impeded by its chemical complexity, driven by its many sources, ranging from biogenic and anthropogenic emissions that produce both primary or secondary particles [*Jacobson, et al.*, 2000; *Rogge, et al.*, 1993; *Seinfeld and Pankow*, 2003; *Turpin, et al.*, 2000]. This leads to large variations in particle sizes, volatility, and/or solubility, with the result of making quantitative measurements of organic carbon aerosol difficult.

A subset of OC is the fraction that is water-soluble. So-called water-soluble organic carbon (WSOC) is of interest since it may have unique and important health effects and indirect impacts on the planetary radiation balance. Studies focused on WSOC can also reduce the complexity of the carbonaceous aerosol and provide new insights. WSOC has two main sources; biomass burning and secondary organic aerosol formation [*Huang and Yu*, 2007; *Huang, et al.*, 2006; *Sullivan, et al.*, 2006; *Weber, et al.*, 2007]. Primary OC oxidizes as it ages producing a more oxygenated OC [*Zhang, et al.*, 2007] and hence water-soluble OC [*Kondo, et al.*, 2007]. WSOC comprises typically 30-80% (gC gC^{-1}) of OC, with lowest ratios generally recorded near sources and highest ratios in aged air masses [*Decesari, et al.*, 2001; *Jaffrezo, et al.*, 2005; *Zappoli, et al.*, 1999].

In the spring of 2006, airborne measurements were made of the major inorganic ions and the water-soluble organic carbon (WSOC) of submicron ($PM_{1.0}$) aerosol with the goal to

study the impact of transported Asian emissions on the Northwestern United States. This research was part of the National Aeronautical Space Administration (NASA) Intercontinental Chemical Transport Experiment, Phase B (INTEX-B). The National Center for Atmospheric Research (NCAR) C130 research aircraft participated in this study, and was based at Paine Field in Everett, Washington, (47.91°N, -122.28°). The C130 conducted 10 research flights (plus two transit flights) that intercepted emissions mainly from Asia as they approached the North American continent. Research flights were conducted from 21 April 2006 to 15 May 2006. Altitude range of the aircraft extended from ~0.1km to ~7.3km asl, with a nominal flight range of ~1300 kilometers from base. Instruments deployed on the NSF C130 pertinent to this study are discussed in the following section.

5.2 Methods

Fine particle bulk chemical composition was measured online from the C130 with two automated systems, each involving a Particle-Into-Liquid Sampler (PILS). The PILS quantitatively transfers ambient aerosol into a liquid stream that can then be analyzed for specific aerosol chemical components. One PILS was coupled to two Metrohm® Ion Chromatographs (Model 761, Houston, TX), while the second was coupled to a Sievers Total Organic Carbon analyzer (GE Water Systems, Model 800T, Boulder, CO). The first instrument package is referred to as PILS-IC (ion chromatography), and the second as PILS-TOC (total organic carbon). Detailed descriptions of these instruments have been published [*Orsini, et al.*, 2003; *Peltier, et al.*, 2007a; *Weber, et al.*, 2001] [*Sullivan, et al.*, 2006; *Sullivan, et al.*, 2004]. Aerosol was sampled with a constant flow nominally

isokinetic inlet, following the design of Clarke et al [*Huebert, et al.*, 2004b], and was located on the underside of the aircraft roughly three quarters the way aft in the air free stream. This inlet was shared with an Aerosol Mass Spectrometer that extracted a portion of flow upstream of the PILS from the centerline of the 1 inch OD sample transport tube. Aerosol was then passed through a non-rotating multi-orifice impactor [*Marple, et al.*, 1991] that had a nominal particle cut size of 1.0μm at 1 atmosphere. Sample temperature, relative humidity, and pressure were measured, and the sample then divided equally using a "Y" to each PILS operating at ~15 L/min.

5.2.1 PILS-IC

The PILS-IC was operating using either 2.45 minute (cations) or 75 second (anions) chromatographic separation. For cation separation, a 'Cation 1-2' resin column (Metrohm-Peak, Houston, TX) was used. Over a 90 second period, PILS effluent was pumped through a 150 μl sample loop for injection onto the column. Eluent with concentrations of 8.5 mM L-tartaric acid and 4.1mM dipicolinic acid was used to isocratically separate cationic components: sodium, ammonium, calcium, potassium, and magnesium. For this setup, cation limits of detection (LOD) for each species were 0.1 μg m^{-3}, with the exception of potassium ion with LOD 0.5 μg m^{-3}. For anion separation, a 'Metrosep Dual 4 – 25' monolithic column (Metrohm-Peak, Houston, TX) was used. Aerosol sample was continually collected over 60 seconds in a 90 μl sample loop and injected into the column. Eluent of 12.0mM p-cyanophenol, pH adjusted (with 1.0N LiOH) to 7.80 ± 0.05, was used to isocratically separate chloride, nitrate, and sulfate. With PILS liquid flow rates used for this anion setup, limits of detection were chloride

0.1 μg m^{-3}, nitrate 0.02 μg m^{-3}, and sulfate 0.02 μg m^{-3}.

The resulting time interval for one PM1.0 ion composition measurement was a 90-second integrated sample every 2.45 minutes for cations, and a 60-second integrated sample every 75 second for anions. All concentrations have been converted to standard temperature and pressure (273.15°K, 1013.25hPa).

A carbon monolith denuder and a set of etched glass honeycomb denuders (citric acid and sodium carbonate coated) were located immediately upstream of the PILS-IC to eliminate gas interferences. Before each flight, a valve diverted sampled aerosol through a HEPA filter for quantification of backgrounds. Sulfate was the only ionic compound measured with detectable background interference, which was generally constant at 0.015 μg l^{-1} (equivalent to ambient aerosol concentration of ~10 ng m^{-3}). The sulfate background was subtracted from the dataset.

The ion chromatographs were calibrated using known dilutions of NIST-traceable ion standards. Linear calibration curves forced through zero were established using five different standards of anions and cations that bracketed the expected range of concentrations typically observed for the flow rates employed and the estimated ambient aerosol concentration. Both cation and anion systems were calibrated using all five standards at the beginning and middle of the research mission. The anion column was also challenged with a single standard before most flights to verify peak retention time (which was very sensitive to eluent concentration and temperature), as well as peak area.

At the end of the mission, the anion column calibration was re-verified; unfortunately, the cation column failed during the last local flight and could not be calibrated. Sensitivity changed by less than ~5% throughout the duration of the mission for the anion and cation systems, based on the series of calibrations.

5.2.2 PILS-WSOC

A second PILS coupled to a Sievers Total Organic Carbon analyzer quantified PM1.0 WSOC. The PILS was operated to produce a total sample liquid flow rate of 1.2 ml min^{-1}. Following the removal of entrained gas bubbles in the liquid sample, this PILS effluent was aspirated by two glass syringe pumps working in alternating tandem to achieve continuous flow, and pumped through a 0.5μm PEEK filter. Liquid sample was re-equilibrated with cabin pressure by using an inline sample line 'tee' that was open to cabin air. Most of this sample (1.0ml/min) was then drawn into the TOC analyzer via its internal peristaltic pump.

The analyzer converts carbonaceous material to CO_2 (carbon dioxide), and measures the evolved CO_2 by conductivity. Oxidation of organic compounds was achieved by acidifying the sample, and then applying a combination of chemical (ammonium persulfate, 15% w/w, flow rate = 1.5μl min^{-1}) and uv (ν = 184 and 254 nm) oxidation. Tests show that no EC and no insoluble OC larger than ~ 0.1 μm can be quantified with this TOC [*Peltier, et al.*, 2007c]. The instrument was operated in 'Turbo' mode to provide a 3-second integrated measurement every 3 seconds. All concentrations have been converted to standard temperature and pressure (273.15°K, 1013.25hPa).

Immediately upstream of the PILS-TOC, the sample was passed through an activated carbon parallel plate denuder [*Eatough, et al.*, 1999] to removed organic gases. During each flight, a computer-actuated valve was triggered every three hours to diverted sample flow through a Teflon filter for a dynamic blank measurement. In general, before aircraft take off, and just after aircraft landing, the filter system was also manually triggered for blank measurements and to limit contamination associated with aircraft maneuvering while taxiing. A linear interpolation of consecutive blanks was calculated and subtracted from the online dataset to determine ambient WSOC concentrations. Though the instrument is factory calibrated, additional calibrations using 4 different concentrations of oxalic acid was conducted before and after the research mission. Near the middle of the mission, a single calibration standard was measured to verify analyzer sensitivity. In each case, analyzer sensitivity was within 5% of factory calibration.

To provide an assessment of instrument accuracy, measurements of identical species made on the NSF C-130 and NASA DC-8 research aircraft were compared during periods of formation flying. A blind intercomparison from flight 12 (15 May 2006) showed that fine particle sulfate measured online with a mist chamber on the DC-8 was essentially identical to fine particle sulfate measured by the PILS-IC on the C130 (slope: 1.00, $1\sigma = 0.03$, range 0.25 to 1.15 $\mu g\ m^{-3}$; n = 40). The PILS-WSOC was only operated on the C130 and thus could not be compared with a similar instrument on the DC-8.

5.2.3 Other Instrumentation

Additional instrumentation used in this work included a CO monitor using a modified UV resonance fluorescence instrument for 1Hz measurements of carbon monoxide (CO). The Trace Organic Gas Analyzer (TOGA) [*Apel, et al.*, 2003] was employed to measure a suite of 33 oxygenated volatile organic compounds that included: carbonyls, alcohols, and C2-C8 nonmethane hydrocarbons. TOGA is a fast gas chromatograph-mass spectroscopy (GC/MS) that provides a 45-second integrated measurement every ~2.5 minutes. In addition, a variety of organic carbon compounds were detected by whole air sampling (WAS). These samples were subsequently analyzed by gas chromatography, mass spectrometry, flame ionization detection, or electron capture detection, depending on species measured. An onboard Proton Transfer Reaction-Mass Spectrometer (PTRMS) [*de Gouw, et al.*, 2003a; *Lindinger, et al.*, 1998] quantified a variety of organic compounds, including hydroxyacetone and acetic acid. The sampling interval of this instrument was ~33 seconds. Water vapor mixing ratio was measured at 1Hz by an onboard hygrometer. Physical measurements, such as altitude and latitude/longitude were provided by the C130 standard instrumentation package.

5.2.4 Identifying air mass sources

Various sources of measured anthropogenic species were identified with Flexpart, an atmospheric trajectory and particle dispersion model [*Stohl, et al.*, 1998]. Flexpart runs were conducted whenever the aircraft changed latitude or longitude by 0.18 degrees, or when the aircraft altitude changed by ~8-15 hPa. In general, Flexpart runs were completed every ~30-60 s for all research flights.

The Flexpart model provides estimates for the fraction of anthropogenic CO, SO_2, and NO_2 from the following continents: Asia, North America, Australia, South America, and Europe. In this analysis, when Asian CO (as determined by Flexpart) exceeded 75% of total observed CO, the air mass is presumed to consist of mainly Asian emissions. When North American CO exceeded 75% of total CO, the air mass was considered to be influenced mainly by North American sources. CO was chosen as a tracer because of the three anthropogenic species Flexpart predicts (CO, NO_2, SO_2), CO is likely the most inert and hence best tracer to identify long range transport. On average, CO from North America and Asia accounted for >90% of total CO that was predicted by the model indicating little influence from other continental sources. Of the 6078 Flexpart model runs analyzed, ~48% (n = 2931) were delineated as influenced by Asian pollution, ~12% (n = 704) were mainly influenced by North American sources of CO, and the remaining ~40% were not dominated by either source. In the following, Asian, North America, and all data are analyzed.

5.3 Results

During the experiment, each research flight had defined objectives that depended on a variety of factors, including meteorological conditions, satellite overpass schedules, coordination with research flights of other aircraft involved in the INTEX campaign, and most importantly, model simulation predictions on the locations of Asian plumes. Figure 5.1 shows the sampling region. Because most INTEX-B research flights focused on measurements within aged plumes from Asia, the data are not statistically representative

of local aerosol climatology; rather it represents measurements weighed by a focus on aged Asian air masses. On several occasions, air masses that were identified to be mainly influenced by more local sources in North America were encountered. These are analyzed as a subset of the North American data set.

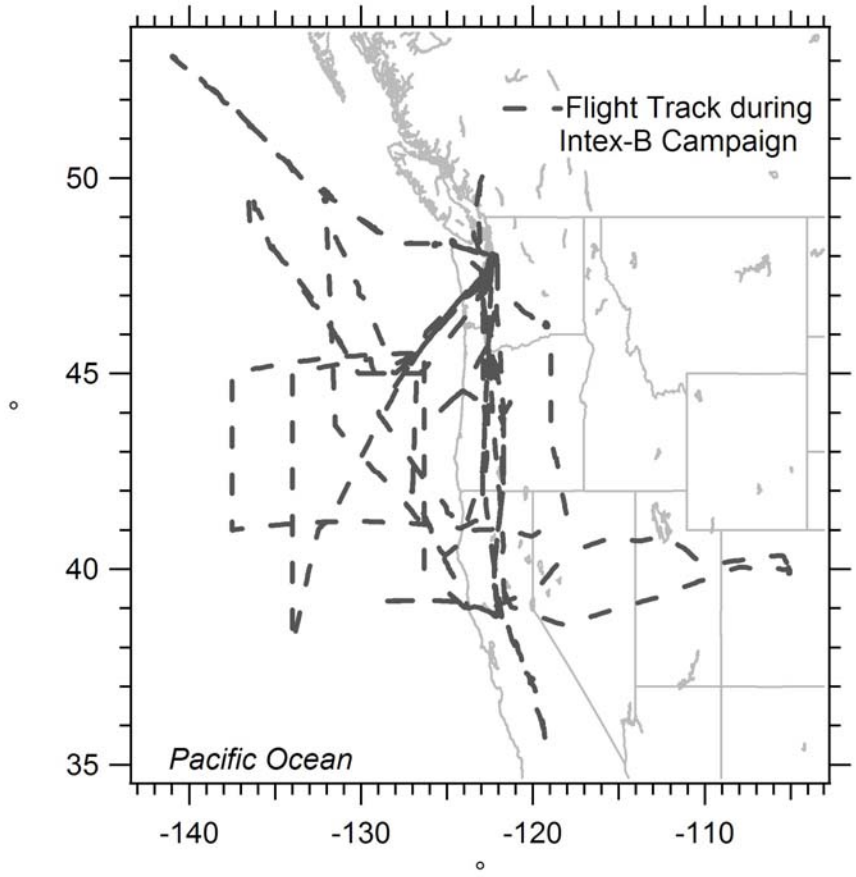

Figure 5.1: NSF C130 research aircraft flight paths. The aircraft was based near Seattle, US (47.91°N, -122.28°) from 21 Apr to 15 May, 2006. Ten local research flights were conducted.

5.3.1 Aerosol composition by continental source

Measured concentrations were generally log-normally distributed and so geometric means and standard deviations are included in the analysis. Of measured components, $PM_{1.0}$ mainly consisted of sulfate and then water-soluble organic carbon, as summarized

in Table 5.1. For all data, median sulfate concentration (± 1σ) was 0.59 ± 0.74 μg m^{-3}, and median WSOC was 0.3 ± 0.8 μgC m^{-3}. Median ammonium concentration was at the detection limit, though mean concentration was 0.2 ± 0.2 μg m^{-3}. Sodium ion was above the detection limit for just 10.2% of observations, and nitrate ion was above the detection limit 5.0% of the time. Calcium and chloride ion were above the detection limit just 0.1% and 0.2%, respectively, and potassium and magnesium ions were not detected during the field campaign. The lack of sea-salt and mineral dust components is consistent with a $PM_{1.0}$ measurement, where these compounds are more frequently observed in supermicron particle sizes [*Fitzgerald*, 1991].

Contrasting air masses with mainly Asian CO sources to North American sources of CO shows that generally both sulfate and WSOC were higher in North American air masses. Median sulfate concentration was 0.84 μg m^{-3} in North American plumes and 0.42 μg m^{-3} in Asian plumes, with substantially more variability in Asian sulfate concentrations (range: LOD to 6.83μg m^{-3} in Asian plumes; LOD to 1.92 μg m^{-3} in North American plumes). This is consistent with large Asian point sources of SO_2. It is noted, however, that our method of identifying North American emissions, based on CO, tends to focus on urban sources located near the west coast of the United States where there are relatively few SO_2 sources.

In contrast to sulfate, median WSOC was a factor of 4 times higher in North American air masses (Table 1) than Asian air masses. Highest concentrations of WSOC could be traced with Flexpart to air masses from the Central Valley of California, as well as the

immediate vicinity of Seattle. Not considering these plumes of highest WSOC concentration, North American plumes still had generally much higher WSOC than Asian plumes (median WSOC without central valley or Seattle plumes was 0.5μgC m^{-3}). California Central Valley plumes are analyzed further in Section 5.3. Plumes from Seattle are not investigated because interceptions were sporadic, recorded briefly during take-off and landing when many instruments were not operational.

Ammonium ion concentration was a factor of two higher in North American air masses compared to Asian air masses. Lastly, mean nitrate ion concentration in North American plumes (0.07 μg m^{-3}) was 7 times higher than observed in Asian air masses (0.01 μg m^{-3}, Table 51), though nitrate was only infrequently observed above LOD for Asia interceptions (1% of measurements were above LOD).

Most of the observations of sulfate and WSOC were representative of more regional conditions. This was especially true for the North American air masses. The ratio of mean to median concentration can provide some indication to the extent of large anomalous plumes in the data set. Interceptions of unique plumes with concentrations significantly above the regional values would lead to mean/median ratios significantly larger than 1. Asian sulfate and WSOC had ratios of 1.6 and 2.5, respectively, whereas North American plumes had ratios of 0.95 (sulfate) and 1.2 (WSOC).

Table 5.1: Statistical summary of PILS observations during INTEX-B field campaign, including all data, observations mainly influenced by Asian emissions, and observations mainly influenced by North American emissions (according to Flexpart continental emissions product). Data includes all 10 local research flights as well as the two transit flights. For measurements below the detection limit, 1/2 the LOD was used in the statistical calculations. Time resolution for ion data is 60 second integral for anions, and 90 second integral for cations. WSOC data has been averaged each Flexpart model run (approx every 30-60 seconds; refer to Flexpart summary for more information). All concentrations are μg m^{-3} for ion data, and μgC m^{-3} for WSOC at standard T and P.

All Data	LOD	n	% above LOD	Median	Mean	1σ	$Mean_{geo}$	$1\sigma_{geo}$	Max	Min
Sodium	0.1	1652	10.2%	0.05	0.09	0.17	0.06	0.66	1.8	0.05
Ammonium	0.1	1846	37.1%	0.10	0.21	0.24	0.08	0.7	3.2	0.05
Calcium	0.1	1664	0.1%	0.05	0.05	0.01	0.05	0.05	0.4	0.05
Potassium	0.5	1664	0.0%	0.25	0.25	0.0	0.25	0.0	0.25	0.25
Magnesium	0.1	1846	0.0%	0.05	0.05	0.0	0.05	0.0	0.05	0.05
Sulfate	0.02	3452	96.7%	0.59	0.77	0.74	0.50	1.10	7.03	0.01
Nitrate	0.02	3464	5.0%	0.01	0.03	0.14	0.01	0.70	1.01	0.01
Chloride	0.1	3452	0.2%	0.05	0.05	0.02	0.05	0.08	1.2	0.05
WSOC	0.1	3644	67.1%	0.3	0.6	0.8	0.25	1.47	5.7	0.1

Asia	LOD	n	% above LOD	Median	Mean	1σ	$Mean_{geo}$	$1\sigma_{geo}$	Max	Min
Sodium	0.1	669	6.7%	0.05	0.08	0.12	0.06	0.56	1.10	0.05
Ammonium	0.1	752	39.9%	0.05	0.16	0.20	0.10	0.93	1.20	0.05
Calcium	0.1	676	0.0%	0.05	0.05	0.00	0.05	0.00	0.05	0.05
Potassium	0.5	676	0.0%	0.25	0.25	0.00	0.25	0.00	0.25	0.25
Magnesium	0.1	752	0.0%	0.05	0.05	0.00	0.05	0.00	0.05	0.05
Sulfate	0.02	1235	96.2%	0.42	0.68	0.82	0.41	1.14	6.83	0.01
Nitrate	0.02	1235	1.5%	0.01	0.01	0.02	0.01	0.29	0.65	0.01
Chloride	0.1	1235	0.2%	0.05	0.05	0.01	0.05	0.06	0.2	0.05
WSOC	0.1	1742	56.5%	0.2	0.5	0.6	0.19	1.37	4.3	0.1

North American	LOD	n	% above LOD	Median	Mean	1σ	$Mean_{geo}$	$1\sigma_{geo}$	Max	Min
Sodium	0.1	110	6.4%	0.05	0.08	0.18	0.06	0.56	1.70	0.05
Ammonium	0.1	119	60.5%	0.10	0.26	0.40	0.14	1.05	3.20	0.05
Calcium	0.1	110	0.0%	0.05	0.05	0.00	0.05	0.00	0.05	0.05
Potassium	0.5	110	0.0%	0.25	0.25	0.00	0.25	0.00	0.25	0.25
Magnesium	0.1	119	0.0%	0.05	0.05	0.00	0.05	0.00	0.05	0.05
Sulfate	0.02	210	98.1%	0.84	0.80	0.34	0.68	0.78	1.92	0.01
Nitrate	0.02	211	0.0%	0.01	0.07	0.38	0.01	0.00	1.01	0.01
Chloride	0.1	210	0.0%	0.05	0.05	0.00	0.05	0.00	0.05	0.05
WSOC	0.1	434	83.4%	0.9	1.1	0.9	0.27	1.24	4.2	0.1

5.3.2 Altitude Profiles of WSOC and Sulfate

To provide a more detailed comparison on the distribution of aerosol composition, and for comparison with other studies, the median WSOC and sulfate altitude profiles are plotted for the Asian and North American air masses. Data were binned into 250m intervals below 2500m, and 500m intervals above this altitude.

5.3.2.1 Asian WSOC and Sulfate

As observed in other studies, Asian air mass WSOC concentrations were highest near the surface. The median WSOC below 3km was ~0.4-0.8 μgC m^{-3}, whereas above this altitude WSOC concentration rapidly decreased to below the limit of detection (0.1 μgC m^{-3}). Measurements of OC on the Asian coast during ACE-ASIA were very different. Huebert et al measured relatively constant OC concentration with altitude [*Huebert, et al.*, 2004a], while Maria et al [2003] measured slightly decreasing concentrations with altitude. In both cases, the OC concentration at higher altitudes ranged from ~2-10 μgC m^{-3}, or approximately 10-20 times higher than WSOC observations at any altitude in our Asian air mass. A number of possibilities may explain the difference. The organic carbon measured in our study may not have been highly soluble and so not detected as WSOC (OC was measured in ACE-ASIA). Emissions from Asia could have been substantially different for these two different study periods. The organic carbon aerosol may have been substantially diluted during transport, or the organic carbon lost, through, for example, precipitation scavenging.

It is unlikely that most of the OC remains insoluble since the air masses were well aged with transport times greater than ~7 days. Aged air has ratios of oxygenated OC to OC, and hence WSOC/OC, typically near 1.0 [*Zhang, et al.*, 2007]. Asian emissions have, if anything, increased in the last few years, so differences in emission cannot likely account for the factor of 10 to 20 lower WSOC measured along the western United States coast. This is further supported by comparisons of CO, an inert tracer for anthropogenic sources. CO recorded from the NASA P-3B aircraft (similar operating altitude range as the NSF C130 of ACE-ASIA) during TRACE-P (held nominally concurrent with ACE-ASIA) had a mean CO of 178.3 ppb ($1\sigma = \pm$ 89.3 ppbv), and median CO was 158.6 ppbv (range: 67-808 ppbv), whereas in this study, INTEX-B Asian air masses had mean CO of 130.7 ($1\sigma = \pm$ 23.9), and median CO was 133.1 ppbv (range: 72-316 ppbv). Assuming emissions from Asia have not substantially changed since Trace-P, this CO data very roughly suggests that pollutant concentrations decreased by 15 –30% by dilution in transport across the Pacific. Based on these arguments it seems reasonable that loss in transport is a major cause for the relatively low WSOC concentrations observed in Asian air masses during INTEX-B.

In contrast to WSOC, sulfate aerosol concentrations in the Asian plumes recorded near North America were relatively constant across the sampled altitude range (Figure 5.2). Figure 5.2 shows that at altitudes below 3km, median sulfate concentration was typically 0.35-0.5 $\mu g\ m^{-3}$. At higher altitudes, median sulfate was 0.40-0.45 $\mu g\ m^{-3}$. This profile is substantially different than the altitude profile that was observed by Lee and coworkers [2003] near the Asian continent, where 8-10 $\mu g\ m^{-3}$ of sulfate was recorded near the

surface and a rapid decrease to ~1-2 μg m^{-3} above 4km. Although the vertical profile is similar, again concentrations were significantly lower after advection, likely due to dilution and loss.

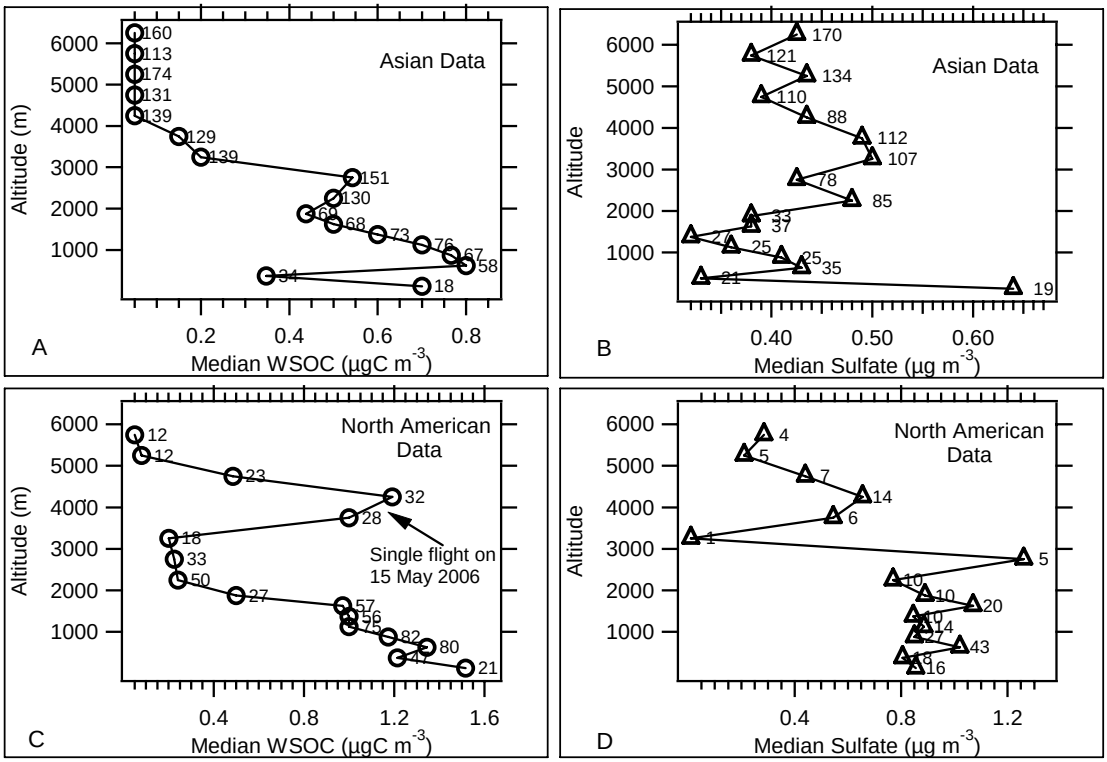

Figure 5.2: Altitude profiles of median WSOC and sulfate concentration. Data is grouped into 250m altitude bins below 2km, and 500m bins above 2km. The numbers on edge of plot is number of observations for each bin

5.3.2.2 North American WSOC and Sulfate

A somewhat similar altitude profile for WSOC was observed when the data is restricted to plumes mainly of North American influence. Overall, WSOC concentration decreased with increasing altitude. Below 2km, WSOC concentration was ~1-1.5 μgC m^{-3} and was mainly due to local Seattle emissions observed during takeoff and landing approaches, as well as some incidental air traffic control transiting. A distinct increase in WSOC concentration was observed between 3-5km. The data were recorded on a single flight

that occurred on 15 May 2006 near Nevada, U.S.A. and was due to air masses from the California Central Valley (this plume is discussed more in Section 5.3.3). At altitudes above ~5km, WSOC concentration decreased to approximately 0.2 μgC m^{-3}. This is higher than similar altitude WSOC concentrations in Asian air masses, which were below the LOD of 0.1 μgC m^{-3}, but similar to the WSOC concentrations of ~0.3μgC m^{-3} at ~ 5 to 6 km altitude reported by Peltier et al [2007a] near the northeastern United States.

For sulfate aerosol, North American air masses were characterized by fairly uniform concentrations below 3 km altitude (~0.8-1.0 μg m^{-3}), and significantly lower concentrations above 3km (~0.4 μg m^{-3}). The free troposphere sulfate concentrations in North America air masses was similar to the free troposphere sulfate from Asian air masses, however, there are significantly fewer data available for an altitude profile of North American sulfate and thus less statistical significance.

5.3.2.3 WSOC Sulfate Ratio with Altitude

As the two main components of fine particles in many regions, the ratio of WSOC to sulfate can provide insight into differences in sources and processing. For example, in the Northeastern United States (NEAQS field campaign), the ratio of WSOC to sulfate was observed to significantly increase with increasing altitude (Figure 5.3) [*Peltier, et al.*, 2007a] suggesting that relative to sulfate, WSOC was either more efficiently lofted, removed less efficiently, and/or produced in situ at faster rates at altitudes between 3 and 5 km. That study concentrated on urban regions of the northeast, as well as a region densely populated with coal-fired power generation facilities located 500-900 km to the

west of New York City. A similar dominance of OC at higher altitudes was also recorded within ~1000 kilometers from the coast of the Korean peninsula, Japan, and the Asian continent during ACE-ASIA [*Heald, et al.*, 2005].

NEAQS and ACE-ASIA observations were of relatively fresh emissions. In contrast, the Asian air masses recorded in this study along the northwestern U.S. coast had undergone long-range transport (6000-7000 km) and the altitude profile of WSOC/sulfate is much different. As shown in Figure 5.3, the INTEX-B Asian WSOC/sulfate profile tends to decrease with increasing altitude with a WSOC/sulfate ratio significantly below 1.0 in the free troposphere. On the other hand, INTEX-B North American observations (e.g. apparently fresher emissions) were similar in trend to the results from NEAQS and ACE-ASIA, with increasing WSOC/sulfate ratios above roughly 2 km asl (Figure 5.3). Free troposphere WSOC/sulfate ratios from North American emissions during INTEX-B were not as high as those observed during NEAQS, This may possibly be a result of Asian influence on the Northwestern United States aerosol climatology, implying background Asian airmasses which are enhanced with sulfate (relative to organics) are mixed with relatively fresh North American emissions. This would result in a lower WSOC/sulfate

ratio, which is consistent with these results.

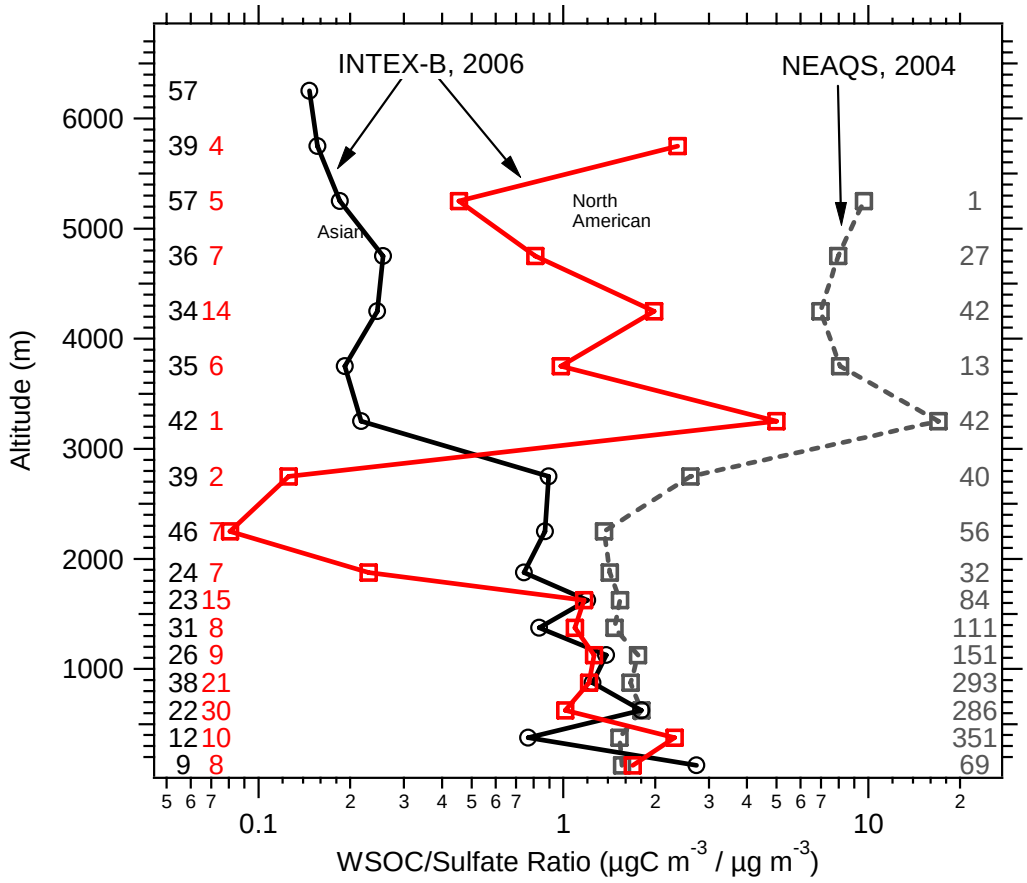

Figure 5.3: Altitude profiles of the ratio between WSOC and sulfate aerosol (PM1.0) as measured by Particle-Into-Liquid Samplers during INTEX-B, including identical measurements in the NEAQS field campaign in New England, US during the summer of 2004 (unpublished data).

The differences in Asian air masses recorded in this study may be due to the effects of Asian transport on WSOC and sulfate. A number of studies have shown that under clear skies, the time constant for secondary organic aerosol (SOA) formation in well defined urban plumes is on the order of ~1 day [*de Gouw, et al.*, 2007; *Sullivan, et al.*, 2006], while the time constant for sulfate formation from SO_2 is larger [*Brock, et al.*, 2007]. Assuming the SOA and sulfate formation time constants described by these studies were

similar for Asian outflow, this mechanism, coupled with precipitation scavenging of aerosols followed by reformation of aerosol during advection from Asia may be responsible for the WSOC/sulfate ratio observed in Asian INTEX-B air masses.

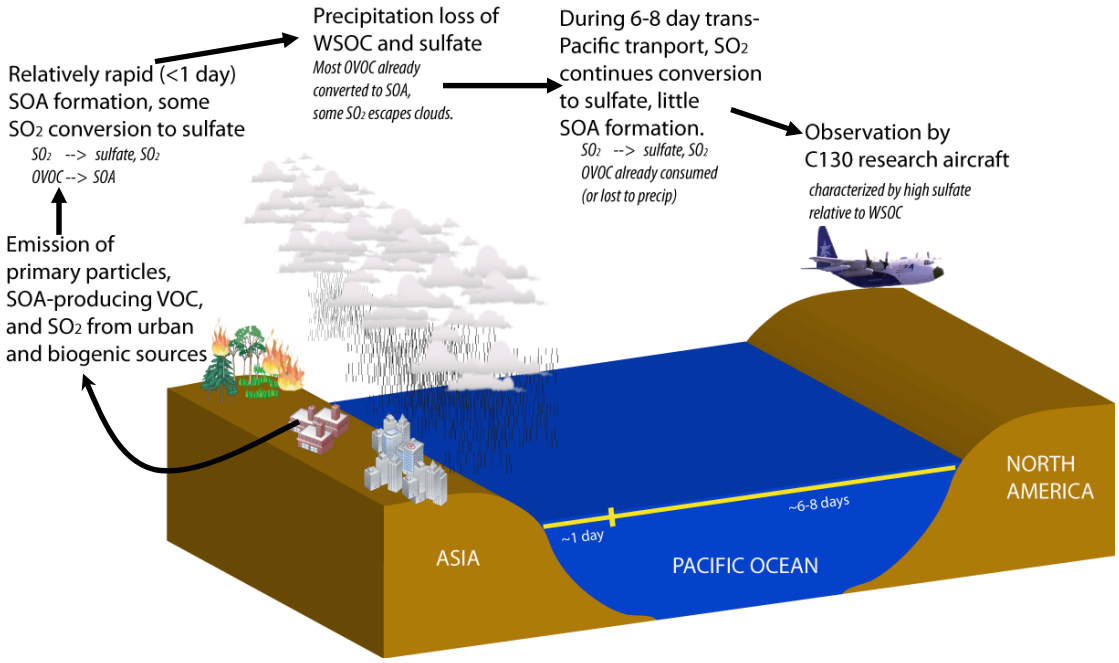

Figure 5.4: Schematic of sulfate and SOA formation near the Asian continent with subsequent precipitation loss and sulfate replenishment during transport. The schematic attempts to explain the differences in observed WSOC/Sulfate ratios recorded near Asia in other studies, and Asian air masses recorded near North America during this study

Eastern Asia and the north central Pacific Ocean regions were subjected to significant precipitation and cloud cover during the INTEX-B study period, according to infrared satellite images of convective influence (http://bocachica.arc.nasa.gov/INTEX_2006/index.html). Figure 5.4 shows schematically a possible explanation for observed differences between WSOC and sulfate at various locations that involve a combination of aerosol formation, loss, and replenishment. If most anthropogenic SOA (hence WSOC) is formed rapidly downwind

of urban regions [*de Gouw, et al.*, 2007; *de Gouw, et al.*, 2005; *Sullivan, et al.*, 2006], much of the WSOC could be lost by precipitation scavenging during advection to North America. Any primary WSOC from biomass burning and sulfate formed prior to precipitation would also be lost. However, aerosols can reform if the precursor gases penetrate the region of precipitation. Measurements show that because SO_2 is not highly water-soluble, sulfate can be reformed down-wind of precipitating clouds [*Brock, et al.*, 2004; *Weber, et al.*, 2001]. Our observation that WSOC concentration was much lower relative to sulfate in the Asian air masses measured near the northwestern United States suggests that there was little reformation of WSOC in comparison to sulfate. One would expect that some VOCs may also penetrate the clouds, but if this line of reasoning is correct, they apparently do not lead to significant concentrations of SOA. The overall result is that Asian sulfur emissions may be more readily transported long distances than organic aerosols precursor VOCs and hence sulfate will tend to dominate Asian anthropogenic impacts in North America.

5.3.3 Investigating sources of WSOC

As the two main components of $PM_{1.0}$ in this study, the sources of sulfate and WSOC are of interest. Sulfate sources are well established and generally well predicted in model simulations [*Heald, et al.*, 2005; *Nowak, et al.*, 2006], whereas this is not the case for carbonaceous aerosols, especially organic carbon. For this reason, possible sources for WSOC measured in this study are now investigated.

5.3.3.1 WSOC and CO and water vapor

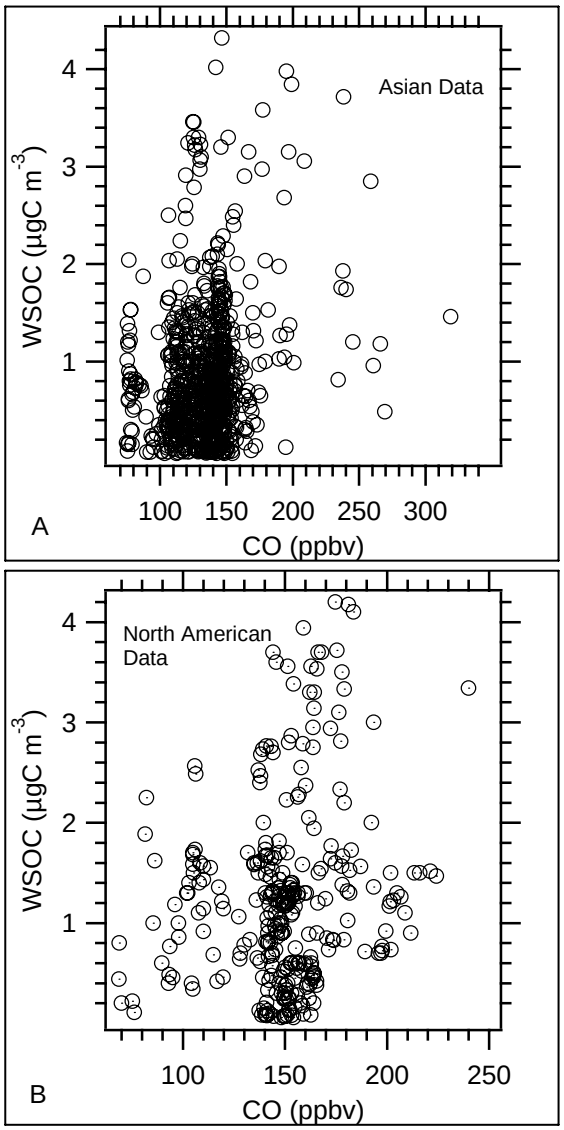

Figure 5.5: Univariate regression analysis of WSOC and CO for data is segregated into Asian (A) and North American (B) background air mass data.

Our previous work focusing on SOA formation in urban plumes showed a strong correlation between WSOC and CO [*de Gouw, et al.*, 2007; *Sullivan, et al.*, 2006; *Weber, et al.*, 2007] indicating that WSOC and CO sources were strongly linked in some manner. Those studies involved airborne measurements in relatively fresh well defined urban

plumes (aged <4 days). In contrast, these INTEX-B measurements of well-aged Asian air masses that had undergone trans-Pacific transport (> 7 days), and North American air masses mainly representative of background conditions, WSOC and CO were not correlated (Figure 5.5, $r^2 = 0.06$, 0.08, respectively) and WSOC could not be linked to specific sources using this method. However, there were two notable interceptions of plumes in the North America data set where enhancements in WSOC concentrations could be linked to a specific source region. On 3 May 2006, measurements were made in the vicinity of the California Central Valley and air trajectory analysis suggested an observation of Central Valley plumes of 1-2 days old. These plumes were intercepted at 21:50:30-22:05:00 UTC and again at 22:16:00-22:33:30 UTC at an altitude range of ~600 m asl. On 15 May 2006, between 20:51 and 22:10 UTC, a region of enhanced WSOC concentration was intercepted over northern Nevada at an altitude of 3 to 5 km asl. This plume can be seen in North American median WSOC profile of Figure 5.2. Flexpart indicated plumes from the Central Valley that were 2-3 days old. Maps showing the locations of both plumes is given in Figure 5.6. The low altitude fresher plume was detected in clear sky with broken cloud cover at altitudes of 6.4 km asl, based on archived METARs from the Central Valley during the flight (available online at: http://vortex.plymouth.edu/sa_parse-u.html). In contrast, the second plume from the central valley was recorded down-wind of a heavily clouded region, based on both video and satellite data (cloud optical thickness based on MODIS aqua).

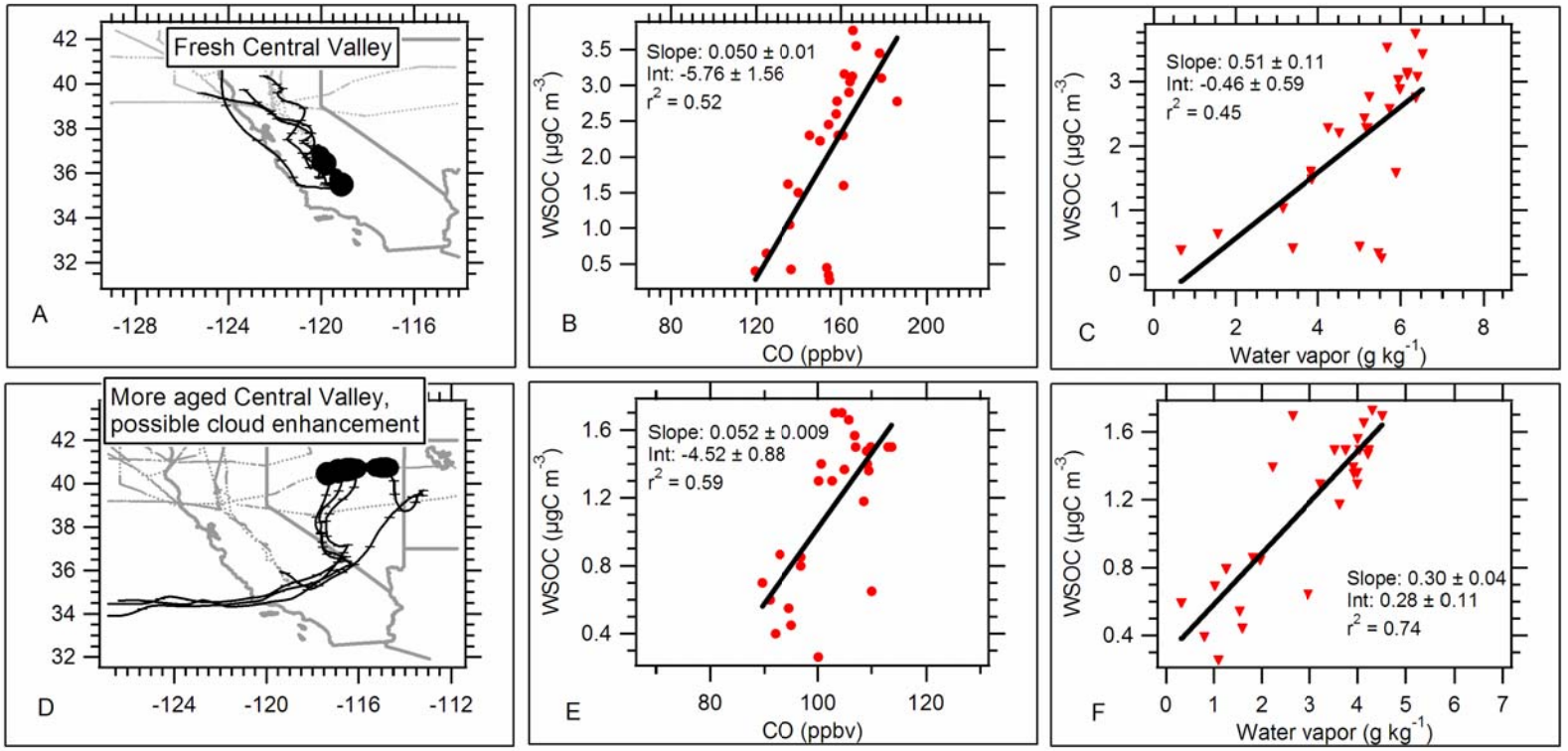

Figure 5.6: A) Location of relatively fresh, low altitude Central Valley plumes with 96 hour HYSPLIT back trajectories. Shaded box represents Central Valley; B) Univariate regression analysis of WSOC and CO; C) WSOC and water vapor for Central Valley California plumes; D) Location of Central Valley plume (black circles) over Nevada with 96 hour HYSPLIT back trajectories. Shaded box represents Central Valley, and cartoon represents region of clouds; E) Univariate regression analysis of WSOC and CO; F) WSOC and water vapor for cloud-influenced Central Valley California plumes

For each flight, WSOC and CO were moderately correlated (Figure 5.6). The correlation coefficient between WSOC and CO during the flight over the Central Valley was 0.52. The Central Valley plume that was intercepted after transport to the northern Nevada region had a higher correlation of $r^2 = 0.59$. Univariate linear regression slopes of 50 ± 10 μgC m^{-3} / ppmv and 52 ± 9 μgC m^{-3} / ppmv, respectively, are also similar to the range of slopes reported for New York City, United States [*Sullivan, et al.*, 2006] and Atlanta, United States, [*Weber, et al.*, 2007] urban plumes. This finding supports a linkage between WSOC and fossil fuel combustion (i.e. CO as a nonspecific tracer of combustion), especially in the case of the more aged plume observed in Nevada.

Correlation between WSOC and water vapor in these plumes was also noteworthy (Figure 5.6). Studies have shown that SOA formation may readily occur in aqueous solutions and may be enhanced by higher relative humidity [*Altieri, et al.*, 2006; *Carlton, et al.*, 2006; *Lim, et al.*, 2005; *Matsunaga, et al.*, 2005]. Water vapor and WSOC are moderately well correlated during the observation above the Central Valley (Figure 5.6, $r^2 = 0.45$), and highly correlated in the observation over northern Nevada ($r^2 = 0.74$) downwind of clouds. These plumes are further discussed in Section 5.3.3.3. In an attempt to discern contributions of anthropogenic and biogenic sources to the WSOC observed in the Asian and North American air masses, and the central valley plumes, a multivariate regression analysis is performed.

5.3.3.2 Multivariate regression to investigate WSOC sources

Measured VOCs, when compared with WSOC, may provide insights into specific WSOC sources. The previous analyses have focused on comparisons of WSOC with single variables (e.g. CO, water vapor, altitude, etc). In order to further identify WSOC sources, a multivariate linear regression model of WSOC and VOC data was constructed. Principle component analysis (PCA) is often used to identify general sources that impact ambient field studies that would not be apparent from a single correlation analyses [*Hopke, et al.*, 1998; *Hopke, et al.*, 2003; *Kim and Hopke*, 2007; *Millet, et al.*, 2005; *Millet, et al.*, 2004; *Quinn, et al.*, 2006, Millet, 2006 #358; *Shim, et al.*, 2007; *Wang, et al.*, 2000]. PCA is used to reduce a large number of variables into smaller and more meaningful sets of variables that account for most of the observed variability in the dataset. Known sources for compounds can then be used to identifying the source for each principle component. This is particularly useful when a large number of variables are correlated. A disadvantage to this technique is that inferences from specific variables are limited because they have been grouped together with like variables. Multivariate linear regression directly relates a dependent variable to a specific set of independent variables. In these techniques, variable coefficients can be compared to one another to provide some indication on the relative importance of each variable. However, a significant disadvantage to this technique is that its results are largely dependant on the variables that are chosen for the regression analysis. The multivariate regression model is described in equation 1, where β_0 is the intercept, and β_1 to β_i are the regression coefficients for independent variables x_1 to x_i.

$$y = \beta_o + \beta_1 x_1 + \beta_2 x_2 + \ldots \beta_i x_i \quad (1)$$

There were a number of VOC measurements made aboard the C130 research aircraft that can be used as tracers of fossil fuel combustion or biogenic (including biomass burning) emissions. Fossil fuel combustion VOCs chosen for this analysis were mainly alkanes and aromatics. Biogenic VOCs were mainly alcohols and organic acids, and also included acetonitrile, a gas tracer for biomass burning. The VOCs selected for fitting with WSOC are summarized in Table 5.2. While none of the selected VOCs are perfect unique tracers for fossil fuel combustion, biomass burning, or biogenic-non-biomass burning sources, compounds that have been shown to be emitted by mainly fossil fuel combustion or mainly biogenic sources were selected [*Guenther, et al.*, 1995; *Heikes, et al.*, 2002; *Jacob, et al.*, 2002; *Jacob, et al.*, 2005; *Lewis, et al.*, 2005; *Singh, et al.*, 2004; *Spaulding, et al.*, 2003]. For example, acetonitrile does have some small industrial sources, and may be formed as a secondary compound, but the largest source of acetonitrile in the atmosphere is from biomass burning [*de Gouw, et al.*, 2003a; *Reiner, et al.*, 2001].

Table 5.2: Summary of independent variables used to fit multivariate regression model. The VOCs are separated into either mainly from fossil fuel combustion, or biogenic sources, which includes biomass burning (acetonitrile) and secondary VOCs lined biogenic emissions.

Fossil Fuel VOCs	Biogenic VOCs
1,1,1-trichloroethane	Methyl chloride
Methylethylketone	Methanol
Isopentane	Hydroxyacetone
Pentane	Acetonitrile
Butane	Isoprene
Acetaldehyde	Acetone
Isobutane	Acetic Acid
Toluene	
Benzene	
Methyl tertiary butyl ether	
Isopropyl nitrate	
o-xylene	
n-pentane	

Prior to regression analysis, the data were converted from a near lognormal to a near normal distribution by calculating the natural log for each data point for all variables. Subtracting the geometric mean concentration or mixing ratio from each measurement, and then dividing by the variable geometric standard deviation, standardized the dataset for each variable. This shifts the mean of the sample to 0 and standardizes the data variability (e.g. $1\sigma = \pm 1$, $2\sigma = \pm 2$, etc). The transformation eliminates potential bias introduced into the model caused by the wide range of concentrations observed in the dataset, giving equal weight to all variables independent of magnitude. Model coefficients can then be compared to one another without consideration to original concentration of the variables [*Kim and Ferree*, 1981]. Our interest here is not so much

on the specific VOCs with highest coefficients, but instead the source of VOCs with highest coefficients (e.g., fossil fuel, biogenic, biogenic from biomass burning).

Backward stepwise multivariate linear regression analysis was performed on the data to model WSOC concentration, where a variable was included when the t-statistic exceeded 2 (i.e., significant at the 5% level). The variables were also checked for multicollinearity and if found, one variable was removed from the model to eliminate redundancy. The independent variables listed in Table 5.2 were used to analyze the dataset, and includes many VOCs that have atmospheric lifetimes greater than the expected transport time from Asia (~5-8 days). Fossil fuel and biogenic VOC variables were combined in the regression model to predict WSOC variability. It should be noted that this analysis does not predict whether specific VOCs form WSOC, rather it uses VOCs as tracers to describe conditions when WSOC can be observed.

As a result of using a linear multivariate regression analysis, it is not likely that the model will fully capture WSOC variability. The C130 research aircraft was equipped to measure just ~60 different VOCs by several different analytical techniques. Since WSOC formation involves highly complex and as of yet, largely unknown VOC chemistry, there are undoubtedly a number of VOCs that play an important role in WSOC formation but were not included in the regression.

Table 5.3 summarizes the multivariate regression analysis for INTEX-B data that is mainly influenced by Asian emissions. The combined VOC sources of WSOC account for 49.3% of the observed variability. Thus, a significant fraction of WSOC variability is

unaccounted for in this analysis. Several factors that were not quantified could explain the missing variability in the regression model. For example, variability in how WSOC aerosol was depleted during transport that differed from impacts on the VOCs. Similarly, VOCs may have been transformed in ways that do not lead to WSOC formation, resulting in a change in VOC concentration but no change in WSOC. Also, since observed WSOC concentration in Asian air masses was frequently below the limit of detection, it is not surprising that this model does not capture all of the variability for well-aged (and traveled) air masses. Regression analysis of North American air masses yielded different results (Table 5.3). Overall, these covariates explain 75.7% of the WSOC variability.

Comparing the standardized regression coefficients (Table 5.3) may provide some insight into generalized sources of WSOC. The absolute values of coefficients have been ranked from largest to smallest (Table 5.3). The absolute value is used since any process that leads to WSOC variability is of interest. For example, a negative coefficient could imply that the processes that produce WSOC is also in some way linked to loss of that VOC. A positive coefficient could result if the VOC and WSOC have similar sources. This points out a limitation with this method that introduces some uncertainty for this analysis; some covariability of a VOC with WSOC may not be linked to WSOC formation in any physical manner. For example, WSOC formed in high oxidizing environments can lead to more WSOC, but some VOCs may also be lost, independent of the VOC source (biogenic or anthropogenic).

Fossil fuel combustion VOC tracers are most closely associated with WSOC concentration in Asian plumes (Table 5.3). Isobutane, methyl ethyl ketone (MEK), and isopropyl nitrate coefficients are significantly larger than the remaining regression variables (it is noted, however, that all variables in this analysis are significant since each has been evaluated by student *t*-test). The remaining coefficients, including acetonitrile, a biomass burning tracer, contribute to variability in WSOC, but fossil fuel combustion VOCs explain most of the variability that could be accounted for in this model.

In contrast, North American WSOC is more closely associated with both biogenic and fossil fuel combustion VOCs. Pentane and hydroxyacetone are the largest contributors to WSOC variability. Pentane is a VOC associated with fossil fuel combustion, and hydroxyacetone is a photo oxidation product of isoprene [*Yu, et al.*, 1995]. Other significant fossil fuel combustion VOCs that contribute to WSOC variability include isobutane and acetaldehyde. Significant biogenic VOCs include acetone, acetic acid, and methyl chloride. These results suggest that both biogenic (but not biomass burning) and anthropogenic sources contributed to WSOC variability in North American air masses. In the North American data set, acetonitrile contributed no significant influence, indicating a limited influence on WSOC by biomass burning.

The contrast between the regression results for Asian versus North American air masses is also consistent with expectations. Higher anthropogenic sources of WSOC relative to biogenic sources in Asian air masses versus northwestern United States air masses are expected, given the proportions of anthropogenic and biogenic sources in the two regions.

Asian emissions from more northern regions (e.g., China) advected westward are heavily influenced by large population centers in, whereas the northwestern United States is not highly populated but is heavily forested.

`

Table 5.3: Regression coefficients for selected VOC independent variables described in Table 5.2. Data has been split (using Flexpart) into air masses mainly influenced by North America, and air masses mainly influenced by Asia.

Asian data			**N American data**		
Significant VOC	Model Coefficient, β_i (Standard error)	Adjusted Model R^2	Significant VOC	Model Coefficient, β_i (Standard error)	Adjusted Model R^2
Isobutane	1.16 (0.27)	49.3%	Pentane	1.43 (0.60)	75.7%
MEK	-0.94 (0.33)		Hydroxyacetone	-1.27 (0.25)	
Isopropyl nitrate	0.90 (0.23)		Isobutane	-1.18 (0.44)	
Isopentane	-0.51 (0.34)		Acetaldehyde	1.18 (0.51)	
Acetaldehyde	0.37 (0.18)		Acetone	-0.87 (0.55)	
1,1,1-trichloroethane	0.33 (0.14)		Acetic acid	0.59 (0.22)	
Acetonitrile	0.27 (0.16)		Methyl chloride	0.56 (0.19)	
Constant, β_0	0.00 (0.15)		Constant, β_0	0.30 (0.31)	

5.3.3.3 Regression Analysis on WSOC Central Valley plumes

The regression was performed in the same manner for the two California Central Valley plumes encountered during INTEX-B. The first Central Valley plume (low altitude measurements made over the valley) was characterized by elevated VOCs and WSOC (2-4 $\mu gC\ m^{-3}$). Due to data availability limitations, hydroxyacetone and acetic acid (both biogenic VOCs) are not included in the analysis. There are, however, a number of other VOCs included in the regression analysis (Table 5.2) that can be used to identify biogenic sources. Thus, we may not be able to directly compare these results with the Asian and North American air mass regressions. Methylethylketone (MEK), methanol, and pentane are statistically significant VOCs that were identified in the regression model predicting

WSOC variability (Table 5.4). Methylethylketone and pentane are associated with fossil fuel combustion. In contrast, methanol sources are predominately biogenic, though there is evidence of small sources related to fossil fuel combustion [*Jacob, et al.*, 2005] (methanol from fossil fuel combustion accounts for ~1-2% of global methanol loading). Comparing coefficients (again, using the absolute value), biogenic sources are similar (0.97 ± 0.13) to fossil fuel combustion sources ($\Sigma_\beta = 1.74 \pm 0.46$ by RMS) for WSOC variability, suggesting that in the Central Valley, WSOC is controlled by both fossil fuel combustion and biogenic sources of VOCs. This model accounts for ~98.2% of the variability of WSOC (Table 5.4).

Table 5.4: Regression coefficients and statistics for selected VOC independent variables described in Table 5.2. Data is from a single plume during a flight on 3 May 2006 in the Central Valley of California.

Parameter	b-coefficient	Standard error	t-statistic	P-Value
MEK	-1.22136	0.429068	-2.84655	0.0159
Methanol	0.97262	0.130999	7.42463	0
Pentane	0.52521	0.174838	3.00398	0.012

Adjusted model $R^2 = 98.2$

The second Central Valley plume intercepted over northern Nevada in a region downwind of clouds was characterized by elevated WSOC concentrations (1-2μgC m^{-3}), elevated oxygenated VOCs (e.g. methanol, acetic acid, acetone), and CO, and relatively low anthropogenic VOCs (e.g. benzene). For this plume, a number of statistically significant VOCs were observed in the multiple regression model of WSOC variability. Methanol and hydroxyacetone – both biogenic VOC tracers - comprise the largest coefficients of all parameters tested (Table 5.2). MEK and 1,1,1-tricholorethane, which

are associated with fossil fuel combustion, and acetone (a biogenic tracer) have similar β-coefficients (Table 5.5), and are somewhat less important. Lastly, pentane and benzene, two VOCs associated with fossil fuel combustion, are also significant determinants of WSOC variability, though their β-coefficients are considerably smaller that the other VOCs (Table 5.5). The model accounts for 92.6% of the variability of WSOC during this plume. By summing the significant VOCs by their β-coefficient, biogenic sources appear to be most responsible for WSOC variability, though fossil fuel combustion VOC tracers also appear to be involved.

Table 5.5: Regression coefficients and statistics for selected VOC independent variables described in Table 5.2. Data is from a single plume during a flight on 15 May 2006 in northern Nevada. Cloud processing is likely evident in this plume.

Parameter	β-coefficient	Standard error	*t*-statistic	P-Value
Methanol	-9.60911	2.54281	-3.77893	0.0129
Hydroxyacetone	6.06393	1.4457	4.19446	0.0085
MEK	4.87372	1.29285	3.76975	0.013
1,1,1-tricholoroethane	4.82808	1.37575	3.50941	0.0171
Acetone	4.33436	1.42781	3.03566	0.0289
Pentane	-2.78377	0.647055	-4.30222	0.0077
Benzene	-2.14162	0.788449	-2.71624	0.042

Adjusted model R^2 = 92.6

Despite having similar source regions (i.e. Central Valley), WSOC for each plume appears to have a different association with VOCs. Based on visual and satellite evidence of clouds in the vicinity during the Nevada flight segment, higher correlations with water vapor (Figure 5.6), and differences in altitudes at which the two Central Valley plumes were detected, the Nevada plume is much more likely to have been influenced by cloud processing. This may account for the differences in multiple regression results. In the cloudy region, the overall analysis results is suggestive of

WSOC formation by heterogeneous processes involving liquid water and biogenic VOCs, as has been proposed in a number of other studies [*Baltensperger, et al.*, 2005; *Hartz, et al.*, 2005; *Hastings, et al.*, 2005; *Lim, et al.*, 2005; *Na, et al.*, 2006; *Pun, et al.*, 2002; *Pun, et al.*, 1999; *Tsigaridis and Kanakidou*, 2003; *Varutbangkul, et al.*, 2006]. This type of mechanism may, at least in part, explain the generally higher WSOC/sulfate ratios (e.g., Figure 5.3) observed in free troposphere continental air masses in this and other studies [*Peltier, et al.*, 2007a], and given the difficulty of simulating cloud processes, may explain poor model prediction of free tropospheric organic aerosol mass and spatial distributions [*Heald, et al.*, 2005; *Heald, et al.*, 2006b]. Furthermore, it may also explain the larger regression slope of ΔWSOC/ΔCO (52 ± 9 μgC m^{-3} per ppmv, Figure 5.6) compared to the plume observed directly over the Central Valley (34 ± 6 μgC m^{-3} per ppmv) despite apparently similar emission sources. The latter Central Valley results of ΔWSOC/ΔCO = 34 ± 6 μgC m^{-3} per ppmv are consistent with other urban studies [*Sullivan, et al.*, 2006; *Weber, et al.*, 2007].

5.4 Conclusions

Airborne measurements in spring 2006 of fine particle ($PM_{1.0}$) bulk chemical composition were made from the surface to ~7 km attitude over Western United States and Canada, and the Eastern Pacific Ocean. The online measurements included ionic species chloride, nitrate, sulfate, sodium, ammonium, potassium, calcium and magnesium, and the water-soluble organic carbon (WSOC) fraction of the organic aerosol. Data were analyzed separately according to continental source by using the

Flexpart dispersion model to identify continental influence. A particular emphasis on WSOC sources is discussed.

Submicron aerosol mass was dominated by water soluble organic carbon and sulfate, with additional contribution to mass by ammonium, nitrate and sodium ions. WSOC concentration was highest in North American air masses (median = 0.9 μgC m^{-3}), and lower in Asian outflow (median = 0.2 μgC m^{-3}). Overall, sulfate aerosol had similar concentrations for Asian and North American observations.

WSOC concentration was highest at lowest altitude ranges in both North American and Asian air masses, though several spikes in particular altitude ranges were observed. WSOC was also compared to sulfate concentration, and analyzed across altitude. Contrary to previous findings near Asia and near the Northeastern United States, the ratio of WSOC-to-sulfate in aged Asian air masses tended to decrease with altitude. We propose this was likely caused by precipitation loss of aerosol prior to observation, and then replenishment of sulfate aerosol as the air mass was transported across the pacific. Since observations were generally not of fresh, urban emissions, WSOC and CO were poorly correlated. However, in distinct plumes, WSOC and CO were well correlated. A similar finding was observed when comparing WSOC with water vapor mixing ratio.

Both Asian and North American plumes were investigated by multivariate regression analysis using a number of tracer VOCs that were representative of fossil fuel combustion or biogenic emissions (including biomass burning). In Asian air masses,

VOCs that are mainly from fossil fuel combustion sources were most closely related to WSOC variability. Biogenic VOCs did not substantially contributed to the observed variability of WSOC in Asian air masses. However, the regression model has significant variability that can not be explained by the measured VOCs, and this is likely related to the long transport time and possible meteorological transformations affecting Asian aerosols. In contrast, a multivariate regression of North American aerosols shows that WSOC variability is driven by a combination of fossil fuel combustion and biogenic VOCs. This regression model explained a greater amount of WSOC variability (~75%).

North American air masses were further refined to include only Central Valley outflow by comparing a relatively fresh plume (aged 1-2 days) with a somewhat aged (2-3 days) plume that may have been processed by nearby clouds. In the case of the relatively fresh plume, by multivariate regression analysis, both biogenic and fossil fuel combustion VOCs were nearly equally responsible for WSOC variability. In contrast, biogenic VOCs appear to have a significantly stronger association with WSOC variability in a plume with stronger evidence for cloud processing. This may also have resulted in a significantly higher ΔWSOC/ΔCO regression slope for cloud-processed air masses, despite having similar emission sources, and higher than what has been observed in other urban plumes. Cloud processing of biogenic VOCs may be an important mechanism for free tropospheric WSOC formation explaining enhanced WSOC concentrations above ~ 2km altitude.

CHAPTER 6

FUTURE WORK

While the PILS-OC technique appears quite useful for fast measurements of OC, there still remains the unanswered question related to the apparent intercept when compared with the Sunset Labs ECOC instrument (Chapter 2). As stated, this intercept may be related to a SVOC background caused by penetration through the denuder leading to positive artifacts in the Sunset Labs OC measurement, or may result from the inability by PILS-OC to detect large, insoluble particles. It is especially interesting that this intercept appears to be larger in regions with larger fractions of mobile sources emissions (e.g. Mexico City > Riverside > Atlanta). A better characterization of this intercept – whether caused by PILS-OC inefficiency or SVOC penetration – is very important because it has significant operational considerations for the Sunset Labs OC analyzer, the PILS-OC technique, or both methods.

A number of improvements could be explored for collecting and analyzing data with a PILS-IC. For example, some uncertainty is introduced into the measurement by the fact that each ion peak in a chromatogram must be integrated by hand. While proprietary software does exist to automate peak detection, it is neither easy to use nor perfectly accurate when selecting peak areas. Thus, the individual operator must check each chromatogram to verify accuracy, a task that is extremely labor intensive and time consuming. This is of particular interest during field measurement campaigns where timely, accurate dissemination of field data is crucial. Furthermore, since different users

may integrate the data differently, bias in calculating peak areas may be introduced. I would encourage future studies to develop an offline, automated method of peak detection and integration, which would improve data turnaround time and reduce operator bias of the data.

Organic carbon aerosol persists at the forefront of aerosol science. Its chemical composition continues to be poorly understood, and in fact, there is still significant uncertainty and disagreement for measurement methodology of bulk carbonaceous material (e.g. bias of volatility concerns, adsorbed SVOCs, etc). Broad classification techniques, such as those described by Sullivan, et al and Sannigrahi, et al [*Sannigrahi, et al.*, 2006; *Sullivan and Weber*, 2006a; b] represent excellent starting points for improved techniques for OC identification. Techniques for classifying organic carbon aerosol, such as by XAD-8 resin separation coupled to SEC (size-exclusion chromatography) categorization are useful because they can be used to group organic aerosol by basic functional groups (e.g. hydrophobic, hydrophilic, and then acidic, basic, or neutral). For example, using these techniques, Sullivan et al [2006a; 2006b] has shown that short chain (less than C-5) aliphatic acids are the dominant secondary organic aerosol product of WSOC in Atlanta during the summer, which is consistent with secondary organic carbon aerosol formation. Though there are limitations to this technique (most notably, relatively high carbon mass requirements for full aerosol recovery by the SEC column), it provides considerable insight into OC aerosol functional groups. While much of the work by Sullivan and Weber was conducted in the laboratory (especially the SEC-related studies) on filter-based samples, full integration of these techniques into online methods

would vastly improve our understanding of organic carbon aerosol by providing specific insight into aerosol sources. Online measurements are advantageous over filter-based methods for mobile sampling of spatially distributed plumes (e.g. aircraft studies) or relatively short time duration SOA formation events. This can be achieved by miniaturizing the inline columns, as well as possibly using preconcentration columns upstream of the sample in order to achieve required mass loading.

Heald et al [2005] noted a significant deviation between observations of organic material at high altitude with model predictions (specifically, with the GEOS-Chem model) in the altitude range of 0-7km. Overall, models can reasonably predict aerosol concentrations – especially for inorganic ions and dust [*Dentener and Crutzen*, 1994; *Pankow*, 1994]. While the poor model/observation correlation may be related to the uncertainty of OC observations, model predictions are frequently off by orders of magnitude and thus need substantial enhancement. Since OC aerosol comprises a large fraction of aerosol mass loading, continued observations – particularly at high altitudes aboard aircraft platforms or mountain-top ground stations – would provide much-needed quantitative results that can be used to improve the understanding of model design. While this (and other) work provides a significant quantity of data with respect to organic aerosol at altitude, it is but a fraction of ambient mass loading and represents only discrete periods of time during sampling. Ideally, development of remote sensing techniques that are sensitive to organic carbon aerosol would provide useful information for model development, and perhaps to future aircraft aerosol observation mission planning. Ideally, one could develop small, quantitative instruments that measure aerosol composition for continuous deployment in

the ambient environment. For example, they could be deployed aboard commercial ships and airplane, much like the current Aircraft Meteorological Data Relay which transmits meteorological information from commercial airplanes to worldwide, governmental weather monitoring and prediction agencies.

CHAPTER 7

CONCLUSIONS

Comprised of a myriad of anthropogenic and biogenic sources, aerosol has a number of effects on our environment ranging from human health impacts to global climate change. After formation, aerosol undergoes substantial transformation as it is transported though the atmosphere by the environment. This leads to substantial chemical complexity in the atmosphere. One way to address this is by quantitative, high time resolution measurements of $PM_{1.0}$ aerosol aboard research aircraft.

As a significant portion of this thesis, a large fraction of observations were made by deployment of a Particle-Into-Liquid sampler aboard aircraft research platforms in North America. This allows for quantitative measurements of submicron aerosol, which, by mass, is mainly organic carbon and ammonium sulfate. Organic carbon aerosol is of particular interest because it continues to be poorly understood, largely because of its numerous sources and high chemical complexity. Ammonium sulfate aerosol is better understood, but plays a significant role in ambient mass loading and aerosol chemistry, particularly in the United States. Aircraft platforms are advantageous because it allows an opportunity to observe aerosol in a range of atmospheric conditions, which provides the opportunity for a more comprehensive understanding of aerosol formation and fate.

Organic carbon aerosol plays a crucial role in the atmosphere, yet quantitative measurements of OC are challenging because it spans a wide range of volatility. This thesis began with review of common aerosol instrumentation and a discussion of a new

method for OC detection. It then discusses the range of aerosol chemical composition across North America. Much of this work is focused on anthropogenic North American aerosol by first discussing how the power generation region and urban areas of the Northeastern United States have affected local aerosol climatology and continental outflow, then tests and refutes a specific mechanism previously thought to significantly contribute to ambient aerosol load, and finally by examining the sources of incoming aerosol to the west coast of North America from Asia. The major findings of this work are summarized below.

Since organic carbon aerosol is a significant fraction of aerosol mass loading, how can existing aerosol instrumentation be modified in order to more easily quantify carbonaceous aerosol?

Replacement of the impaction plate with a mini cyclone on the PILS system appears to significantly increase droplet collection efficiency. By coupling this instrument with a Sievers TOC analyzer, this new technique appears to successfully measure the organic fraction of submicron aerosol. The instrument was tested with various calibration aerosol generated in the laboratory, as well as in ambient conditions in Atlanta and Riverside. By linear regression slope (± 1σ), the PILS-OC measured ~101% ± 2% of OC in Atlanta, and ~93% ± 5% of OC in Riverside, not statistically different from one considering the combined uncertainties associated with each measurement (10% PILS-OC, 20% Sunset OCEC). As a result of this work, a possibly significant positive bias was observed with data from the Sunset Labs ECOC instrument. This was characterized in a side-by-side

comparison with the PILS-OC, as well as with a TEOM and BAM analyzer. It is noted that the PILS-OC can not adequately detect the completely insoluble fraction of organic carbon aerosol that has aerodynamic diameters greater than ~110nm.

A consequence of this work illustrates a potentially important issue with the Sunset Labs analyzer. Assuming the PILS modification discussed here results in a quantitative measurement of OC aerosol, it suggests that the Sunset Labs instrument deployed during these studies may have had an instrument bias of ~1-3 $\mu gC\ m^{-3}$. This was a significant artifact, and may be a result on SVOC penetration through the denuder, NDIR detection uncertainty, sample flow rate error, or another unknown artifact. This artifact appears to be related to the relative influence of fossil fuel combustion sources of VOC (and thus OC aerosol) – in cases where there were fewer fossil fuel VOC sources, the bias appears smaller. This is important because as a widely-used instrument for OC detection, this may suggest that the Sunset Labs OC measurement may report higher than actual concentrations (due to the positive bias), which would reduce the importance of organic carbon to aerosol mass loading. Furthermore, this calls into question the efficacy of the Sunset Labs analyzer since it appears as though the artifact may be related to specific aerosol sampling conditions (e.g. high or low fraction of mobile sources of organics) and indicates that the instrument bias is not uniform across possible ambient sampling conditions, and therefore can not be easily corrected. Thus, it calls into question the limit of detection and instrument precision of the Sunset Labs OC analyzer.

How does aerosol transformation and transportation affect pollution within the northeastern United States?

Aerosol exiting the eastern coast of North America mainly consisted of sulfate and ammonium ion, and water soluble organic carbon, and this work summarized overall chemical climatology of submicron aerosol in this region. At times, the sulfate aerosol was highly acidic and was secondarily formed after emission from the coal-fired power generating regions of the Ohio River Valley and along the eastern seaboard. Particle acidity was highest at lowest altitude ranges, and is consistent with sulfate sources on the surface. $PM_{1.0}$ Nitrate, chloride, sodium, calcium, magnesium, and potassium ions were rarely observed during the NEAQS field campaign.

By comparing particle volume measurements with bulk composition, we estimate particle density and the ratio of organic matter (OM). This was performed using an iterative linear equation solver. The measured $PM_{1.0}$ particle volume concentrations and inferred density were then used to estimate $PM_{1.0}$ particle mass concentrations. Although the particle density varied with composition, the analysis predicted a fairly constant ratio of OM to WSOC of 3.1 ± 1.6 μg μgC^{-1}.

WSOC (and inferred OM) was detected throughout the sampling locations, and was observed in highest concentrations (WSOC >25 $\mu gC\ m^{-3}$, inferred OM > 75 $\mu g\ m^{-3}$) within the Yukon/Alaskan biomass burning plumes. Although, like sulfate, WSOC concentrations decreased rapidly with increasing altitude, the ratio of WSOC to sulfate increased sharply at about 2.5 km altitude, in the region of transition from the boundary layer to the free troposphere. This indicates that WSOC formation (via SOA) is likely

occurring at VOCs are lofted to altitude. Apart from biomass burning plumes, WSOC was more spatially uniform than sulfate and highest concentrations appeared to be mainly associated with urban emissions and WSOC concentrations generally ranged in between 2 and 4 μgC m^{-3}. Overall, in this study, sulfate comprised ~35 % of the $PM_{1.0}$ mass and OM ~55%, however, the fractions varied depending on altitude, and the proximity to various sources, such as power generating facilities and urban regions.

Aerosol mass loading in the Northeastern United States was largely influenced by anthropogenic sources of aerosol, mainly sulfate and WSOC. Most sulfate, as expected, was formed downwind of coal-fired power generation facilities in the region. While the United States heavily relies on coal for power production, this represents a relatively homogenous and concentrated source of a significant aerosol component. Thus, in order to reduce aerosol mass loading in the Northeastern United States, sulfur controls would be an effective and efficient way to reduce aerosols. This reduction would have increased benefits beyond just reducing aerosol mass, because SO_2 point sources are also associated with acidic aerosol, which has known effects on human health. WSOC, on the other hand, is somewhat more complex. There are both distinct biogenic sources (e.g. biomass burning), as well as sources that appears related to anthropogenic emissions. Biomass burning sources may substantially contribute to overall global mass loading of organic aerosol, but had minimal effect on the surface of the Northeastern US since most observations of biomass WSOC were discrete, high altitude interceptions. Anthropogenic WSOC is somewhat more complicated because point sources are far less obvious. In addition, broad, regional concentration of WSOC were observed, even in

conditions that were not directly downwind of urban sources. Thus, WSOC is present in background concentrations (possibly from biogenic sources), but was enhanced downwind of urban outflow. In contrast to sulfate, control strategies for WSOC are not clear, and need to consider anthropogenic emissions of WSOC precursors (e.g. VOCs), but must also consider that aerosol mass loading of organics may also be influenced by broader, regional background concentrations possibly linked to biogenic (non biomass burning) emissions.

Does ambient organic aerosol form under acid-catalyzing conditions?

A case study near northern Georgia, US was presented that examined possible acid-catalyzed SOA formation caused by distinct power plant plumes. Acid-catalyzed SOA has been suggested as a significant source of organic aerosol in a number of chamber studies, and WSOC is a good (though not completely specific) measurement of SOA. By examining a spatially broad regional dome of WSOC, five power plant plumes were intercepted which where highly acidic (ammonium to sulfate molar ratios were generally less than 1). However, no detectable increase in WSOC concentration was observed when comparing WSOC concentration within the plume (where acid catalyzed SOA formation would be most likely to occur) with WSOC concentration immediately outside of the plume.

At the time of the measurements, the findings of this work were somewhat unexpected. Since then, several studies have shown (though not as direct as in this work) that acid-

catalyzed SOA may not be significant in the ambient atmosphere. This work does not seek to diminish the chamber study work of others, but shows that chamber studies may not accurately reflect on atmospheric processes under ambient conditions. While there are many reactions that are responsible for aerosol formation – particularly in organic carbon aerosol formation - acid catalyzed reactions are unlikely to be a significant source of OC, and thus efforts to better identify OC formation mechanisms should be focused elsewhere.

To what extent does long range transport from Asia play in the role of carbonaceous aerosol in North America?

Long range transport of Asian aerosols can be detected at altitude over North America. WSOC, a fraction of organic carbon aerosol, was generally less then 0.5 mgC m-3 at low (0-3km) altitudes, and was below the detection limit (<0.1μgC m^{-3}) at high altitudes. This is in contrast to other work that showed organic carbon aerosol concentrations that ranged from ~2-10 mgC m-3. In contrast, sulfate aerosol was generally observed to be uniform in concentration throughout the sampled altitudes. This, along with other evidence presented in this thesis, suggest that the air mass may have been affected by aerosol dilution and precipitation loss during transport over the Pacific, resulting in significant aerosol losses. However, sulfate aerosol apparently reformed during transport, presumably replacing some of the sulfate lost during transit. This resulted in a decreasing fraction of WSOC-to-sulfate ratio with increasing altitude, and is different from the findings in the Northeastern United States, as well as in fresher emissions closer

to the Asian continent. Nonetheless, total measured submicron aerosol mass loading using a PILS aboard a research aircraft near the west coast of the US was generally less than 1-2 μg m^{-3}, suggesting, relative to current USEPA NAAQS standards, only a small fraction of ambient aerosol in the US is advected from Asia. Since there continues to be significant disagreement with current aerosol models (which tend to poorly predict organic carbon aerosol concentration), this finding suggests the plausibility of a significant aerosol transformation mechanism that could be important for improving aerosol chemical models.

A multivariate regression analysis of WSOC variability results in general source identification of WSOC by using specific VOC tracers in the regression. For Asian air masses, WSOC variability tended to be more associated with fossil fuel combustion VOCs, whereas in observations restricted to North American emissions, WSOC was nearly equally associated with biogenic (non biomass burning) and fossil fuel combustion VOCs. Two specific plumes from the North American data subset were further analyzed by regression. In the case of a relatively fresh, low altitude plume over the Central Valley of California, WSOC variability was nearly equally associated with fossil fuel combustion and biogenic VOCs. In contrast, a plume that also originated in the Central Valley, but had passed near the vicinity of a cloud was also analyzed, and the multivariate regression results suggest a larger impact of biogenic VOCs than fossil fuel combustion (though fossil fuel combustion VOCs were still somewhat important). The regression evidence is suggestive of WSOC formation by heterogeneous processes

involving liquid water and biogenic VOCs, and may be a more important mechanism for WSOC formation than previously thought.

To summarize the entire these, aerosol chemical composition is incredibly complex and requires quantitative, in situ approaches to better understand its significance in the ambient environment. The diverse sets of measurements included in this thesis contribute salient findings that help define ambient aerosol chemistry and composition. We now better understand processes such as ambient acid-catalyzed secondary organic aerosol formation, as well as altitude profiles of aerosol composition which suggest time scales of secondary formation that depend on chemical composition (which also led to an assessment of sulfate and SOA reformation during long range transport from Asia after loss due to apparent precipitation scavenging). Relative contributions to ambient aerosol mass loading and chemical transformation due to coal-fired power generation facilities, large megalopolis regions, distant biomass burning, and long range transport from Asia have been better defined, especially in the populated Northeastern US. Finally, we have developed a better understanding of the relationship between VOC sources and their affect on WSOC variability.

APPENDIX A

CONCENTRATION CALCULATIONS AND CALIBRATION

This appendix summarizes the equations used to convert data acquired from analyzers to atmospheric concentration. It also provides typical concentration ranges when constructing calibration curves.

A1: Calculations for online instruments

A1.1 Inorganic Ions

Using a PILS-IC, the concentrations of measured ions in air must be converted from liquid concentration that is detected by the ion chromatographs. Normally, the PILS-IC transport liquid flows at 0.19 ml min^{-1}. Thus, collected droplets must account for this flow, as well as the air flow rate of the system. Because of the operational design of the PILS collector, the conversion must also account for sample dilution caused by condensed steam water on the collected droplets. This is accomplished by an internal standard (usually lithium ion, which is not normally found in detectable concentrations in the atmosphere). The general conversion equation is presented below, and is followed with a sample calculation using realistic parameters.

$$[ion] = \frac{volumetric\ \ flowrate\ at\ impactor \times liquid\ \ concentration}{air\ \ flow\ rate}$$

Where:

$$volumetric\ \ flowrate\ at\ impactor = impactor\ \ flowrate \times \left(\frac{initial\ \ std\ conc}{measured\ \ std\ conc} \right)$$

$$\frac{(0.19ml/mi + ((1.17 \times 0.19ml/\min) - 0.19ml.\min) \times (350\mu g/l)}{15l/\min} = 5.19\mu g/m^3$$

A1.2 WSOC

The PILS-WSOC collection mechanism is similar to the PILS-IC system, except that it uses a different analyzer. However, unlike PILS-IC, the internal standard normally used to measure sample dilution can not be used. Thus, this dilution is estimated by replicating PILS-WSOC operational characteristics (air flow rate, steam flow rate, transport liquid flow rate). The dilution is assumed to be 17% ± 0.5%, and is included in the equation. In addition, the interpolated background measurement is subtracted from the data.

$$[WSOC] = \frac{volumetric\ \ flowrate\ at\ impactor \times (liquid\ \ conc - background\ \ conc)}{air\ \ flow\ rate}$$

$$\frac{(0.60ml/mi + ((1.17 \times 0.19ml/\min) - 0.19ml.\min) \times (140\,ppb - 30\,ppb)}{15l/\min} = 4.6\mu gC/m^3$$

A1.2.1 Interpolation

The background measurements of PILS-WSOC on research aircraft are normally measured every 180 minutes (for 10 minutes). Thus, they are not a continuous assessment of background artifact. The background measurement is therefore linearly interpolated between successive measurements.

$$y = \left(y_a + \frac{(x - x_a)(y_b - y_a)}{(x_b - x_a)} \right) at\ the\ point(x, y)$$

A1.3 OC and EC

OC and EC are calculated by the manufacturer's software, and represent the integrated area underneath a plot of NDIR response curve and time in the thermogram. Care is taken to eliminate carbonate, as well as correctly define the thermogram split that determines the EC and OC split. Figure A1 shows a typical thermogram from the Sunset Labs analyzer, and each integration component is identified.

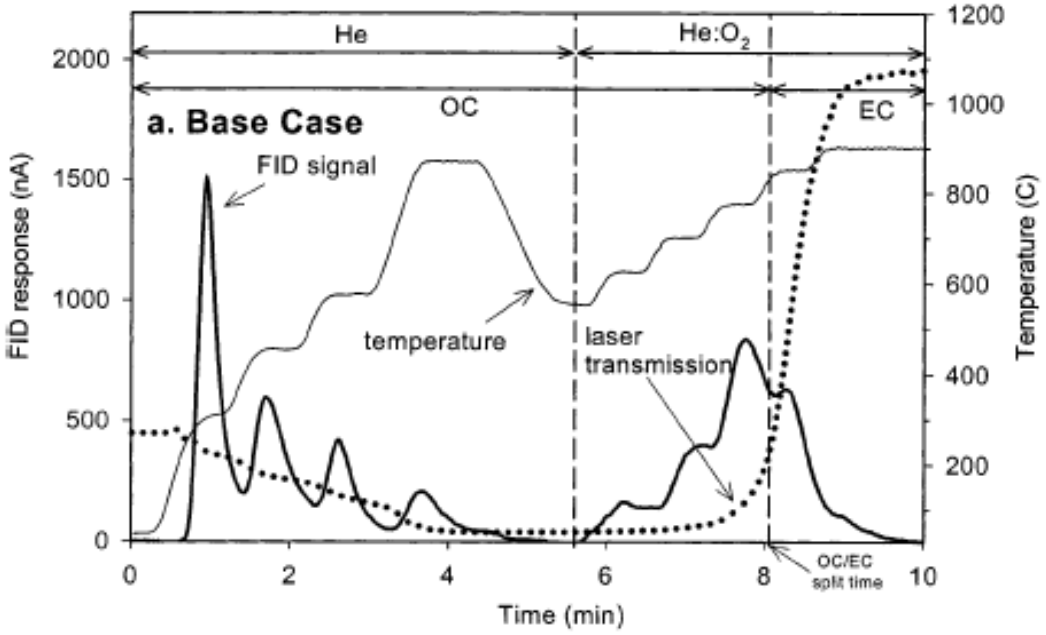

Figure A1: Screen capture of a thermogram from the Sunset Labs ECOC analyzer. Figure from Schauer, et al. [2003]

A2 Instrument calibration

A2.1 Ion chromatography calibration

Calibration curves were constructed for each ion measured prior to each field campaign. The calibration was usually generated using at least 5 NIST-traceable concentration standards, and was typically verified near the middle, and at the end of the field campaign.

Typical NIST-traceable standard concentrations used in calibration are described in Table A1 and A2.

Table A1: Typical concentrations used in NIST-traceable anion standards used for ion chromotograph.

Std ID	[bromide] (μg/L)	[chloride] (μg/L)	[nitrate, nitrite] (μg/L)	[phosphate] (μg/L)	[sulfate] (μg/L)
1	0.32	0.4768	1.6176	2.4	2.4
2	2.8	4.172	14.154	21	21
3	8	11.92	40.44	60	60
3a	16	23.84	80.88	120	120
4	40	59.6	202.2	300	300
5	80	119.2	404.4	600	600
6	120	178.8	606.6	900	900
7	240	357.6	1213.2	1800	1800
8	560	834.4	2830.8	4200	4200

Table A2: Typical concentrations used in NIST-traceable cation standards used for ion chromotograph.

Std ID	[lithium] (μg/L)	[sodium] (μg/L)	[ammonium] (μg/L)	[potassium] (μg/L)	[calcium] (μg/L)	[magnesium] (μg/L)
1	0.59004	2.3964	4.8132	2.376	11.946	2.3964
2	1.2312168	5.000488	10.043544	4.95792	24.92732	5.000488
2a	1.9668	7.988	16.044	7.92	39.82	7.988
2b	5.9004	23.964	48.132	23.76	119.46	23.964
2c	9.834	39.94	80.22	39.6	199.1	39.94
2d	15.7344	63.904	128.352	63.36	318.56	63.904
2e	19.668	79.88	160.44	79.2	398.2	79.88
3	24.585	99.85	200.55	99	497.75	99.85
4	39.336	159.76	320.88	158.4	796.4	159.76
5	98.34	399.4	802.2	396	1991	399.4

Using typical flow rates, approximate concentration ranges of sulfate are 0.027 μg m^{-3} (Std 1) to 47.60 μg m^{-3} (Std 8). Approximate concentration ranges of ammonium are 0.02 μg m^{-3} (Std 1) to 9.09 μg m^{-3} (Std 5).

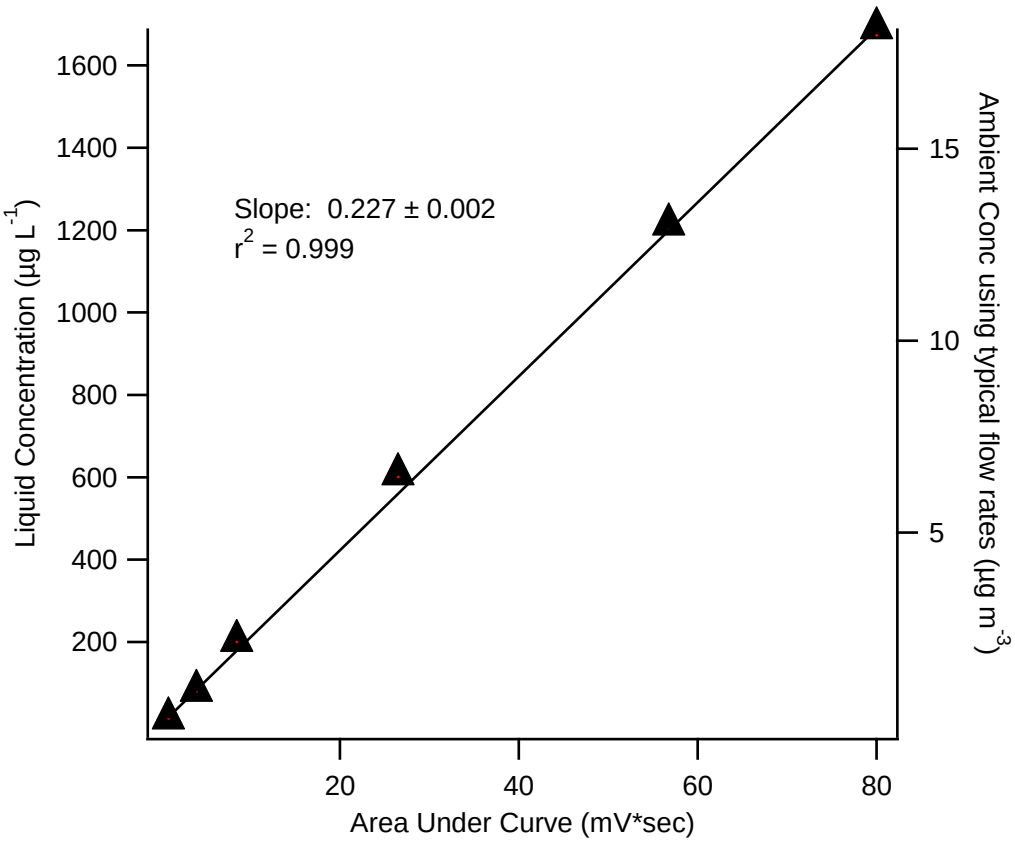

Figure A2: A typical ion calibration curve for ion chromatographs.

The standard concentrations depicted in Table A1 and A2 are used to generate a linear calibration curve that plots liquid concentration of the standard versus instrument response (as Area Under Curve). The line is forces through zero, and a linear regression fit is calculated. The slope is used to convert instrument response to liquid concentration of the sample, which is then converted to ambient concentration using the equations in section A1.1. Figure A2 is a typical calibration curve for a single ion species. Similar curves (though generally with different regression slopes) are generated for each ion measured.

A2.2 TOC calibration

The Sievers TOC analyzer is factory-calibrated and does not require ongoing calibration. The calibration, however, was tested for linearity prior to, during, and just after field deployment using an oxalic acid. Three points were checked: 50ppbC, 200ppbc, and 1000ppbC. In addition, fresh, ultrapurified water was injected directly into the analyzer prior to research flights and ground experiments. TOC concentration in fresh, purified water is typically 20-25 ppbC, and though not quantitative, this single-point check verified instrument functionality at low concentrations.

REFERENCES

Altieri, K. E., et al. (2006), Evidence for oligomer formation in clouds: Reactions of isoprene oxidation products, *Environmental Science & Technology*, *40*, 4956-4960.

Andreae, M. O., and P. J. Crutzen (1997), Atmospheric aerosols: biogeochemical sources and role in atmospheric chemistry, *Science*, *276*, 1052-1058.

Apel, E. C., et al. (2003), A fast-GC/MS system to measure C_2 to C_4 carbonyls and methanol aboard aircraft, *Journal of Geophysical Research*, *108*, 15-11 10.1029/2002JD003199.

Bae, M. S., et al. (2004), Validation of a semi-continuous instrument for elemental carbon and organic carbon using a thermal-optical method, *Atmospheric Environment*, *38*, 2885-2893.

Bae, M. S., et al. (2006), Estimation of the monthly average ratios of organic mass to organic carbon for fine particulate matter at an urban site, *Aerosol Science and Technology*, *40*, 1123-1139.

Baltensperger, U., et al. (2005), Secondary organic aerosols from anthropogenic and biogenic precursors, *Faraday Discussions*, *130*, 265-278.

Beattie, B. L., and D. M. Whelpdale (1989), Meteorological characteristics of large acidic deposition events at Kejimkujik, Nova Scotia, *Water, Air and Soil Pollution*, *46*, 45-59.

Bertschi, I. T., and D. A. Jaffe (2005), Long-range transport of ozone, carbon monoxide, and aerosols to the NE Pacific troposphere during the summer of 2003: Observations of smoke plumes from Asian boreal fires, *Journal of Geophysical Research-Atmospheres*, *110* 10.1029/2004JD005135.

Birch, M. E. (1998), Analysis of carbonaceous aerosols: interlaboratory comparison, *Analyst*, *123*, 851-857.

Biswas, P., and C. Y. Wu (1998), Control of toxic metal emissions from combustors using sorbents: A review, *Journal of the Air & Waste Management Association*, *48*, 113-127.

Bond, T. C. (2001), Spectral dependence of visible light absorption by carbonaceous particles emitted from coal combustion, *Geophysical Research Letters*, *28*, 4075-4078 10.1029/2001GL013652.

Boucher, O., and U. Lohmann (1995), The Sulfate-Ccn-Cloud Albedo Effect - a Sensitivity Study with 2 General-Circulation Models, *Tellus Series B-Chemical and Physical Meteorology*, *47*, 281-300.

Brasseur, G. P., et al. (1999), *Atmospheric chemistry and global change*, xviii, 654 p. pp., Oxford University Press, New York.

Brauer, M., et al. (1995), Measurement of Acidic Aerosol Species in Eastern-Europe - Implications for Air-Pollution Epidemiology, *Environmental Health Perspectives*, *103*, 482-488.

Brock, C. A., et al. (2004), Particle characteristics following cloud-modified transport from Asia to North America, *Journal of Geophysical Research*, *109*, 1-18 10.1029/2003JD004198.

Brock, C. A., et al. (2000), Ultrafine particle size distributions measured in aircraft exhaust plumes, *Journal of Geophysical Research*, *105*, 26555-26567.

Brock, C. A., et al. (2007), Sources of Particulate Matter in the Northeastern United States: 2. Evolution of Chemical and Microphysical Properties, *In Review - J Geophysical Research*.

Brock, C. A., et al. (2003), Particle growth in urban and industrial plumes in Texas, *Journal of Geophysical Research*, *108*, 11-11 10.1029/2002JD002746.

Brock, C. A., et al. (2002), Particle growth in the plumes of coal-fired power plants, *Journal of Geophysical Research*, *107*, 9-1 10.1029/2001JD001062.

Brook, J. R., et al. (1997), Temporal and spatial relationships in fine particle strong acidity, sulphate, PM10 and PM2.5 across multiple Canadian locations, *Atmospheric Environment*, *31*, 4223-4236.

Brown, S. S., et al. (2006), Variability in nocturnal nitrogen oxide processing and its role in regional air quality, *Science*, *311*, 67-70.

Carlson, R. M. (1980), Method and Apparatus for the Determination of Volatile Electrolytes, edited, licensed by Sievers, USA.

Carlton, A. G., et al. (2006), Link between isoprene and secondary organic aerosol (SOA): Pyruvic acid oxidation yields low volatility organic acids in clouds, *Geophysical Research Letters*, *33* 10.1029/2005GL025374.

Charlson, R. J., et al. (1992), Climate Forcing by Anthropogenic Aerosols, *Science*, *255*, 423-430.

Chow, J. C. (1995), Measurement Methods to Determine Compliance with Ambient Air-Quality Standards for Suspended Particles, *Journal of the Air & Waste Management Association*, *45*, 320-382.

Chow, J. C., et al. (2004), Equivalence of elemental carbon by thermal/optical reflectance and transmittance with different temperature protocols, *Environmental Science & Technology*, *38*, 4414-4422.

Chow, J. C., et al. (2001), Comparison of IMPROVE and NIOSH carbon measurements, *Aerosol Science and Technology*, *34*, 23-34.

Chow, J. C., et al. (1994), Temporal and spatial variations of $PM_{2.5}$ and PM_{10} aerosol in the Southern California Air Quality Study, *Atmospheric Environment*, *28*, 2061-2080.

Chow, J. C., et al. (1993), DRI thermal/optical reflectance carbon analysis system: Description, evaluation and applications in U.S. air quality studies, *Atmospheric Environment, Part A: General Topics*, *27A*, 1185-1201.

Collins, W. J., et al. (2002), The oxidation of organic compounds in the troposphere and their global warming potentials, *Climatic Change*, *52*, 453-479.

CRC (2005), *Handbook of chemistry and physics*, 57 v. pp., Chemical Rubber Pub. Co. , Cleveland, OH.

Davidson, C. I., et al. (2005), Airborne particulate matter and human health: A review, *Aerosol Science and Technology*, *39*, 737-749.

de Gouw, J., et al. (2003a), Sensitivity and specificity of atmospheric trace gas detection by proton-transfer-reaction mass spectrometry, *International Journal of Mass Spectrometry*, *223*, 365-382.

de Gouw, J. A., et al. (2007), Sources of Particulate Matter in the Northeastern United States: 1. Direct Emissions and Secondary Formation of Organic Matter in Urban Plumes, *In Review - J Geophysical Research*.

de Gouw, J. A., et al. (2004), Chemical composition of air masses transported from Asia to the U.S. West Coast during ITCT 2K2: fossil fuel combustion versus biomass-burning signatures, *Journal of Geophysical Research*, *109*, 15 pp. 10.1029/2003JD004202.

de Gouw, J. A., et al. (2005), Budget of organic carbon in a polluted atmosphere: Results from the New England Air Quality Study in 2002, *Journal of Geophysical Research*, *110*, 22 10.1029/2004JD005623.

de Gouw, J. A., et al. (2003b), Emission sources and ocean uptake of acetonitrile (CH3CN) in the atmosphere, *Journal of Geophysical Research*, *108* 10.1029/2002JD002897.

de Gouw, J. A., et al. (2006), Volatile organic compounds composition of merged and aged forest fire plumes from Alaska and western Canada, *Journal of Geophysical Research*, *111*, 20 10.1029/2005JD006175.

Decesari, S., et al. (2000), Characterization of water-soluble organic compounds in atmospheric aerosol: A new approach, *Journal of Geophysical Research-Atmospheres*, *105*, 1481-1489 10.1029/1999JD900950.

Decesari, S., et al. (2001), Chemical features and seasonal variation of fine aerosol water-soluble organic compounds in the Po Valley, Italy, *Atmospheric Environment*, *35*, 3691-3699.

Decesari, S., et al. (2002), Water soluble organic compounds formed by oxidation of soot, *Atmospheric Environment*, *36*, 1827-1832.

Delfino, R. J., et al. (1997), Effects of air pollution on emergency room visits for respiratory illnesses in Montreal, Quebec, *American Journal of Respiratory and Critical Care Medicine*, *155*, 568-576.

Dentener, F. J., and P. J. Crutzen (1994), A 3-Dimensional Model of the Global Ammonia Cycle, *Journal of Atmospheric Chemistry*, *19*, 331-369.

Dockery, D. W., et al. (1993), An association between air pollution and mortality in six U.S. cities, *The New England Journal of Medicine.*, *329*, 1753-1759.

Eatough, D. J., et al. (1999), Integrated and real-time diffusion denuder sampler for $PM_{2.5}$, *Atmospheric Environment*, *33*, 2835-2844.

Eatough, D. J., et al. (1993), Multiple-system, multi-channel diffusion denuder sampler for the determination of fine-particulate organic material in the atmosphere, *Atmospheric Environment, Part A: General Topics*, *27A*, 1213-1219.

Even, A., et al. (2000), Online Analysis of Organic Aerosol Samples - A contribution to subproject 'AEROSOL', paper presented at EUROTRAC-2 Symposium, Garmisch Partenkirchen, Germany, 27-31 Mar 2000.

Facchini, M. C., et al. (1999), Partitioning of the organic aerosol component between fog droplets and interstitial air, *Journal of Geophysical Research-Atmospheres*, *104*, 26821-26832 10.1029/1999JD900349.

Fehsenfeld, F. C., et al. (2006), International Consortium for Atmospheric Research on Transport and Transformation (ICARTT): North America to Europe - Overview of the 2004 summer field study, *Journal of Geophysical Research*, *111*, 36 10.1029/2006JD007829.

Fine, P. M., et al. (2001), Chemical characterization of fine particle emissions from fireplace combustion of woods grown in the northeastern United States, *Environmental Science & Technology*, *35*, 2665-2675.

Fitzgerald, J. W. (1991), Marine Aerosols - a Review, *Atmospheric Environment Part a-General Topics*, *25*, 533-545.

Fuzzi, S., et al. (2001), A simplified model of the water soluble organic component of atmospheric aerosols, *Geophysical Research Letters*, *28*, 4079-4082 10.1029/2001GL013418.

Gao, S., et al. (2004), Particle phase acidity and oligomer formation in secondary organic aerosol, *Environmental Science and Technology*, *38*, 6582-6589.

Gao, S., et al. (2006), Characterization of polar organic components in fine aerosols in the southeastern United States: Identity, origin, and evolution, *Journal of Geophysical Research-Atmospheres*, *111* 10.1029/2005JD006601.

Greenwald, R., et al. (2006), The influence of aerosols on crop production: A study using the CERES crop model, *Agricultural Systems*, *89*, 390-413.

Guenther, A., et al. (1995), A Global-Model of Natural Volatile Organic-Compound Emissions, *Journal of Geophysical Research-Atmospheres*, *100*, 8873-8892 10.1029/94JD02950.

Gussman, R. A., et al. (2002), Design, calibration, and field test of a cyclone for PM1 ambient air sampling, *Aerosol Science and Technology*, *36*, 361-365.

Gwynn, R. C., et al. (2000), A time-series analysis of acidic particulate matter and daily mortality and morbidity in the Buffalo, New York, region, *Environmental Health Perspectives*, *108*, 125-133.

Hartz, K. E. H., et al. (2005), Cloud condensation nuclei activation of monoterpene and sesquiterpene secondary organic aerosol, *Journal of Geophysical Research-Atmospheres*, *110* 10.1029/2004JD005754.

Hastings, W. P., et al. (2005), Secondary organic aerosol formation by glyoxal hydration and oligomer formation: Humidity effects and equilibrium shifts during analysis, *Environmental Science & Technology*, *39*, 8728-8735.

Heald, C. L., et al. (2006a), Transpacific transport of Asian anthropogenic aerosols and its impact on surface air quality in the United States, *Journal of Geophysical Research-Atmospheres*, *111* 10.1029/2005JD006847.

Heald, C. L., et al. (2005), A large organic aerosol source in the free troposphere missing from current models, *Geophysical Research Letters*, *32*, 4 10.1029/2005GL023831.

Heald, C. L., et al. (2006b), Concentrations and sources of organic carbon aerosols in the free troposphere over North America, *Journal of Geophysical Research*, *111*, D23S47 10.1029/2006JD007705.

Heikes, B. G., et al. (2002), Atmospheric methanol budget and ocean implication, *Global Biogeochemical Cycles*, *16* 10.1029/2002GB001895.

Holloway, J. S., et al. (2000), Airborne intercomparison of vacuum ultraviolet fluorescence and tunable diode laser absorption measurements of tropospheric carbon monoxide, *Journal of Geophysical Research*, *105*, 24251-24261 10.1029/2000JD900237.

Hopke, P. K., et al. (1998), Three-way (PARAFAC) factor analysis: examination and comparison of alternative computational methods as applied to ill-conditioned data, *Chemometrics and Intelligent Laboratory Systems*, *43*, 25-42.

Hopke, P. K., et al. (2003), Receptor modeling of ambient and personal exposure samples: 1998 Baltimore Particulate Matter Epidemiology-Exposure Study, *Atmospheric Environment*, *37*, 3289-3302.

Horvath, H. (1993), Atmospheric Light-Absorption - a Review, *Atmospheric Environment Part a-General Topics*, *27*, 293-317.

Huang, X. F., and J. Z. Yu (2007), Is vehicle exhaust a significant primary source of oxalic acid in ambient aerosols?, *Geophysical Research Letters*, *34* 10.1029/2006GL028457.

Huang, X. F., et al. (2006), Water-soluble organic carbon and oxalate in aerosols at a coastal urban site in China: Size distribution characteristics, sources, and formation

mechanisms, *Journal of Geophysical Research-Atmospheres*, *111* 10.1029/2006JD007408.

Huebert, B., et al. (2004a), Measurements of organic and elemental carbon in Asian outflow during ACE-Asia from the NSF/NCAR C-130, *Journal of Geophysical Research-Atmospheres*, *109* 10.1029/2004JD004700.

Huebert, B. J., et al. (2003), An overview of ACE-Asia: Strategies for quantifying the relationships between Asian aerosols and their climatic impacts, *Journal of Geophysical Research-Atmospheres*, *108* 10.1029/2003JD003550.

Huebert, B. J., et al. (2004b), PELTI: Measuring the passing efficiency of an airborne low turbulence aerosol inlet, *Aerosol Science and Technology*, *38*, 803-826.

Huey, L. G. (2007), Measurement of trace atmospheric species by chemical ionization mass spectrometry: Speciation of reactive nitrogen and future directions, *Mass Spectrometry Reviews*, *26*, 166-184.

Hughes, L. S., et al. (2000), Evolution of atmospheric particles along trajectories crossing the Los Angeles basin, *Environmental Science and Technology*, *34*, 3058-3068.

Huntzicker, J. J., et al. (1982), Analysis of Organic and Elemental Carbon in Ambient Aerosol by a Thermal-Optical Method, in *Particulate Carbon: Atmospheric Life Cycle*, edited by G. T. Wolff and R. L. Klimisch, pp. 79-88, Plenum Press, New York.

Husar, R. B., et al. (2001), Asian dust events of April 1998, *Journal of Geophysical Research-Atmospheres*, *106*, 18317-18330.

Iinuma, Y., et al. (2004), Aerosol-chamber study of the α-pinene/O_3 reaction: Influence of particle acidity on aerosol yields and products, *Atmospheric Environment*, *38*, 761-773.

Iinuma, Y., et al. (2007), Source characterization of biomass burning particles: The combustion of selected European conifers, African hardwood, savanna grass, and German and Indonesian peat, *Journal of Geophysical Research-Atmospheres*, *112* 10.1029/2006JD007120.

IPCC (2007), *Climate change 2007: The Physical Science Basis. Summary for Policymakers*, x, 18 p. pp., IPCC Secretariat, Geneva, Switzerland.

Jacob, D. J., et al. (2003), Transport and Chemical Evolution over the Pacific (TRACE-P) aircraft mission: Design, execution, and first results, *Journal of Geophysical Research-Atmospheres*, *108*, 1-19 10.1029/2002JD003276.

Jacob, D. J., et al. (2002), Atmospheric budget of acetone, *Journal of Geophysical Research-Atmospheres*, *107* 10.1029/2001JD000694.

Jacob, D. J., et al. (2005), Global budget of methanol: Constraints from atmospheric observations, *Journal of Geophysical Research-Atmospheres*, *110* 10.1029/2004JD005172.

Jacobson, M. C., et al. (2000), Organic atmospheric aerosols: review and state of the science, *Reviews of Geophysics*, *38*, 267-294.

Jaffe, D., et al. (2003), Six 'new' episodes of trans-Pacific transport of air pollutants, *Atmospheric Environment*, *37*, 391-404.

Jaffe, D., et al. (2005), Seasonal cycle and composition of background fine particles along the west coast of the US, *Atmospheric Environment*, *39*, 297-306.

Jaffrezo, J. L., et al. (2005), Seasonal variations of the water soluble organic carbon mass fraction of aerosol in two valleys of the French Alps, *Atmospheric Chemistry and Physics*, *5*, 2809-2821.

Jang, M., and R. M. Kamens (2001), Atmospheric secondary aerosol formation by heterogeneous reactions of aldehydes in the presence of a sulfuric acid aerosol catalyst, *Environmental Science and Technology*, *35*, 4758-4766.

Jimenez, J. L., et al. (2003), Ambient aerosol sampling using the Aerodyne Aerosol Mass Spectrometer, *Journal of Geophysical Research-Atmospheres*, *108* 10.1029/2001JD001213.

Johnson, D., et al. (2006), Simulating the detailed chemical composition of secondary organic aerosol formed on a regional scale during the TORCH 2003 campaign in the southern UK, *Atmospheric Chemistry and Physics*, *6*, 419-431.

Jones, A., et al. (1994), A Climate Model Study of Indirect Radiative Forcing by Anthropogenic Sulfate Aerosols, *Nature*, *370*, 450-453.

Kalberer, M., et al. (2004), Identification of Polymers as Major Components of Atmospheric Organic Aerosols, *Science*, *303*, 1659-1662.

Keeler, G. J., et al. (1991), Acid Aerosol Measurements at a Suburban Connecticut Site, *Atmospheric Environment Part a-General Topics*, *25*, 681-690.

Kenny, L. C., and R. A. Gussman (2000), A direct approach to the design of cyclones for aerosol-monitoring applications, *Journal of Aerosol Science*, *31*, 1407-1420.

Khlystov, A., et al. (1995), The Steam-Jet Aerosol Collector, *Atmospheric Environment*, *29*, 2229-2234.

Kim, E., and P. K. Hopke (2007), Comparison between sample-species specific uncertainties and estimated uncertainties for the source apportionment of the speciation trends network data, *Atmospheric Environment*, *41*, 567-575.

Kim, J. O., and G. D. Ferree (1981), Standardization in Causal-Analysis, *Sociological Methods & Research*, *10*, 187-210.

Kleeman, M. J., et al. (2000), Size and composition distribution of fine particulate matter emitted from motor vehicles, *Environmental Science and Technology*, *34*, 1132-1142.

Kondo, Y., et al. (2007), Oxygenated and water-soluble organic aerosols in Tokyo, *Journal of Geophysical Research-Atmospheres*, *112* 10.1029/2006JD007056.

Langford, A. O., and F. C. Fehsenfeld (1992), Natural Vegetation as a Source or Sink for Atmospheric Ammonia - a Case-Study, *Science*, *255*, 581-583.

Law, K. S., and A. Stohl (2007), Arctic air pollution: Origins and impacts, *Science*, *315*, 1537-1540.

Lee, Y. N., et al. (2003), Airborne measurement of inorganic ionic components of fine aerosol particles using the particle-into-liquid sampler coupled to ion chromatography technique during ACE-Asia and TRACE-P, *Journal of Geophysical Research*, *108*, 14-11 10.1029/2002JD003265.

Lewis, A. C., et al. (2005), Sources and sinks of acetone, methanol, and acetaldehyde in North Atlantic marine air, *Atmospheric Chemistry and Physics*, *5*, 1963-1974.

Lighty, J. S., et al. (2000), Combustion aerosols: Factors governing their size and composition and implications to human health, *Journal of the Air & Waste Management Association*, *50*, 1565-1618.

Likens, G. E., et al. (1996), Long-term effects of acid rain: Response and recovery of a forest ecosystem, *Science*, *272*, 244-246.

Lim, H.-J., and B. J. Turpin (2002), Origins of primary and secondary organic aerosol in Atlanta: Results of time-resolved measurements during the Atlanta Supersite Experiment, *Environmental Science and Technology*, *36*, 4489-4496.

Lim, H. J., et al. (2005), Isoprene forms secondary organic aerosol through cloud processing: Model simulations, *Environmental Science & Technology*, *39*, 4441-4446.

Lim, H. J., et al. (2003), Semicontinuous aerosol carbon measurements: Comparison of Atlanta Supersite measurements, *Journal of Geophysical Research-Atmospheres*, *108* 10.1029/2001JD001214.

Limbeck, A., et al. (2003), Secondary organic aerosol formation in the atmosphere via heterogeneous reaction of gaseous isoprene on acidic particles, *Geophysical Research Letters*, *30*, 6-1 10.1029/2003GL017738.

Lindinger, W., et al. (1998), On-line monitoring of volatile organic compounds at pptv levels by means of proton-transfer-reaction mass spectrometry (PTR-MS) - Medical applications, food control and environmental research, *International Journal of Mass Spectrometry*, *173*, 191-241.

Liu, W., et al. (2003), Application of receptor modeling to atmospheric constituents at Potsdam and Stockton, NY, *Atmospheric Environment*, *37*, 4997-5007.

Lohmann, U., and J. Feichter (2005), Global indirect aerosol effects: a review, *Atmospheric Chemistry and Physics*, *5*, 715-737.

Lynch, J. A., et al. (2000), Changes in sulfate deposition in eastern USA following implementation of Phase I of Title IV of the Clean Air Act Amendments of 1990, *Atmospheric Environment*, *34*, 1665-1680.

Ma, Y., et al. (2003), Characteristics and influence of biosmoke on the fine-particle ionic composition measured in Asian outflow during the Transport and Chemical Evolution Over the Pacific (TRACE-P) experiment, *Journal of Geophysical Research*, *108*, GTE 37-31 to GTE 37-16 10.1029/2002JD003128.

Ma, Y., et al. (2004), Intercomparisons of airborne measurements of aerosol ionic chemical composition during TRACE-P and ACE-Asia, *Journal of Geophysical Research*, *109*, 13 pp.

Maria, S. F., et al. (2003), Source signatures of carbon monoxide and organic functional groups in Asian Pacific Regional Aerosol Characterization Experiment (ACE-Asia) submicron aerosol types, *Journal of Geophysical Research*, *108*, ACE 5-1 to ACE 5-14 10.1029/2003JD003703.

Marple, V. A., et al. (1991), Microorifice uniform deposit impactor (MOUDI): description, calibration, and use, *Aerosol Science and Technology*, *14*, 434-446.

Matsunaga, S. N., et al. (2005), Isoprene oxidation products are a significant atmospheric aerosol component, *Atmospheric Chemistry and Physics*, 5, 11143-11156 1680-7375/acpd/2005-5-11143.

Maxwell-Meier, K., et al. (2004), Inorganic composition of fine particles in mixed mineral dust-pollution plumes observed from airborne measurements during ACE-Asia, *Journal of Geophysical Research-Atmospheres*, *109* 10.1029/2003JD004464.

Mayol-Bracero, O. L., et al. (2002), Carbonaceous aerosols over the Indian Ocean during the Indian Ocean Experiment (INDOEX): chemical characterization, optical properties, and probable sources, *Journal of Geophysical Research*, *107*, 2-29 10.1029/2000JD000039.

McDonald, J. D., et al. (2003), Source apportionment of airborne fine particulate matter in an underground mine, *Journal of the Air & Waste Management Association*, *53*, 386-395.

McKeown, P. J., et al. (1991), Online Single-Particle Analysis by Laser Desorption Mass-Spectrometry, *Analytical Chemistry*, *63*, 2069-2073.

McMurry, P. H. (2000), A review of atmospheric aerosol measurements, *Atmospheric Environment*, *34*, 1959-1999.

Millet, D. B., et al. (2005), Atmospheric volatile organic compound measurements during the Pittsburgh Air Quality Study: Results, interpretation, and quantification of primary and secondary contributions, *Journal of Geophysical Research-Atmospheres*, *110* 10.1029/2004JD004601.

Millet, D. B., et al. (2004), Volatile organic compound measurements at Trinidad Head, California, during ITCT 2K2: Analysis of sources, atmospheric composition, and aerosol residence times, *Journal of Geophysical Research-Atmospheres*, *109* 10.1029/2003JD004026.

Mitchell, J. F. B., et al. (1995), Climate Response to Increasing Levels of Greenhouse Gases and Sulfate Aerosols, *Nature*, *376*, 501-504.

Miyazaki, Y., et al. (2006), Time-resolved measurements of water-soluble organic carbon in Tokyo, *Journal of Geophysical Research-Atmospheres*, *111* 10.1029/2006JD007125.

Moulin, C., et al. (1997), Control of atmospheric export of dust from North Africa by the North Atlantic oscillation, *Nature*, *387*, 691-694.

Murphy, D. M., and D. S. Thomson (1995), Laser Ionization Mass-Spectroscopy of Single Aerosol-Particles, *Aerosol Science and Technology*, *22*, 237-249.

Murphy, D. M., et al. (1998), In situ measurements of organics, meteoritic material, mercury, and other elements in aerosols at 5 to 19 kilometers, *Science*, *282*, 1664-1669.

Na, K., et al. (2006), Formation of secondary organic aerosol from the reaction of styrene with ozone in the presence and absence of ammonia and water, *Atmospheric Environment*, *40*, 1889-1900.

Nenes, A., et al. (1998), ISORROPIA: A new thermodynamic equilibrium model for multiphase multicomponent inorganic aerosols, *Aquatic Geochemistry*, *4*, 123-152.

Neuman, J. A., et al. (1999), Study of inlet materials for sampling atmospheric nitric acid, *Environmental Science & Technology*, *33*, 1133-1136.

NIOSH (1996), Elemental carbon (diesel particulate): method 5040, in *NIOSH Manual of Analytical Methods*, edited by P. M. Eller and M. E. Cassinelli, National Institute for Occupational Safety and Health, Cincinatti.

Noble, C. A., and K. A. Prather (1996), Real-time measurement of correlated size and composition profiles of individual atmospheric aerosol particles, *Environmental Science & Technology*, *30*, 2667-2680.

Novakov, T., et al. (1997), Airborne measurements of carbonaceous aerosols on the East Coast of the United States, *Journal of Geophysical Research*, *102*, 30023-30030 10.1029/97JD02793.

Nowak, J. B., et al. (2006), Analysis of urban gas phase ammonia measurements from the 2002 Atlanta Aerosol Nucleation and Real-Time Characterization Experiment (ANARChE), *Journal of Geophysical Research-Atmospheres*, *111* 10.1029/2006JD007113.

Orsini, D. A., et al. (2003), Refinements to the particle-into-liquid sampler (PILS) for ground and airborne measurements of water soluble aerosol composition, *Atmospheric Environment*, *37*, 1243-1259.

Pandis, S. N., et al. (1995), Dynamics of Tropospheric Aerosols, *Journal of Physical Chemistry*, *99*, 9646-9659.

Pang, Y., et al. (2002), $PM_{2.5}$ semivolatile organic material at Riverside, California: Implications for the $PM_{2.5}$ Federal Reference Method sampler, *Aerosol Science and Technology*, *36*, 277-288.

Pankow, J. F. (1994), An Absorption-Model of the Gas Aerosol Partitioning Involved in the Formation of Secondary Organic Aerosol, *Atmospheric Environment*, *28*, 189-193.

Park, R. J., et al. (2003), Sources of carbonaceous aerosols over the United States and implications for natural visibility, *Journal of Geophysical Research*, *108*, AAC 5-1 to AAC 5-14 10.1029/2002JD003190.

Peltier, R. E., et al. (2007a), Fine aerosol bulk composition measured on WP-3D research aircraft in vicinity of the Northeastern United States – results from NEAQS, *Atmospheric Chemistry and Physics*, *7*, 3231–3247.

Peltier, R. E., et al. (2007b), No evidence for acid-catalyzed secondary organic aerosol formation in power plant plumes over metropolitan Atlanta, Georgia, *Geophysical Research Letters*, *34*, 5 10.1029/2006GL028780.

Peltier, R. E., et al. (2007c), Investigating a Method for Online OC Detection with a Particle-Into-Liquid Sampler, *Aerosol Science and Technology*, *In Review*.

Perry, K. D., et al. (1997), Long-range transport of North African dust to the eastern United States, *Journal of Geophysical Research-Atmospheres*, *102*, 11225-11238.

Peters, A., et al. (1997), Respiratory effects are associated with the number of ultrafine particles, *American Journal of Respiratory and Critical Care Medicine*, *155*, 1376-1383.

Pfister, G., et al. (2005), Quantifying CO emissions from the 2004 Alaskan wildfires using MOPITT CO data, *Geophysical Research Letters*, *32*, 5 10.1029/2005GL022995.

Pope, C. A. (1996), Particulate pollution and health: A review of the Utah Valley experience, *Journal of Exposure Analysis and Environmental Epidemiology*, *6*, 23-34.

Pope, C. A. (2000), Review: Epidemiological basis for particulate air pollution health standards, *Aerosol Science and Technology*, *32*, 4-14.

Prati, P., et al. (2000), Source apportionment near a steel plant in Genoa (Italy) by continuous aerosol sampling and PIXE analysis, *Atmospheric Environment*, *34*, 3149-3157.

Prospero, J. M. (1999), Long-term measurements of the transport of African mineral dust to the southeastern United States: Implications for regional air quality, *Journal of Geophysical Research-Atmospheres*, *104*, 15917-15927 10.1029/1999JD900072.

Pun, B. K., et al. (2002), Secondary organic aerosol - 2. Thermodynamic model for gas/particle partitioning of molecular constituents, *Journal of Geophysical Research-Atmospheres*, *107* 10.1029/2001JD000542.

Pun, B. K., et al. (1999), Gas-phase formation of water-soluble organic compounds in the atmosphere: A retrosynthetic analysis, *Journal of Atmospheric Chemistry*, *35*, 199-223.

Quinn, P. K., et al. (2006), Impacts of sources and aging on submicrometer aerosol properties in the marine boundary layer across the Gulf of Maine, *Journal of Geophysical Research-Atmospheres*, *111* 10.1029/2006JD007582.

Reid, J. S., et al. (2005), A review of biomass burning emissions part III: intensive optical properties of biomass burning particles, *Atmospheric Chemistry and Physics*, *5*, 827-849.

Reiner, T., et al. (2001), Chemical characterization of pollution layers over the tropical Indian Ocean: Signatures of emissions from biomass and fossil fuel burning, *Journal of Geophysical Research-Atmospheres*, *106*, 28497-28510 10.1029/2000JD900695.

Reiss, R., et al. (2007), Evidence of health impacts of sulfate- and nitrate-containing particles in ambient air, *Inhal. Toxicol.*, *19*, 419-449.

Riddle, E. E., et al. (2006), Trajectory model validation using newly developed altitude-controlled balloons during the International Consortium for Atmospheric Research on Transport and Transformations 2004 campaign, *Journal of Geophysical Research-Atmospheres*, *111* 10.1029/2006JD007456.

Rogge, W. F., et al. (1998), Sources of fine organic aerosol. 9. Pine, oak and synthetic log combustion in residential fireplaces, *Environmental Science & Technology*, *32*, 13-22.

Rogge, W. F., et al. (1993), Quantification of urban organic aerosols at a molecular level: Identification, abundance and seasonal variation, *Atmospheric Environment, Part A: General Topics*, *27A*, 1309-1330.

Ryerson, T. B., et al. (1999), Design and initial characterization of an inlet for gas-phase NOy measurements from aircraft, *Journal of Geophysical Research-Atmospheres*, *104*, 5483-5492 10.1029/1998JD100087.

Sannigrahi, P., et al. (2006), Characterization of water-soluble organic carbon in urban atmospheric aerosols using solid-state ^{13}C NMR spectroscopy, *Environmental Science and Technology*, *40*, 666-672.

Santarpia, J. L., et al. (2004), Direct measurement of the hydration state of ambient aerosol populations, *Journal of Geophysical Research*, *109*, 1-16 10.1029/2004JD004653.

Sardar, S. B., et al. (2005a), Size-fractionated measurements of ambient ultrafine particle chemical composition in Los Angeles using the NanoMOUDI, *Environmental Science and Technology*, *39*, 932-944.

Sardar, S. B., et al. (2005b), Seasonal and spatial variability of the size-resolved chemical composition of particulate matter (PM10) in the Los Angeles Basin, *Journal of Geophysical Research-Atmospheres*, *110* 10.1029/2004JD004627.

Saxena, P., and L. M. Hildemann (1996), Water-Soluble Organics in Atmospheric Particles: A Critical Review of the Literature and Application of Thermodynamics to Identify Candidate Compounds, *Journal of Atmospheric Chemistry*, *24*, 57.

Schauer, J. J., et al. (2003), ACE-Asia intercomparison of a thermal-optical method for the determination of particle-phase organic and elemental carbon, *Environmental Science & Technology*, *37*, 993-1001.

Schindler, D. W. (1988), Effects of Acid-Rain on Fresh-Water Ecosystems, *Science*, *239*, 149-157.

Seinfeld, J. H., and S. N. Pandis (1998), *Atmospheric chemistry and physics : from air pollution to climate change*, xxvii, 1326 p. pp., Wiley, New York.

Seinfeld, J. H., and J. F. Pankow (2003), Organic atmospheric particulate material, in *Annual review of physical chemistry, Volume 54, 2003*, edited, pp. 121-140, Annual Review.

Shim, C. S., et al. (2007), Source characteristics of oxygenated volatile organic compounds and hydrogen cyanide, *Journal of Geophysical Research-Atmospheres*, *112* 10.1029/2006JD007543.

Simpson, D., et al. (1999), Inventorying emissions from nature in Europe, *Journal of Geophysical Research-Atmospheres*, *104*, 8113-8152.

Singh, H. B. (1995), *Composition, chemistry, and climate of the atmosphere*, xii, 527 p. pp., Van Nostrand Reinhold, New York.

Singh, H. B., et al. (2004), Analysis of the atmospheric distribution, sources, and sinks of oxygenated volatile organic chemicals based on measurements over the Pacific during TRACE-P, *Journal of Geophysical Research-Atmospheres*, *109* 10.1029/2003JD003883.

Smith, G. D., and J. D. Hearn (2006), Studies of radical-initiated oxidation of organic particles using aerosol CIMS, *Abstracts of Papers of the American Chemical Society*, *231*.

Song, C. H., et al. (2005), Dust composition and mixing state inferred from airborne composition measurements during ACE-Asia C130 Flight #6, *Atmospheric Environment*, *39*, 359-369.

Sorooshian, A., et al. (2006a), Modeling and characterization of a particle-into-liquid sampler (PILS), *Aerosol Science and Technology*, *40*, 396-409.

Sorooshian, A., et al. (2006b), Oxalic acid in clear and cloudy atmospheres: Analysis of data from International Consortium for Atmospheric Research on Transport and Transformation 2004, *Journal of Geophysical Research-Atmospheres*, *111* 10.1029/2005JD006880.

Spaulding, R. S., et al. (2003), Characterization of secondary atmospheric photooxidation products: Evidence for biogenic and anthropogenic sources, *Journal of Geophysical Research-Atmospheres*, *108* 10.1029/2002JD002478.

Stier, P., et al. (2006), Impact of nonabsorbing anthropogenic aerosols on clear-sky atmospheric absorption, *Journal of Geophysical Research-Atmospheres*, *111* 10.1029/2006JD007147.

Stohl, A., et al. (1998), Validation of the Lagrangian particle dispersion model FLEXPART against large-scale tracer experiment data, *Atmospheric Environment*, *32*, 4245-4264.

Streets, D. G. (2007), Dissecting future aerosol emissions: Warming tendencies and mitigation opportunities, *Climatic Change*, *81*, 313-330.

Streets, D. G., et al. (2003), An inventory of gaseous and primary aerosol emissions in Asia in the year 2000, *Journal of Geophysical Research-Atmospheres*, *108* 10.1029/2002JD003093.

Streets, D. G., and S. T. Waldhoff (2000), Present and future emissions of air pollutants in China: SO2, NOx, and CO, *Atmospheric Environment*, *34*, 363-374.

Sullivan, A. P., et al. (2006), Airborne measurements of carbonaceous aerosol soluble in water over northeastern United States: Method development and an investigation into water-soluble organic carbon sources, *Journal of Geophysical Research*, *111*, 1-14 10.1029/2005JD006485.

Sullivan, A. P., and R. J. Weber (2006a), Chemical characterization of the ambient organic aerosol soluble in water. 1. Isolation of hydrophobic and hydrophilic fractions with a XAD-8 resin, *Journal of Geophysical Research*, *111*, 9 pp. 10.1029/2005JD006485.

Sullivan, A. P., and R. J. Weber (2006b), Chemical characterization of the ambient organic aerosol soluble in water: 2. Isolation of acid, neutral, and basic fractions by modified size-exclusion chromatography, *Journal of Geophysical Research*, *111*, 19 pp. 10.1029/2005JD006486.

Sullivan, A. P., et al. (2004), A method for on-line measurement of water-soluble organic carbon in ambient aerosol particles: results from an urban site, *Geophysical Research Letters*, *31*, 4 pp. 10.1029/2004GL019681.

Takegawa, N., et al. (2005), Characterization of an Aerodyne Aerosol Mass Spectrometer (AMS): Intercomparison with other aerosol instruments, *Aerosol Science and Technology*, *39*, 760-770 10.1029/2006GL025815.

Talbot, R. W., et al. (1992), Soluble Species in the Arctic Summer Troposphere - Acidic Gases, Aerosols, and Precipitation, *Journal of Geophysical Research-Atmospheres*, *97*, 16531-16543.

Thurston, G. D., et al. (2005), Workgroup report: Workshop on source apportionment of particulate matter health effects - Intercomparison of results and implications, *Environmental Health Perspectives*, *113*, 1768-1774.

Tolbert, P. E., et al. (2000), Interim results of the study of particulates and health in Atlanta (SOPHIA), *Journal of Exposure Analysis and Environmental Epidemiology*, *10*, 446-460.

Tolocka, M. P., et al. (2004), Formation of Oligomers in Secondary Organic Aerosol, *Environmental Science and Technology*, *38*, 1428-1434.

Tolocka, M. P., et al. (2001), East versus West in the US: Chemical Characteristics of $PM_{2.5}$ during the Winter of 1999, *Aerosol Science and Technology*, *34*, 88-96.

Tsigaridis, K., and M. Kanakidou (2003), Global modelling of secondary organic aerosol in the troposphere: a sensitivity analysis, *Atmospheric Chemistry and Physics*, *3*, 1849-1869.

Turpin, B. J., and J. J. Huntzicker (1991), Secondary Formation of Organic Aerosol in the Los-Angeles Basin - a Descriptive Analysis of Organic and Elemental Carbon Concentrations, *Atmospheric Environment Part a-General Topics*, *25*, 207-215.

Turpin, B. J., et al. (1990), Intercomparison of Photoacoustic and Thermal Optical Methods for the Measurement of Atmospheric Elemental Carbon, *Atmospheric Environment Part a-General Topics*, *24*, 1831-1835.

Turpin, B. J., et al. (1994), Investigation of organic aerosol sampling artifacts in the Los Angeles basin, *Atmospheric Environment*, *28*, 3061-3071.

Turpin, B. J., and H. J. Lim (2001), Species contributions to PM2.5 mass concentrations: Revisiting common assumptions for estimating organic mass, *Aerosol Science and Technology*, *35*, 602-610.

Turpin, B. J., et al. (2000), Measuring and simulating particulate organics in the atmosphere: problems and prospects, *Atmospheric Environment*, *34*, 2983-3013.

USEPA (2002), Health assessment document for diesel engine exhaust, edited by O. o. R. a. D. N. C. f. E. Assessment, National Center for Environmental Assessment, Office of Research and Development, U.S. Environmental Protection Agency,, Washington, D.C.

USEPA; Review of the national ambient air quality standards for particulate matter policy sssessment of scientific and technical information - Accessed: Available online, Government web site, 2005: http://purl.access.gpo.gov/GPO/LPS62787

VanCuren, R. A., and T. A. Cahill (2002), Asian aerosols in North America: Frequency and concentration of fine dust, *Journal of Geophysical Research-Atmospheres*, *107* 10.1029/2002JD002204.

VanCuren, R. A., et al. (2005), Asian continental aerosol persistence above the marine boundary layer over the eastern North Pacific: Continuous aerosol measurements from Intercontinental Transport and Chemical Transformation 2002 (ITCT 2K2), *Journal of Geophysical Research-Atmospheres*, *110* 10.1029/2004JD004973.

Varutbangkul, V., et al. (2006), Hygroscopicity of secondary organic aerosols formed by oxidation of cycloalkenes, monoterpenes, sesquiterpenes, and related compounds, *Atmospheric Chemistry and Physics*, *6*, 2367-2388.

Verma, S., et al. (2006), Sulfate aerosols forcing: An estimate using a three-dimensional interactive chemistry scheme, *Atmospheric Environment*, *40*, 7953-7962.

Volkamer, R., et al. (2006), Secondary organic aerosol formation from anthropogenic air pollution: Rapid and higher than expected, *Geophysical Research Letters*, *33* 10.1029/2006GL026899.

Voss, P. B., et al. (2005), Altitude control of long-duration balloons, *Journal of Aircraft*, *42*, 478-482.

Wang, Y., et al. (2000), Evidence of convection as a major source of condensation nuclei in the northern midlatitude upper troposphere, *Geophysical Research Letters*, *27*, 369-372 10.1029/1999GL010930.

Warneke, C., et al. (2006), Biomass burning and anthropogenic sources of CO over New England in the summer 2004, *Journal of Geophysical Research*, *111*, 13 10.1029/2005JD006878.

Weber, R. J., et al. (2001), A particle-into-liquid collector for rapid measurement of aerosol bulk chemical composition, *Aerosol Science and Technology*, *35*, 718-727.

Weber, R. J., et al. (2007), A Study of Secondary Organic Aerosol Formation in the Anthropogenic-Influenced Southeastern USA., *Journal of Geophysical Research* 10.1029/2007JD008408.

Wilson, J. C., et al. (2004), Function and performance of a low turbulence inlet for sampling supermicron particles from aircraft platforms, *Aerosol Science and Technology*, *38*, 790-802.

Wilson, W. E., et al. (2006), The measurement of fine-particulate semivolatile material in urban aerosols, *Journal of the Air & Waste Management Association*, *56*, 384-397.

Yamasoe, M. A., et al. (2006), Effect of smoke and clouds on the transmissivity of photosynthetically active radiation inside the canopy, *Atmospheric Chemistry and Physics*, *6*, 1645-1656.

Yu, J. Z., et al. (1995), Identifying Airborne Carbonyl-Compounds in Isoprene Atmospheric Photooxidation Products by Their Pfbha Oximes Using Gas-Chromatography Ion-Trap Mass-Spectrometry, *Environmental Science & Technology*, *29*, 1923-1932.

Zappoli, S., et al. (1999), Inorganic, organic and macromolecular components of fine aerosol in different areas of Europe in relation to their water solubility, *Atmospheric Environment*, *33*, 2733-2743.

Zhang, Q., et al. (2007), Ubiquity and dominance of oxygenated species in organic aerosols in anthropogenically-influenced Northern Hemisphere midlatitudes *Geophysical Research Letters*, *32* 10.1029/2007GL029979

Zhang, Q., et al. (2004), Insights into the chemistry of new particle formation and growth events in Pittsburgh based on aerosol mass spectrometry, *Environmental Science and Technology*, *38*, 4797-4809.

Zheng, M., et al. (2002), Source apportionment of PM2.5 in the southeastern United States using solvent-extractable organic compounds as tracers, *Environmental Science and Technology*, *36*, 2361-2371.